THE ASTROPHYSICAL JOURNAL SUPPLEMENT SERIES, 111:95–142, 1997 July

VLBA OBSERVATIONS OF RADIO REFERENCE FRAME SOURCES. II. ASTROMETRIC SUITABILITY BASED ON OBSERVED STRUCTURE

ALAN L. FEY
US Naval Observatory, Code EO, 3450 Massachusetts Avenue, NW, Washington, DC 20392-5420; afey@alf.usno.navy.mil
AND
PATRICK CHARLOT
Observatoire de Paris, CNRS/URA 1125, 61 avenue de l'Observatoire, F-75014 Paris, France; charlot@obspm.fr
Received 1996 December 2; accepted 1997 January 14

ABSTRACT

We present simultaneous dual-frequency Very Long Baseline Array 2 and 8 GHz observations of 133 of the 560 extragalactic sources for which positions were reported by Johnston et al. These observations represent the second in a series of observations intended to image the entire set of sources presented by Johnston et al. and, together with previously reported observations, bring the total number of sources observed so far to 169. We use the data to quantify the magnitude of the expected effect of intrinsic source structure on astrometric bandwidth synthesis VLBI observations. We also define a source "structure index," which can be used as an estimate of the astrometric quality of the sources.

Subject headings: quasars: general — radio continuum: galaxies — surveys

1. INTRODUCTION

A catalog based on the radio positions of 560 extragalactic sources distributed over the entire sky was presented by Johnston et al. (1995). The positional accuracy of these sources was estimated to be better than 3 mas in both coordinates, with the majority of the sources having uncertainties better than 1 mas. This catalog marks a milestone in defining a global, self-consistent, quasi-inertial radio reference frame accurate at the milliarcsecond level.

Despite its significance and accuracy, the current radio reference frame suffers from errors that are primarily due to intrinsic source structure (Johnston et al. 1995). The compact extragalactic sources that comprise the radio reference frame have variable emission structure on scales larger than the accuracy of their position estimates. Therefore, maintenance of the frame at a high level of accuracy requires measuring and monitoring changes in source structure. To this end, we have started an observing program to image the reference frame sources on a regular basis. The goal of these observations is to establish a database of images of all of the reference frame sources at the same frequencies as those used for precise astrometry. Despite the initial effort of Charlot (1990a), who imaged 14 sources using geodetic very long baseline interferometry (VLBI) data, most of the reference frame sources have never been imaged, either with sufficient sensitivity, sufficient resolution, or at these frequencies. In addition to providing a larger data set to improve positional accuracy, the observations reported here will allow us primarily to monitor sources for variability or structural changes so that they can be evaluated for continued suitability as reference frame objects. Furthermore, these observations will aid in our understanding of the underlying astrophysical phenomena responsible for variations of the intrinsic structure of extragalactic radio sources.

Of the 560 extragalactic sources for which positions were reported by Johnston et al. (1995), a total of 436 sources were used to "define" a radio reference frame. Positions for an additional 124 sources were also presented, in the same frame as that of the defining sources. Fey, Clegg, & Fomalont (1996) presented dual-frequency Very Long Baseline Array (VLBA) observations of 42 of these sources. In this paper, we report dual-frequency VLBA 2 and 8 GHz observations of an additional 127 sources, together with second or third epoch observations of six of the 42 sources previously observed by Fey et al. (1996). This brings the total number of sources observed so far to 169. The sources presented in this paper were chosen more or less randomly from the total list of sources. The observations reported here represent the second in a series of observations intended to image the entire set of sources presented by Johnston et al. (1995). Observations from subsequent epochs will be reported as they are reduced and analyzed.

2. OBSERVATIONS AND DATA ANALYSIS

Observations were made during two 24 hr periods on 1995 April 12–13 and on 1995 October 12–13 using the VLBA telescope (Napier et al. 1994) of the National Radio Astronomy Observatory (NRAO).[1] Eight intermediate frequencies (IFs; frequency channels) were recorded simultaneously, each 4 MHz wide, with four at the *S* band (centered at 2.22, 2.23, 2.29, and 2.32 GHz) and four at the *X* band (centered at 8.15, 8.23, 8.41, and 8.55 GHz) for a total bandwidth of 16 MHz in each frequency band. Due to a damaged dichroic plate, data were recorded only at the *X* band at the St. Croix, VI station during the 1995 October 12–13 session. Observations were made in a dual-frequency bandwidth synthesis mode to facilitate delay measurements for astrometry. The multiplicity of channels allows for the determination of a precise group delay (Rogers 1970), while simultaneous observations in two bands allow for an accurate calibration of the frequency-dependent propagation delay introduced by the ionosphere. The results of the precise astrometry afforded by these observations will be presented elsewhere. Observations in this mode also allow simultaneous dual-frequency imaging, which is the focus of the work discussed here.

A total of 133 sources were observed using short-duration ($\approx$3 minutes) "snapshots" over a number of different hour angles to maximize the (u, v)-plane coverage.

[1] NRAO is operated by Associated Universities, Inc., under cooperative agreement with the National Science Foundation.

Observations were scheduled to maximize mutual visibility between the VLBA antennas, so low-declination sources were usually observed less often than those at higher declinations. Most sources were observed during at least four or five scans, while a few sources were observed during as many as eight scans. No source was observed during fewer than three scans.

The raw data bits were correlated with the VLBA correlator at the Array Operations Center in Socorro, New Mexico. The correlated data were calibrated and corrected for residual delay and delay rate using the NRAO Astronomical Image Processing System (AIPS). The initial amplitude calibration for each of the eight IFs was accomplished using system temperature measurements taken during the observations and the NRAO-supplied gain curves. Fringe-fitting was done in AIPS using solution intervals equal to the scan durations and a point-source model in all cases. After correction for residual delay and delay rate, the data were written to FITS disk files. All subsequent processing was carried out using the Caltech VLBI imaging software, primarily DIFMAP (Pearson et al. 1994). After phase self-calibration with a point-source model, the 2 s correlator records were coherently averaged to 10 s records and then edited.

The amplitude calibration was improved by observations of the compact source 1749+096. A single amplitude gain correction factor for 1749+096 was derived for each antenna for each IF, based on fitting a simple Gaussian source model to the 1749+096 visibility data after applying only the initial calibration based on the measured system temperatures and gain curves. Gain correction factors were calculated based on the differences between observed and model visibilities. The resulting set of amplitude gain correction factors was then applied to the visibility data of 1749+096 as well as to the visibility data of the remaining sources. The evaluation of amplitude ratios at crossing points in the (u, v)-plane on a sample of sources confirmed that the relative amplitude calibration at this stage was better than 5% for most antennas, but in no case exceeded 10%.

The flux density of 1749+096 was measured at both epochs of the VLBA observations by the NRAO Green Bank Interferometer (GBI) and at the same frequencies (E. Waltman 1996, private communication). At epoch 1995 April 12–13, the *S*-band flux density of 1749+096 as measured by the VLBA was found to be $\approx$23% higher than the value measured by the GBI. The *X*-band VLBA flux density of 1749+096 was $\approx$8% higher than the GBI value. At epoch 1995 October 12–13, the *S*-band flux density of 1749+096 as measured by the VLBA was found to be $\approx$14% higher than the value measured by the GBI. The *X*-band VLBA flux density of 1749+096 was approximately equal to the GBI value. The flux density of 1741−038 was also measured by the GBI at epoch 1995 October 12–13. The *S*-band flux density of 1741−038 as measured by the VLBA was found to be $\approx$13% higher than the value measured by the GBI. The *X*-band VLBA flux density of 1741−038 was $\approx$3% higher than the GBI value. The visibility data were not corrected for these amplitude discrepancies.

The visibility data for each frequency band were self-calibrated, Fourier inverted, and CLEANed using DIFMAP in an automatic mode (Shepherd, Pearson, & Taylor 1995). DIFMAP combines the visibilities for each IF of an observation in the (u, v)-plane during gridding, taking into account frequency differences. However, DIFMAP makes no attempt to correct for spectral index effects. The spanned bandwidth of the four IFs in each band is relatively small (0.1 GHz [4% fractional bandwidth] at the *S* band and 0.4 GHz [5% fractional bandwidth] at the *X* band), so we assume that source structure and flux density variations across each of the two frequency bands are negligible. The data were self-calibrated following the hybrid-mapping technique (Pearson & Readhead 1984) in order to correct for residual amplitude and phase errors. The data were initially phase self-calibrated and mapped using uniform weighting in the (u, v)-plane before switching to natural weighting after several iterations. A point-source model was used as a starting model for the iterative procedure in all cases. Convergence was usually obtained on average in 15 iterations (including both phase-only and phase-plus-amplitude self-calibration) but went as high as 55 iterations for some of the more extended sources at the *S* band. Convergence was defined basically as the iteration at which the peak in the residual image became less than a specified factor times the rms noise of the residual image from the previous iteration.

3. OBSERVATIONAL RESULTS

Contour plots of the final, naturally weighted images of 133 sources at both the *S* band and the *X* band are shown in Figure 1. For convenience, the resulting images for each band are identified by only a single fiducial frequency (2.32 and 8.55 GHz, respectively), even though they were made using the data from all frequency channels. Table 1 lists parameters of the final images. The maximum dynamic range is $\sim$2900:1 at the *S* band and $\sim$3400:1 at the *X* band. The average dynamic range is $\sim$860:1 at the *S* band and $\sim$930:1 at the *X* band. The average rms noise is $\sim$1.3 mJy beam^{-1} at the *S* band and $\sim$1.0 mJy beam^{-1} at the *X* band. Figure 2 shows the rms noise plotted against the peak of the images for most of the sources at both the *S* band and the *X* band. One source at the *S* band and three sources at the *X* band have values that lie outside the plotted range in this figure. Figure 2 shows that the rms noise in the images at both frequencies increases only slightly with increasing peak flux density. Most values of the rms noise are less than $\sim$2.5 mJy beam^{-1} at the *S* band and less than $\sim$2.0 mJy beam^{-1} at the *X* band. This suggests that we have come close to reaching the thermal noise limit for these sources, a remarkable result considering the variation in the (u, v)-plane coverage from source to source [see Fey et al. 1996 for sample (u, v) plots]. The expected thermal noise is estimated to be $\sim$0.6 mJy beam^{-1} at both frequencies for a 20-minute observation (assuming a value of the VLBA system inefficiency, $1/\eta_s \approx 2$).

Gaussian models were fitted to the self-calibrated *visibility data* using DIFMAP. The results of the model fitting are listed in Table 2. The last column in this table lists the reduced χ^2 of the fit between the model and the visibility data. Only fitted models with a reduced $\chi^2 \lesssim 1.4$ are included in this table. The reduced χ^2 has an expected value of 1.0 (however, when the data are self-calibrated, the number of degrees of freedom is reduced so that the expected value of the reduced χ^2 may actually be significantly less than 1.0; cf. Henstock et al. 1995). At the *S* band, the sources 0116+319, 0518+165, 0831+557, 1117+146, 1458+718, 2021+317, and 2023+336 are too complex to

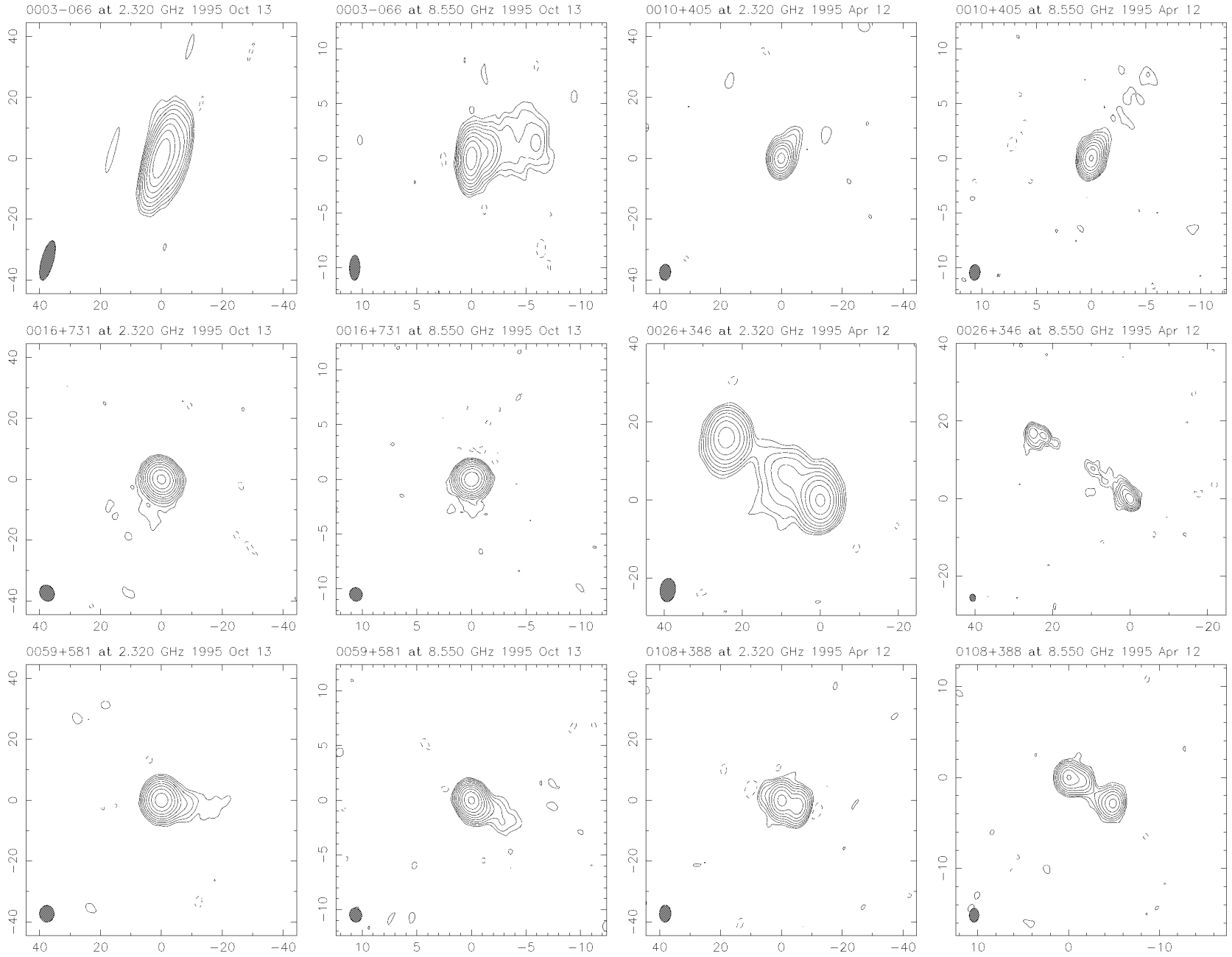

FIG. 1.—Contour plots of 133 extragalactic radio sources at both the *S* band and the *X* band. Image parameters are listed in Table 1. Gaussian models fitted to the visibility data at each frequency are listed in Table 2. The scale of each image is in milliarcseconds. The FWHM Gaussian restoring beam applied to the images is shown as a hatched ellipse in the lower left-hand corner of each panel. For convenience, the images for each band are labeled only by a single fiducial frequency (2.32 and 8.55 GHz, respectively), even though they were made using the data from all frequency channels (see text). Milliarcsecond accurate positions for these sources can be obtained from Johnston et al. (1995).

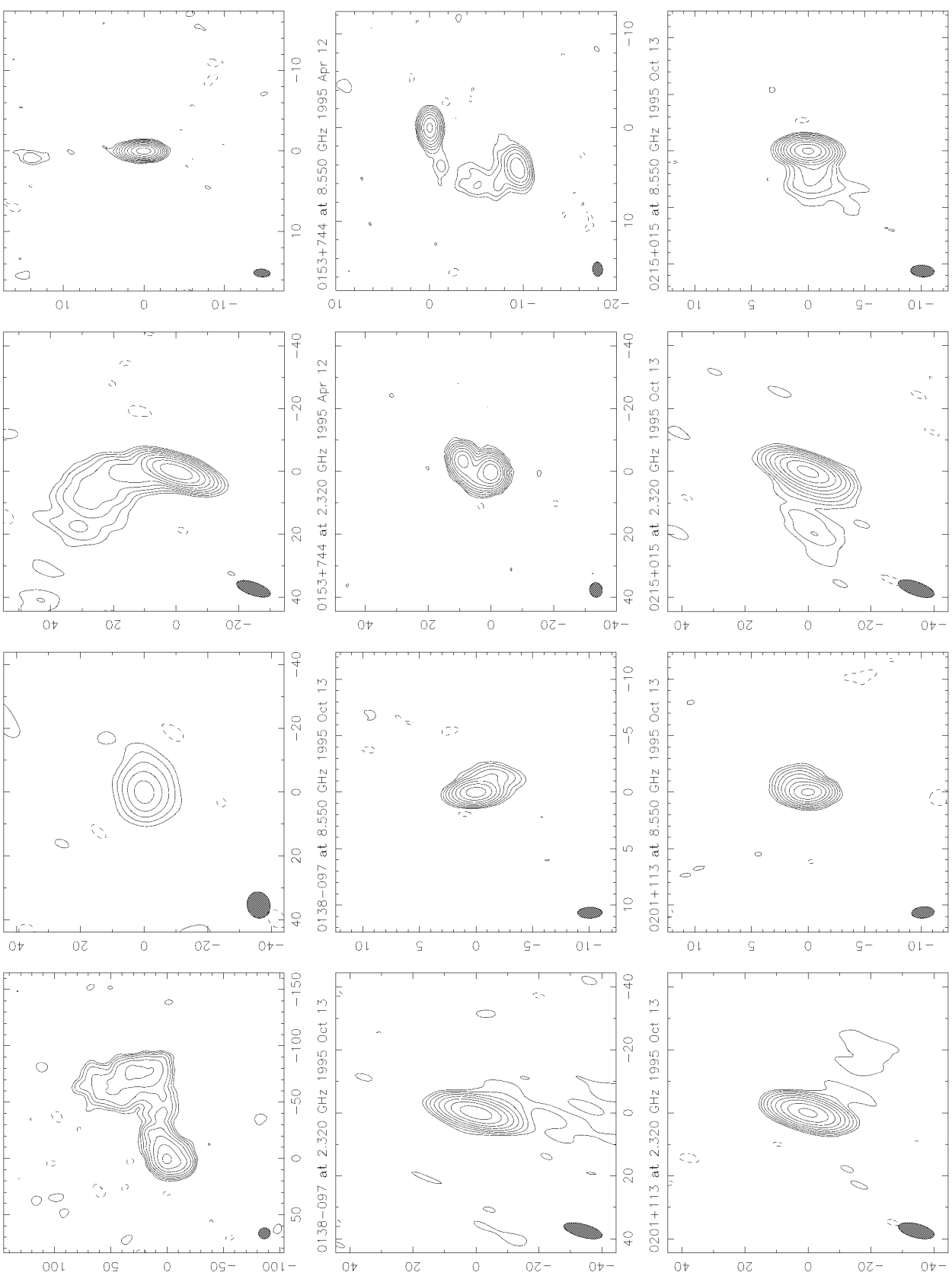

FIG. 1—*Continued*

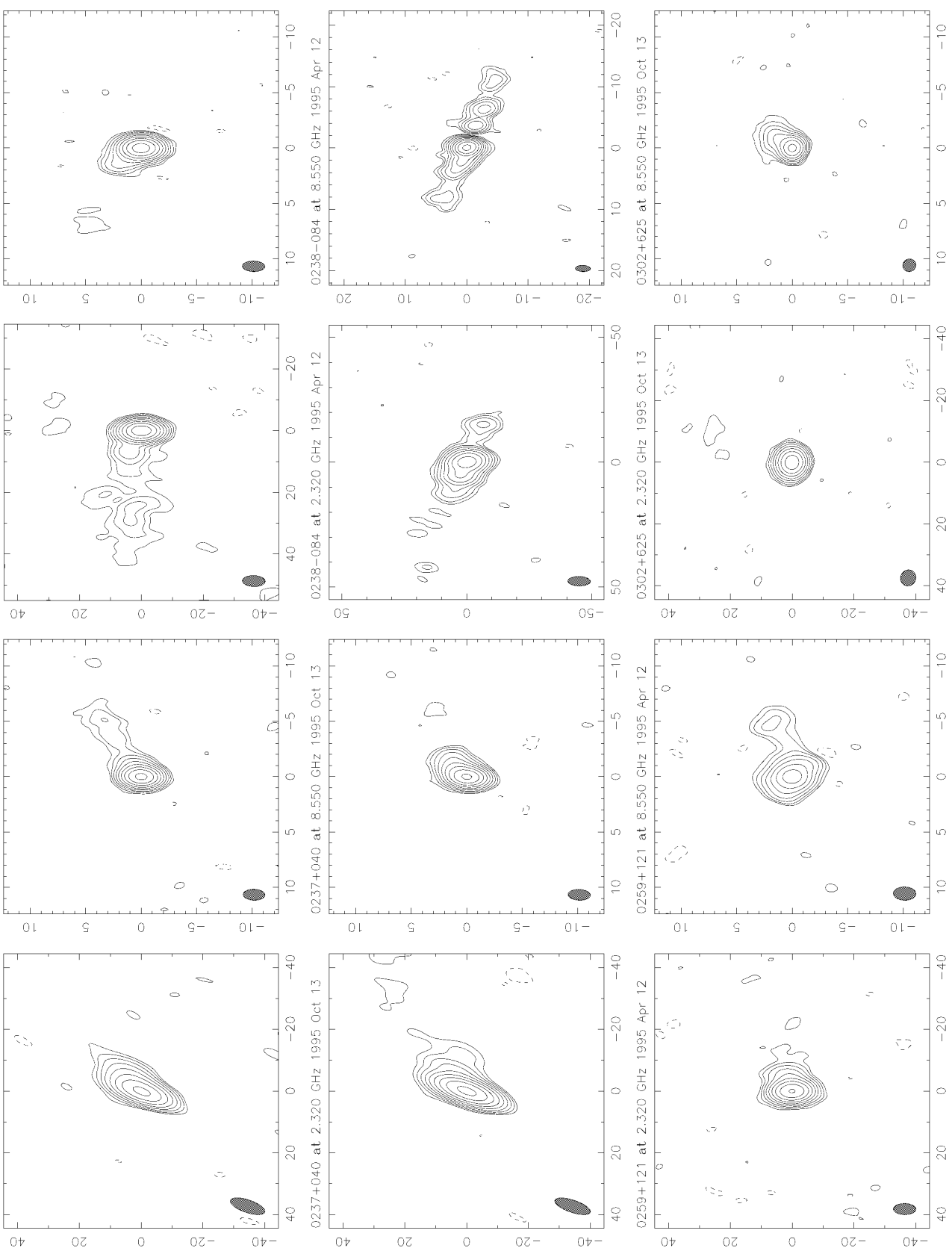

FIG. 1—*Continued*

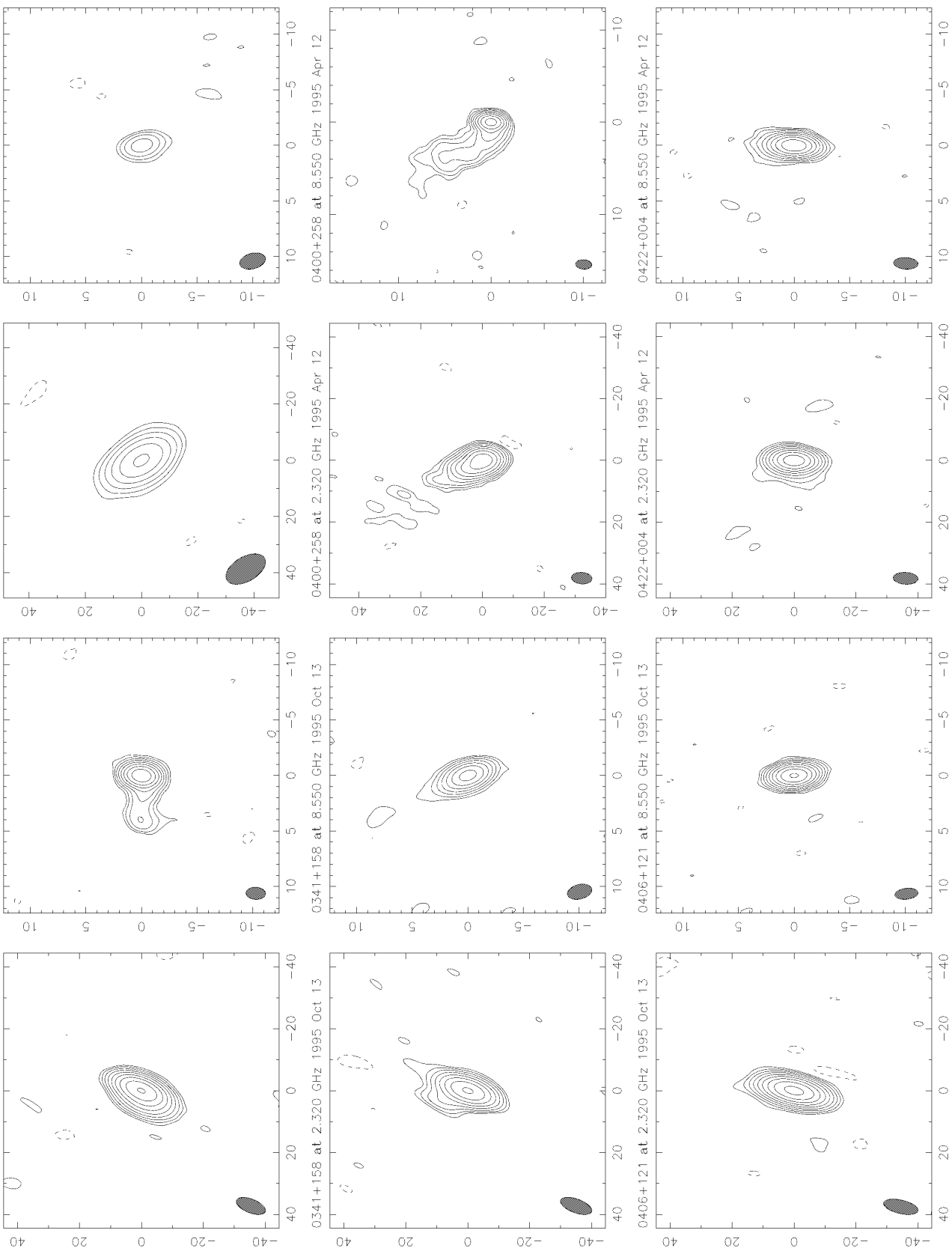

FIG. 1—*Continued*

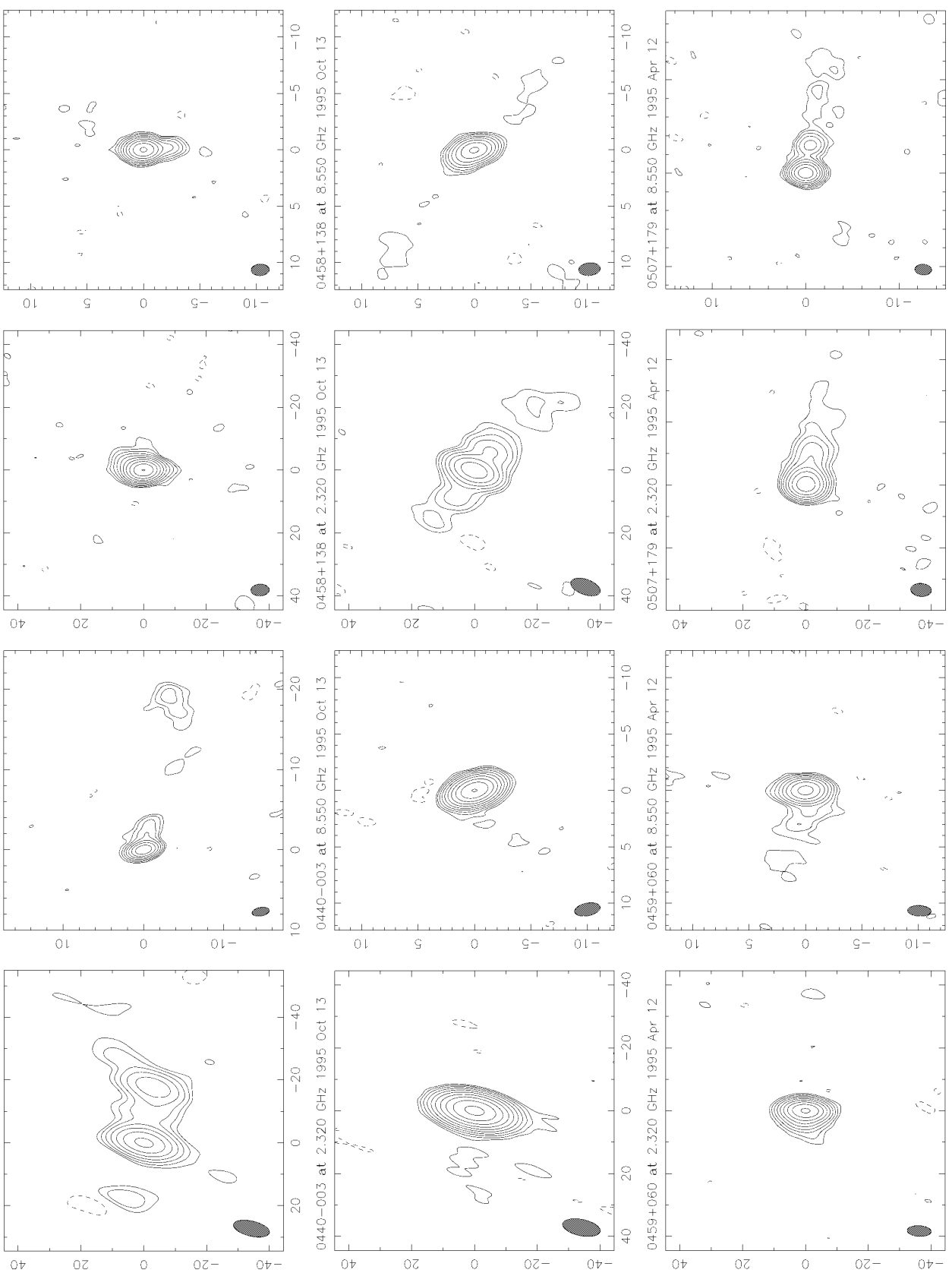

FIG. 1—*Continued*

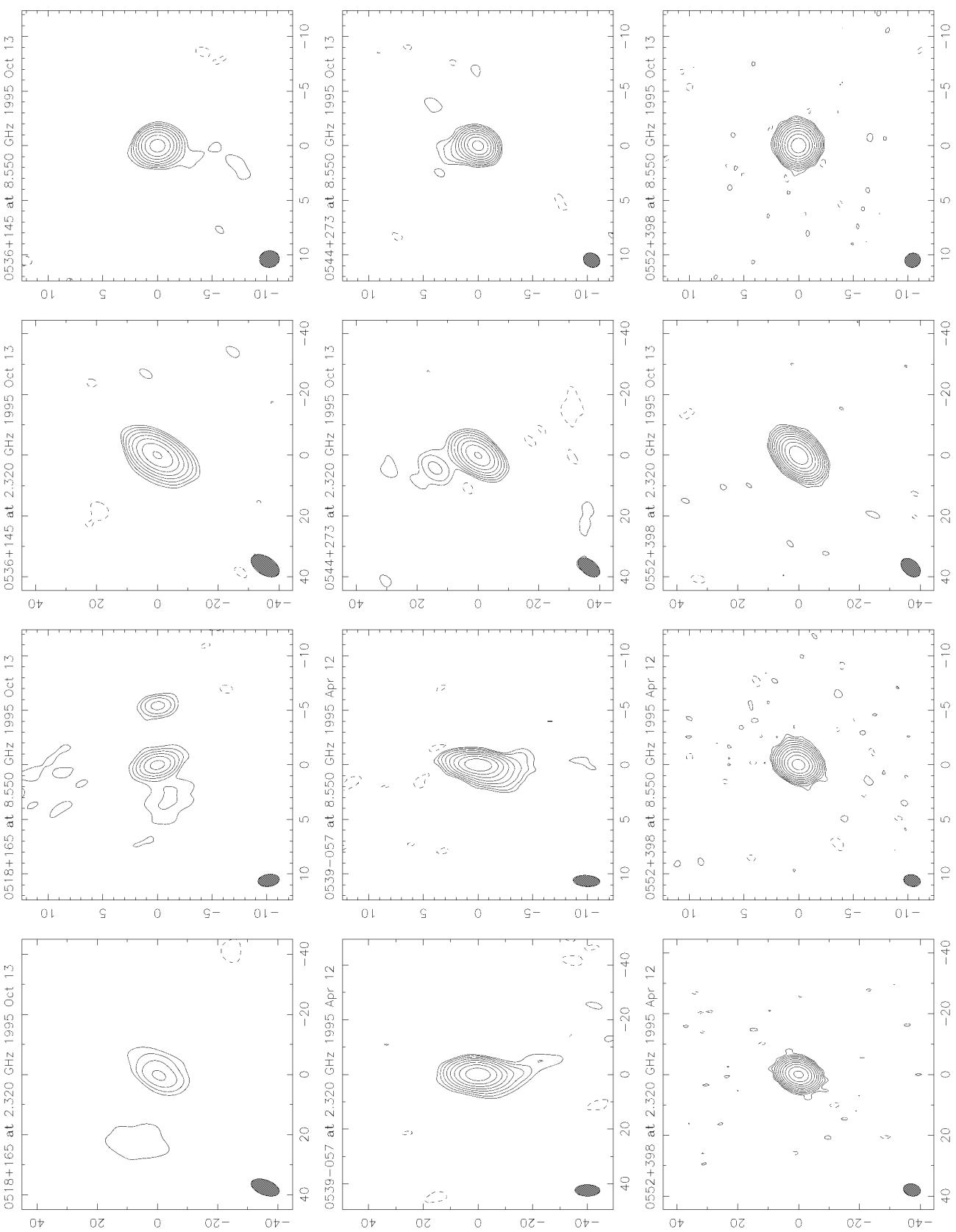

FIG. 1—*Continued*

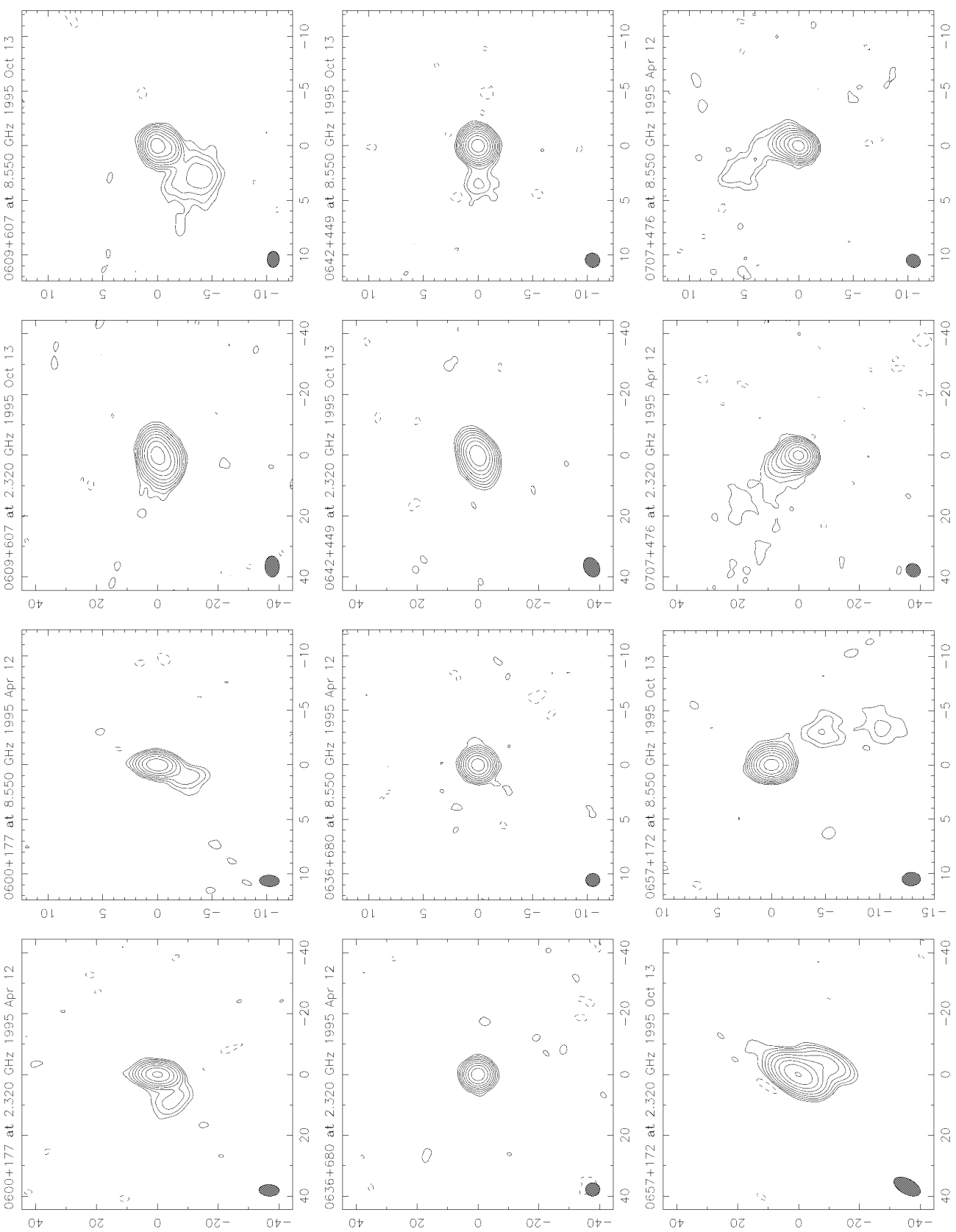

FIG. 1—*Continued*

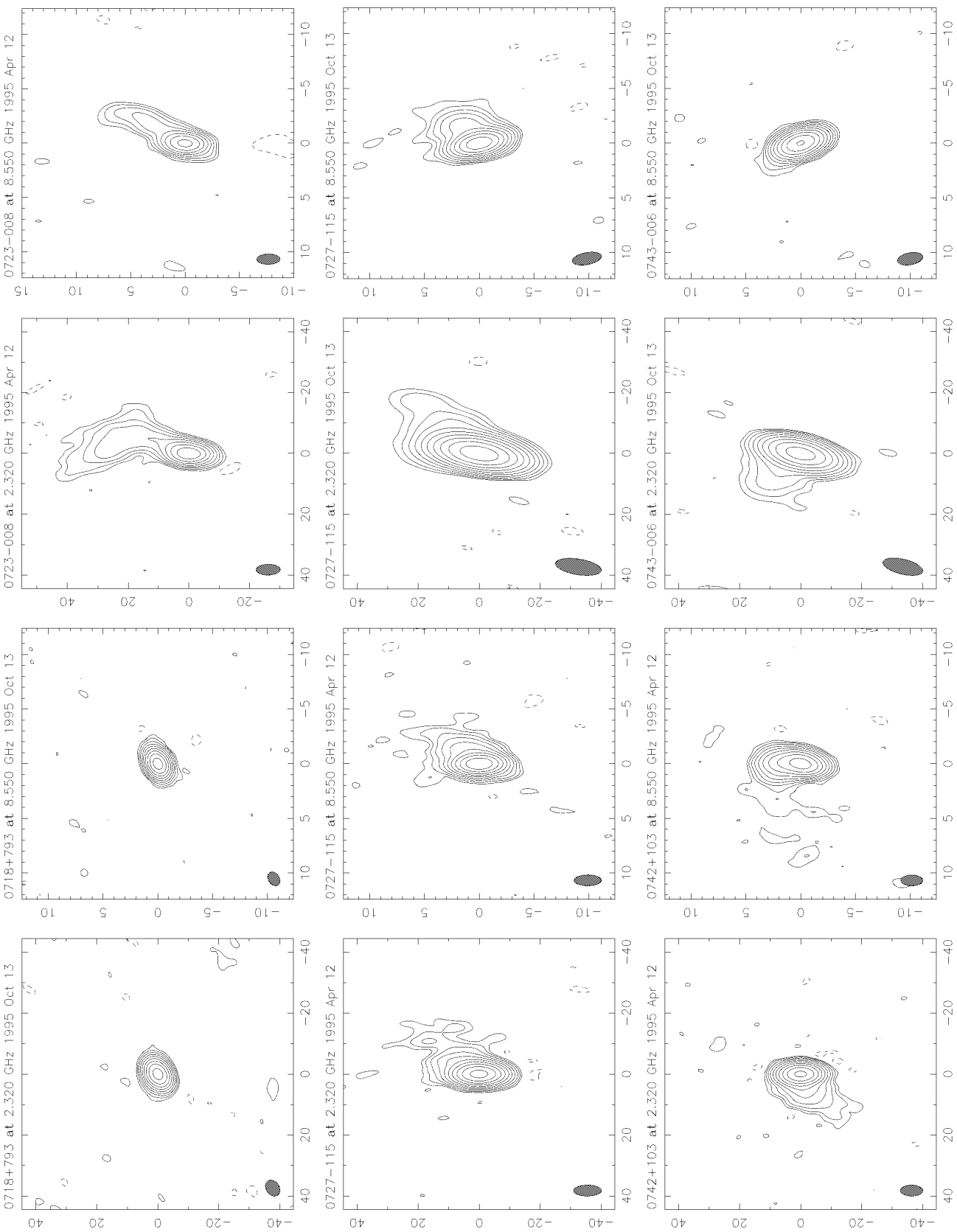

FIG. 1—*Continued*

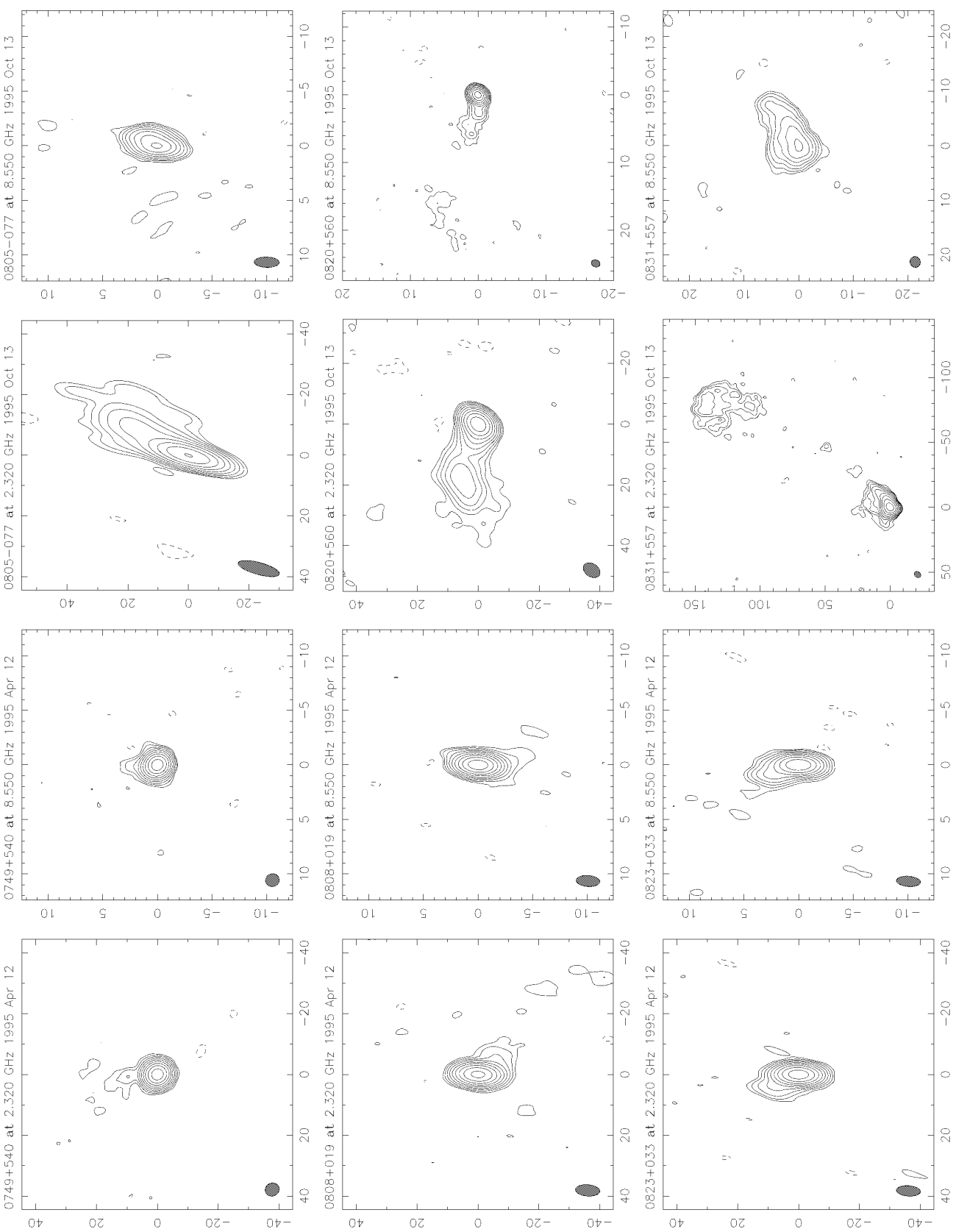

FIG. 1—*Continued*

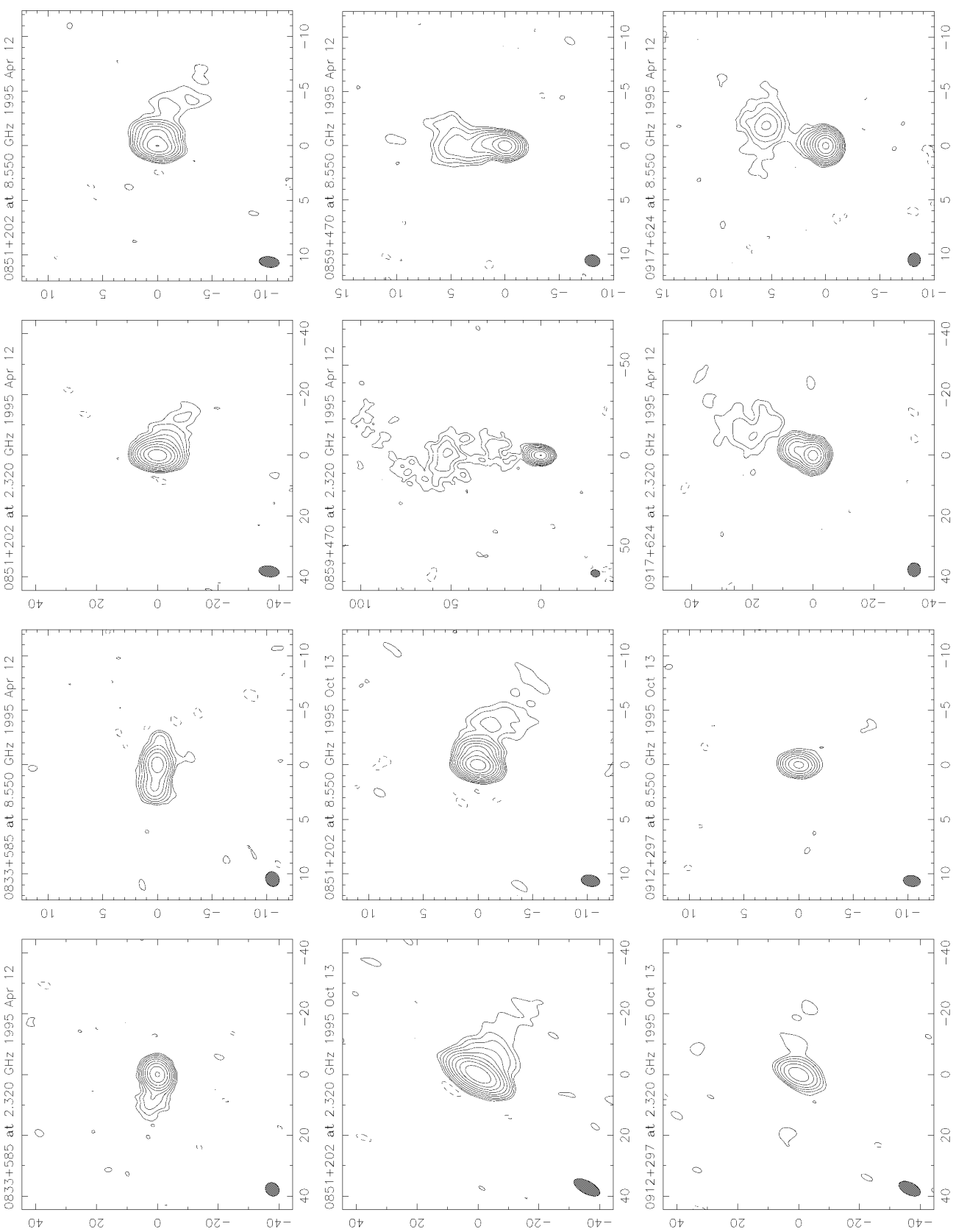

FIG. 1—*Continued*

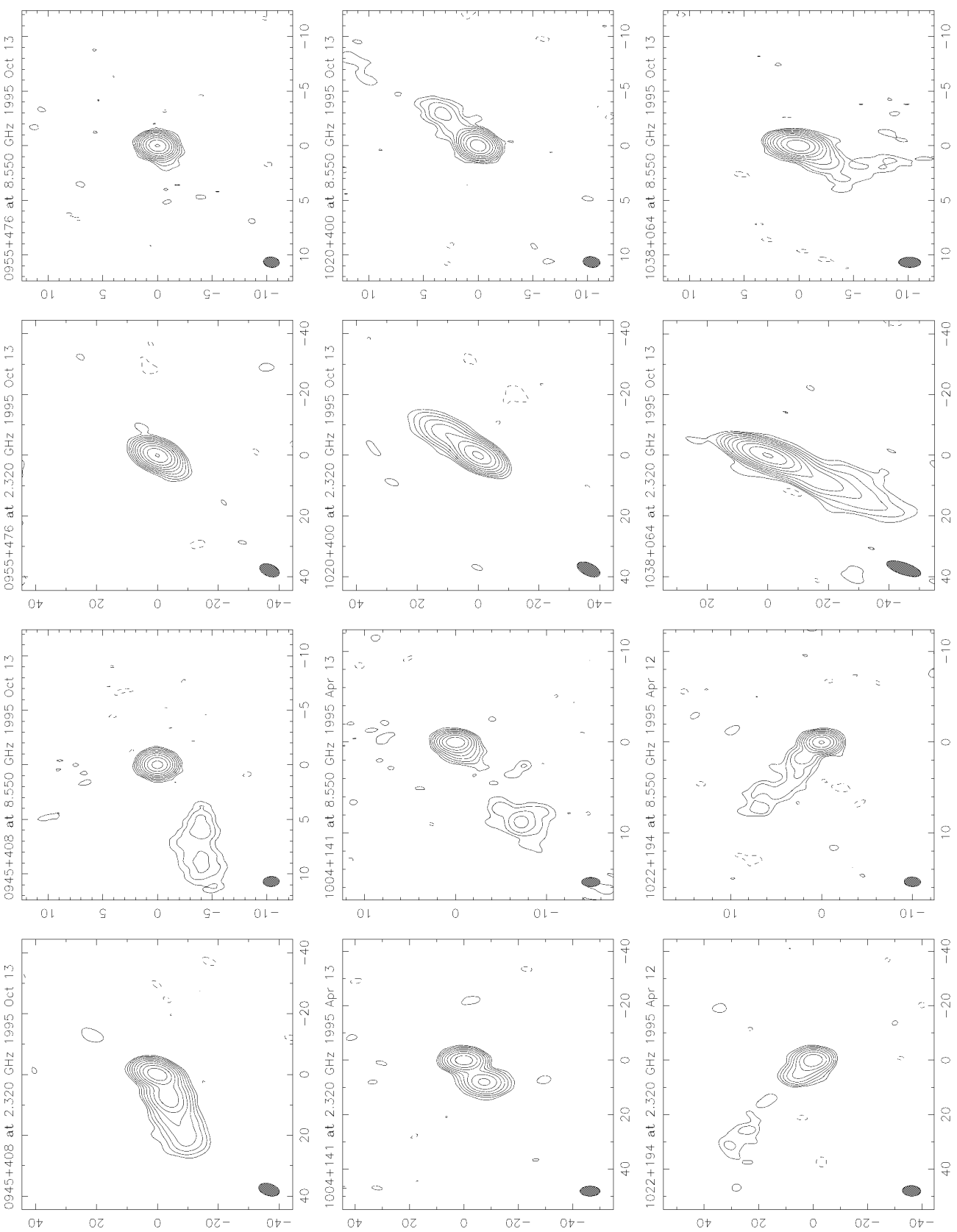

FIG. 1—*Continued*

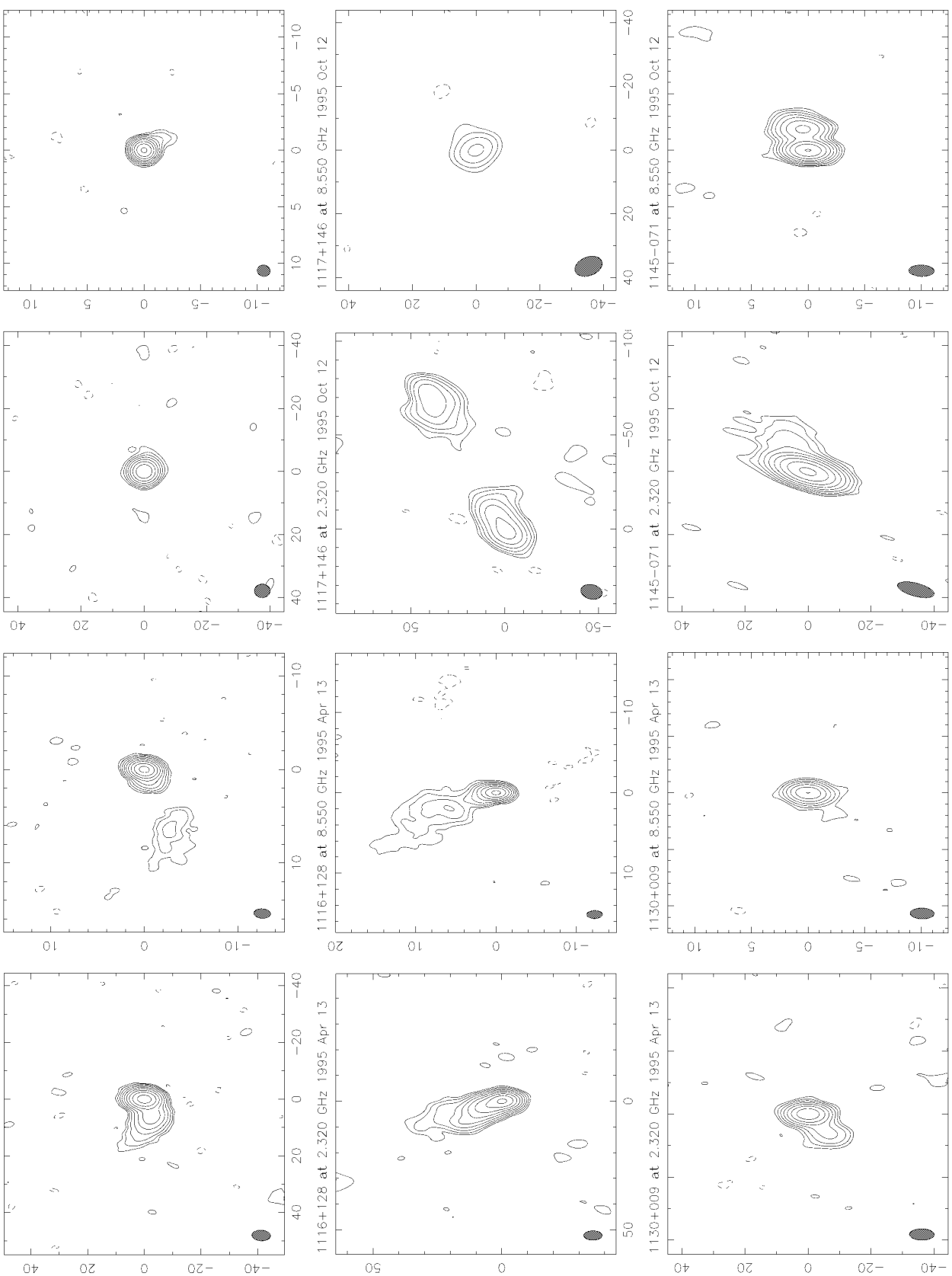

FIG. 1—*Continued*

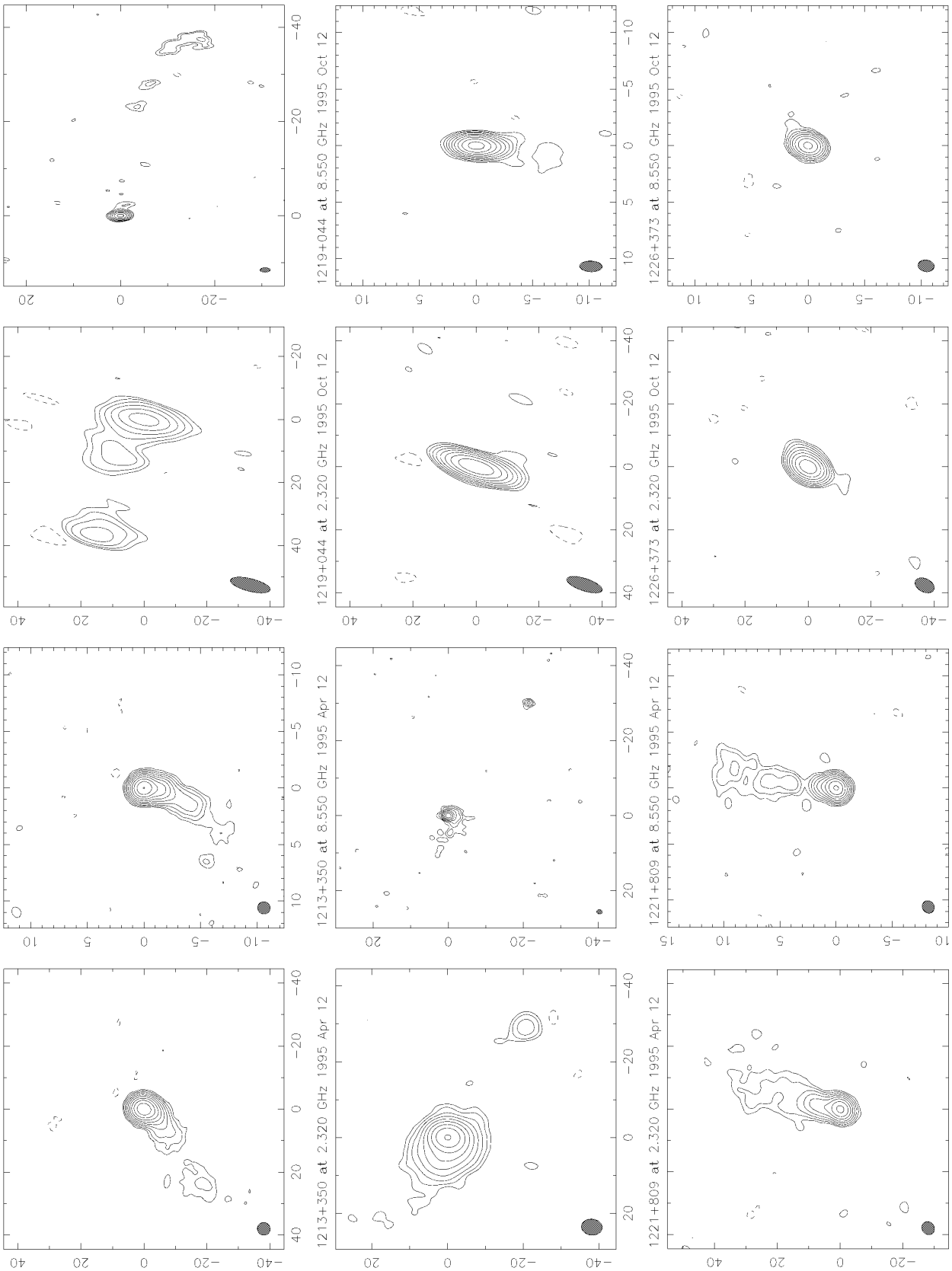

FIG. 1—*Continued*

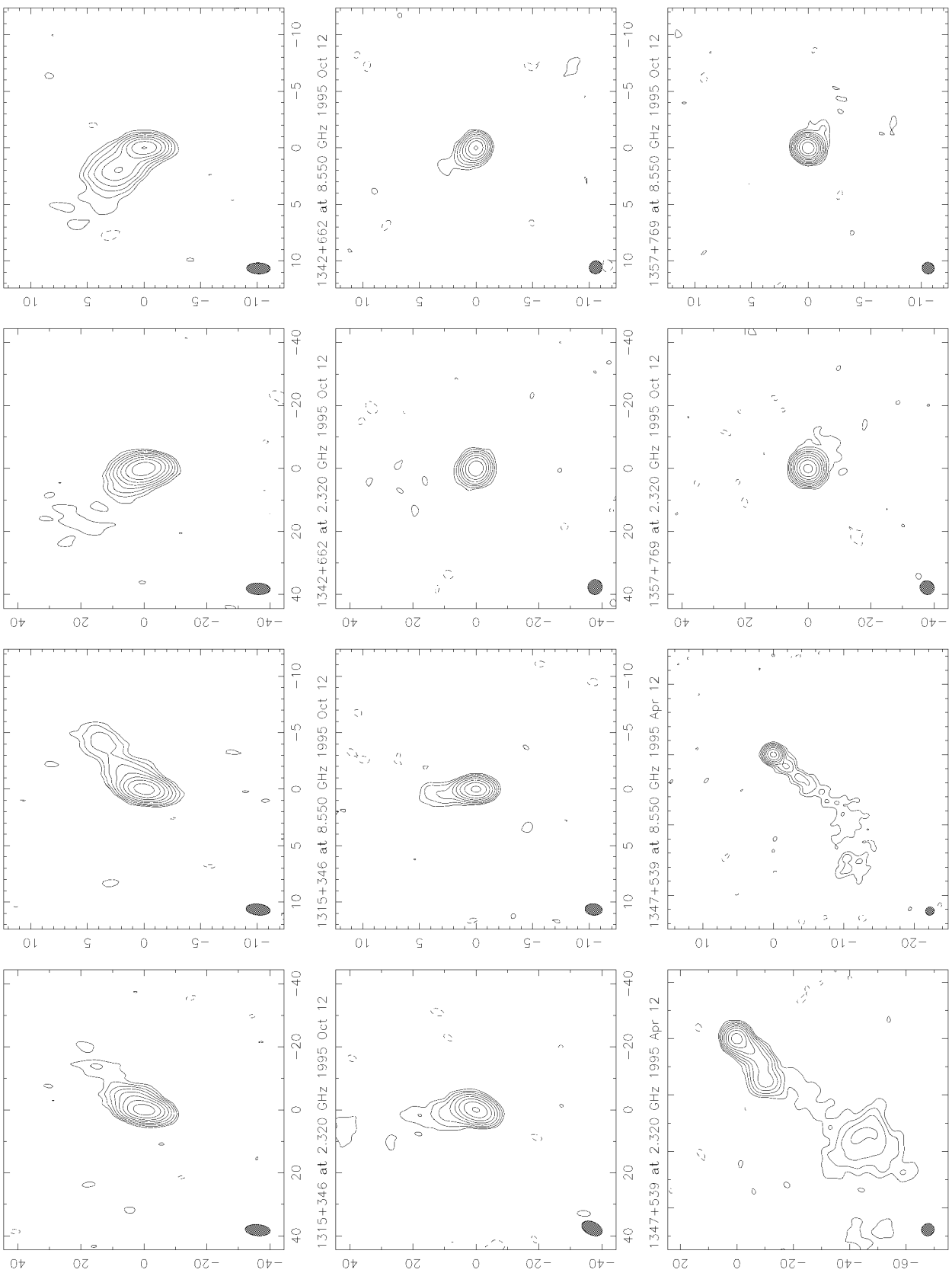

FIG. 1—*Continued*

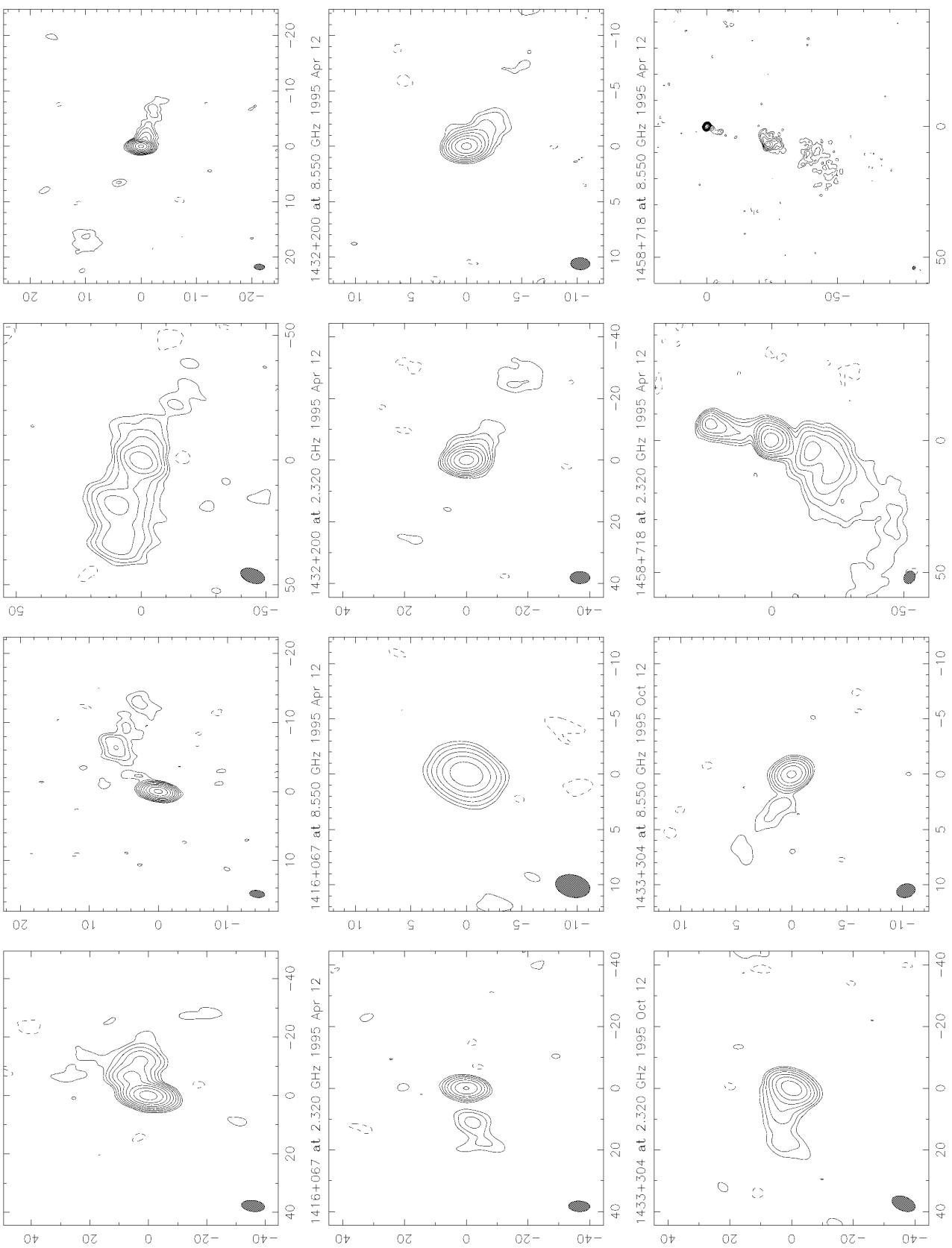

FIG. 1—*Continued*

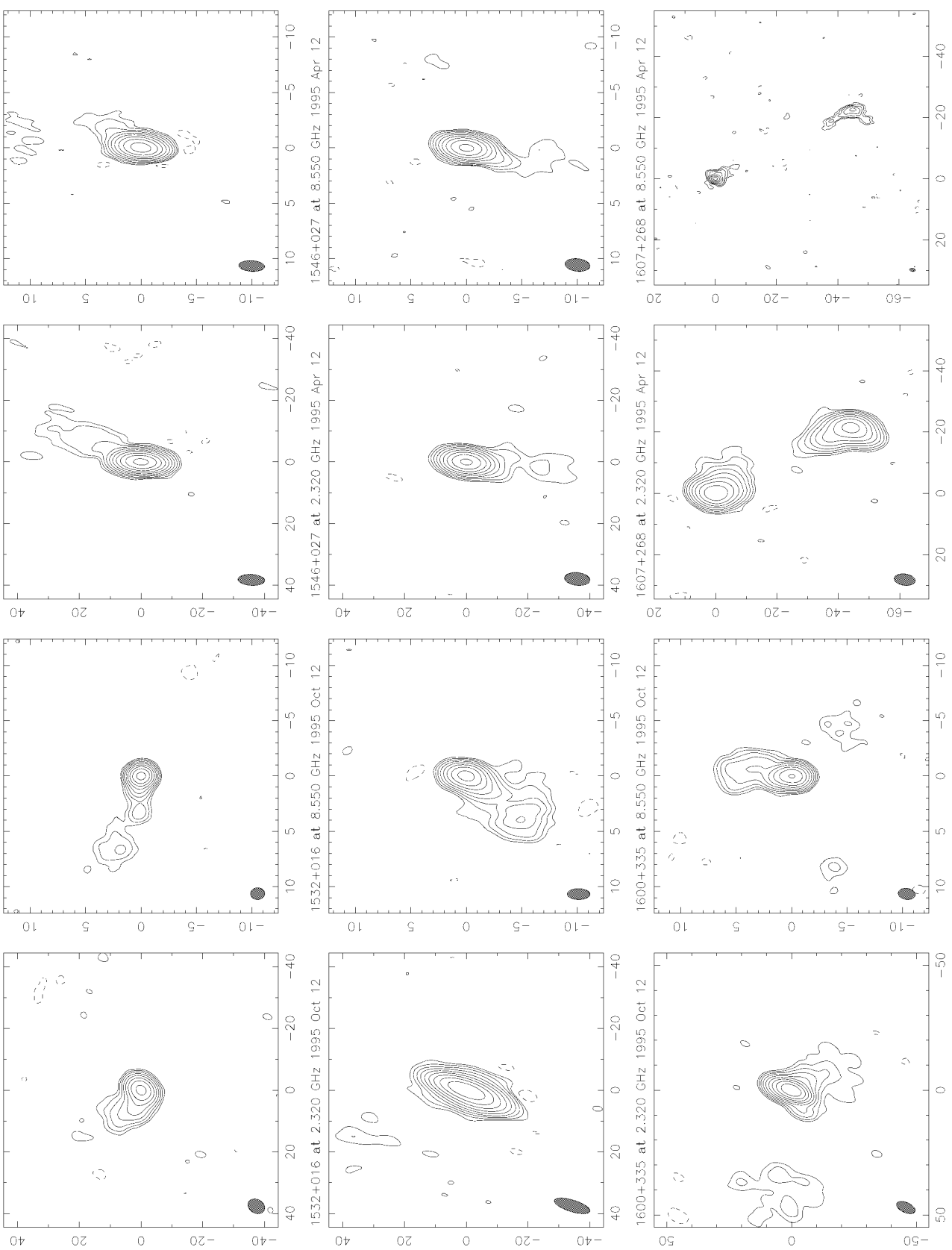

FIG. 1—*Continued*

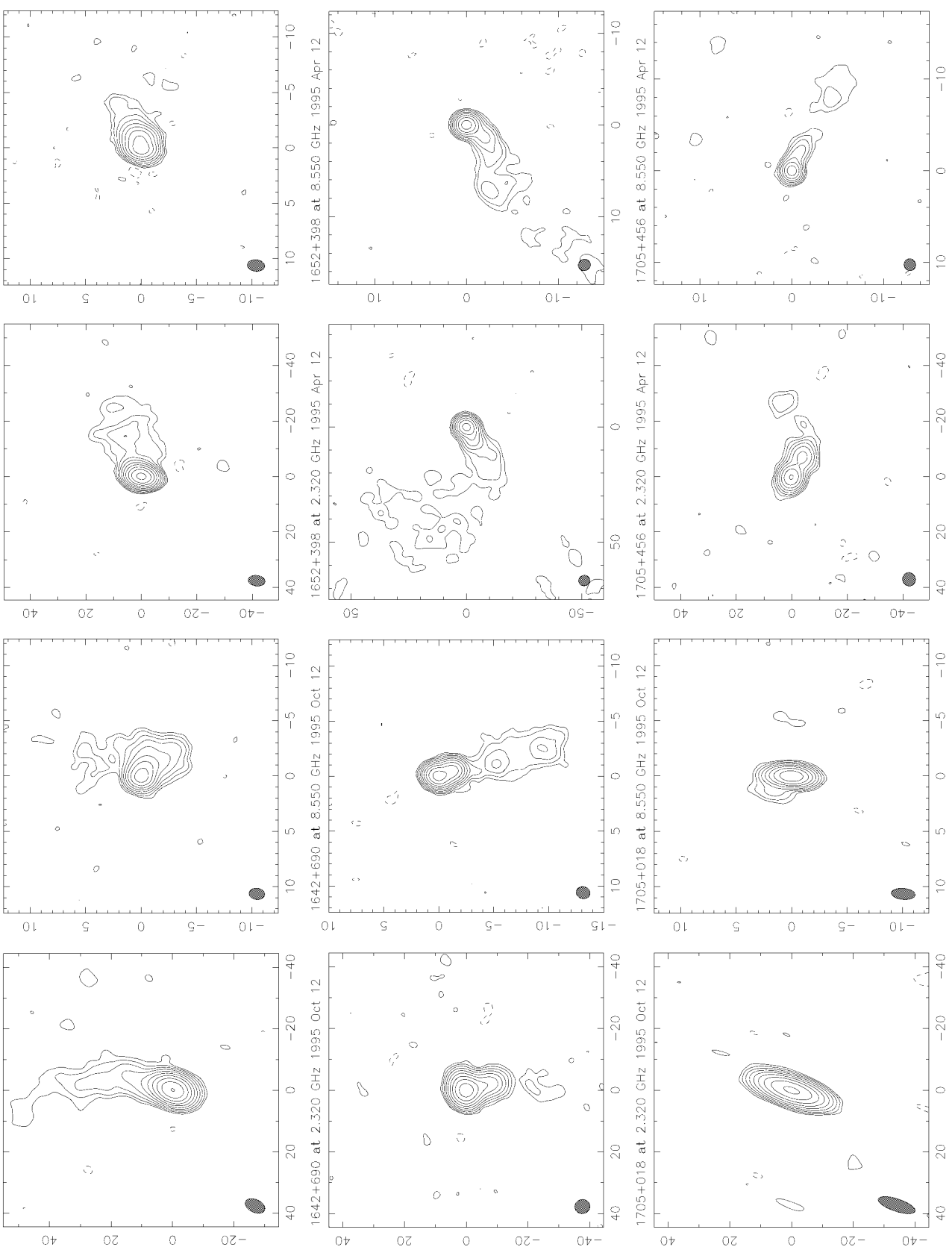

FIG. 1—*Continued*

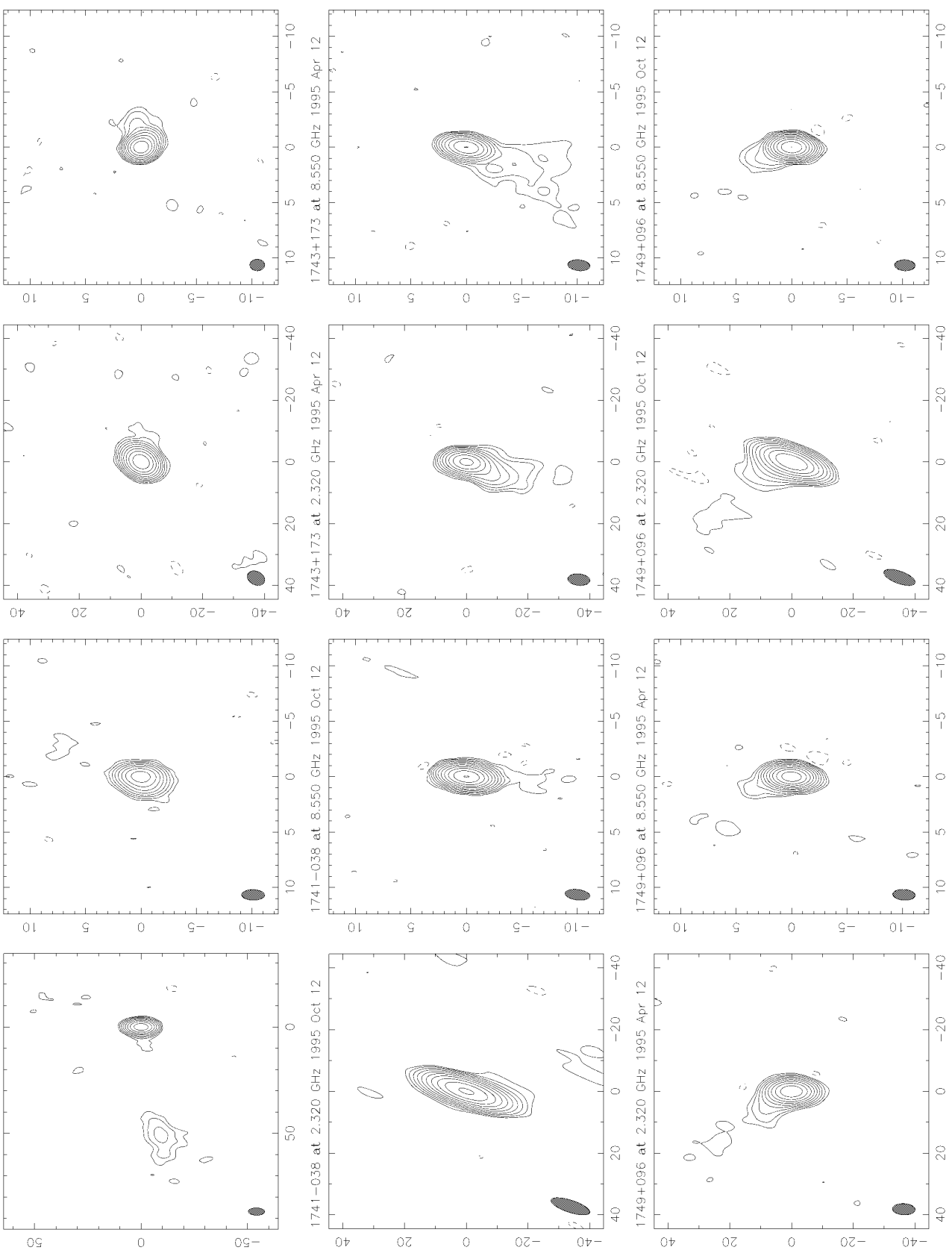

FIG. 1—*Continued*

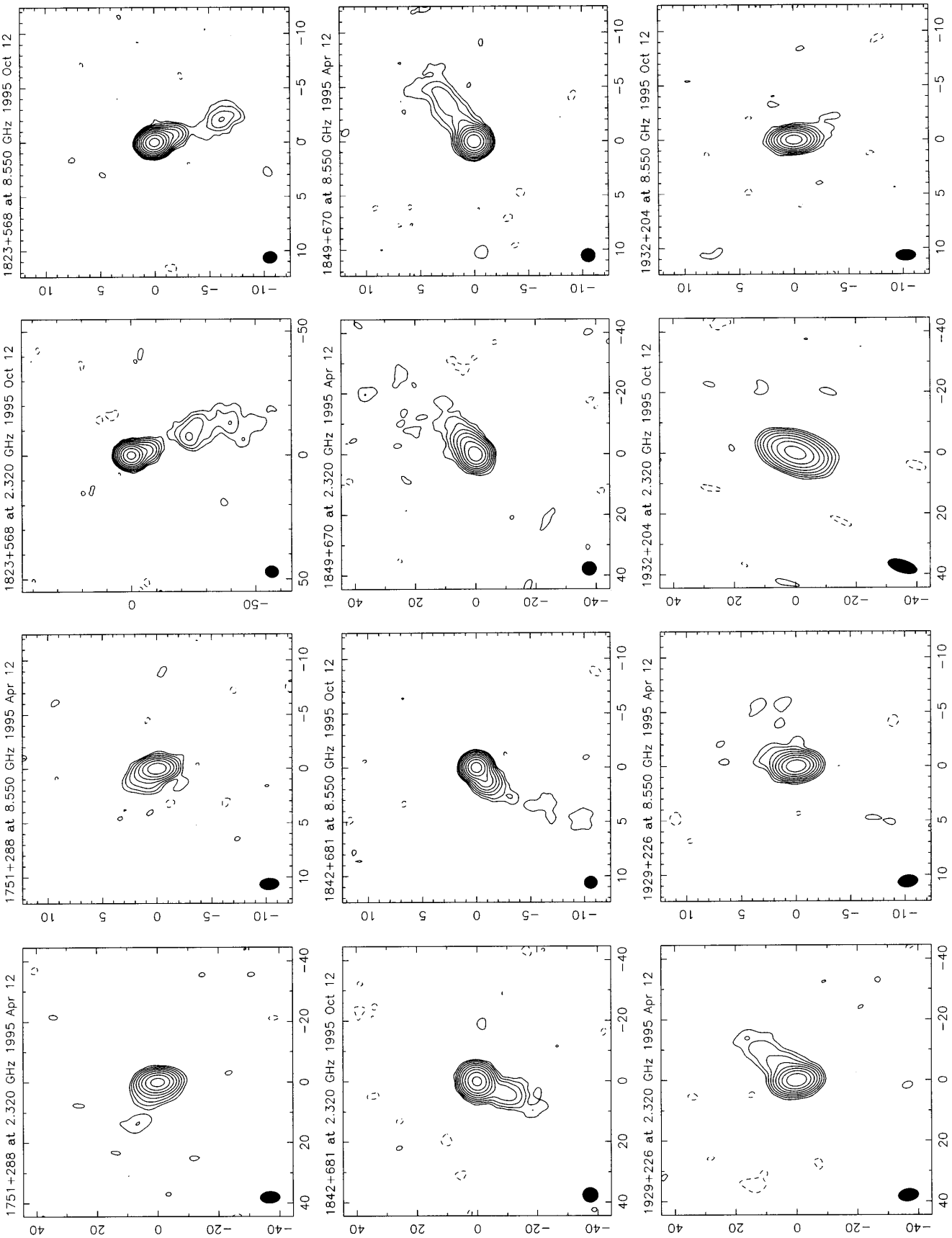

FIG. 1—*Continued*

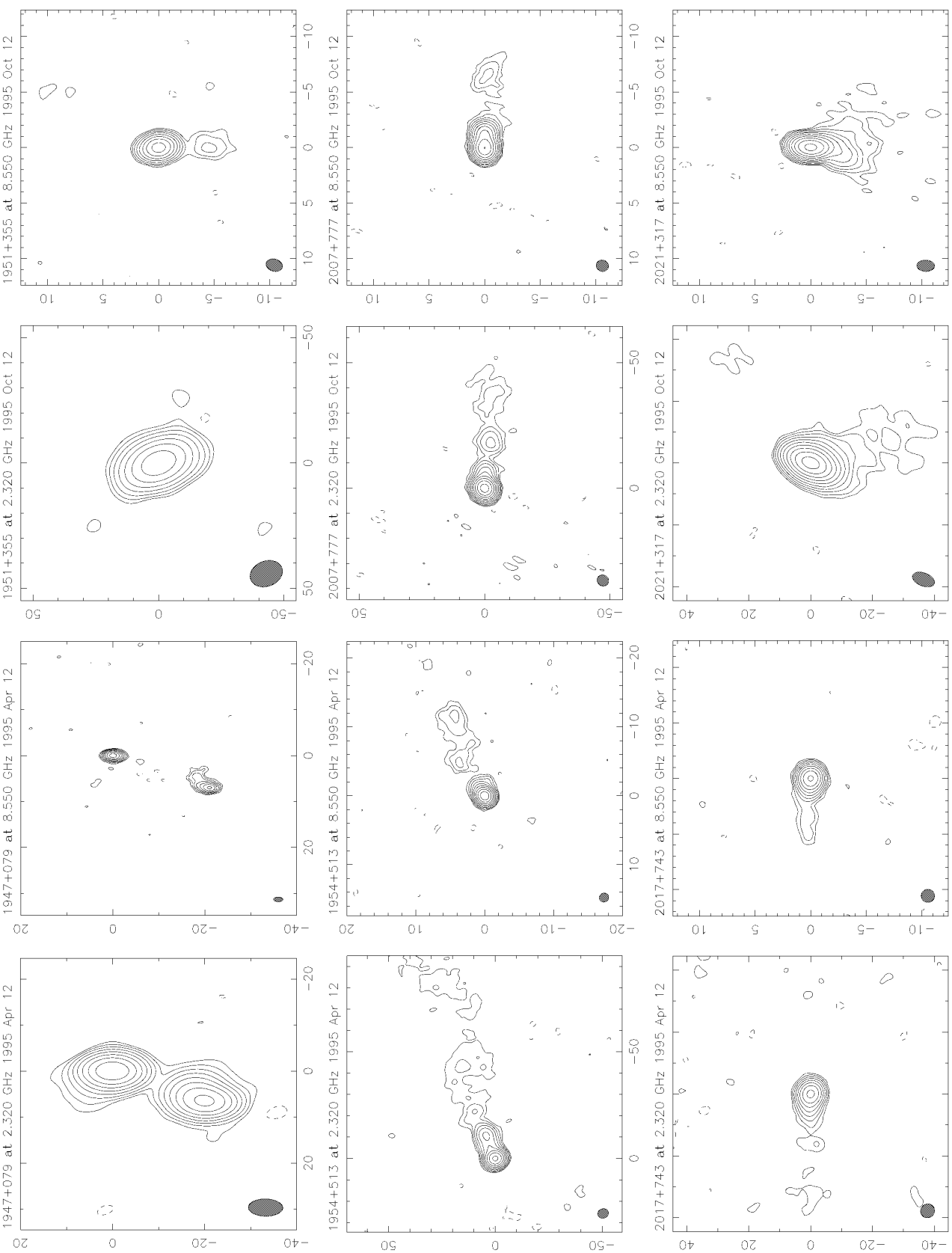

FIG. 1—*Continued*

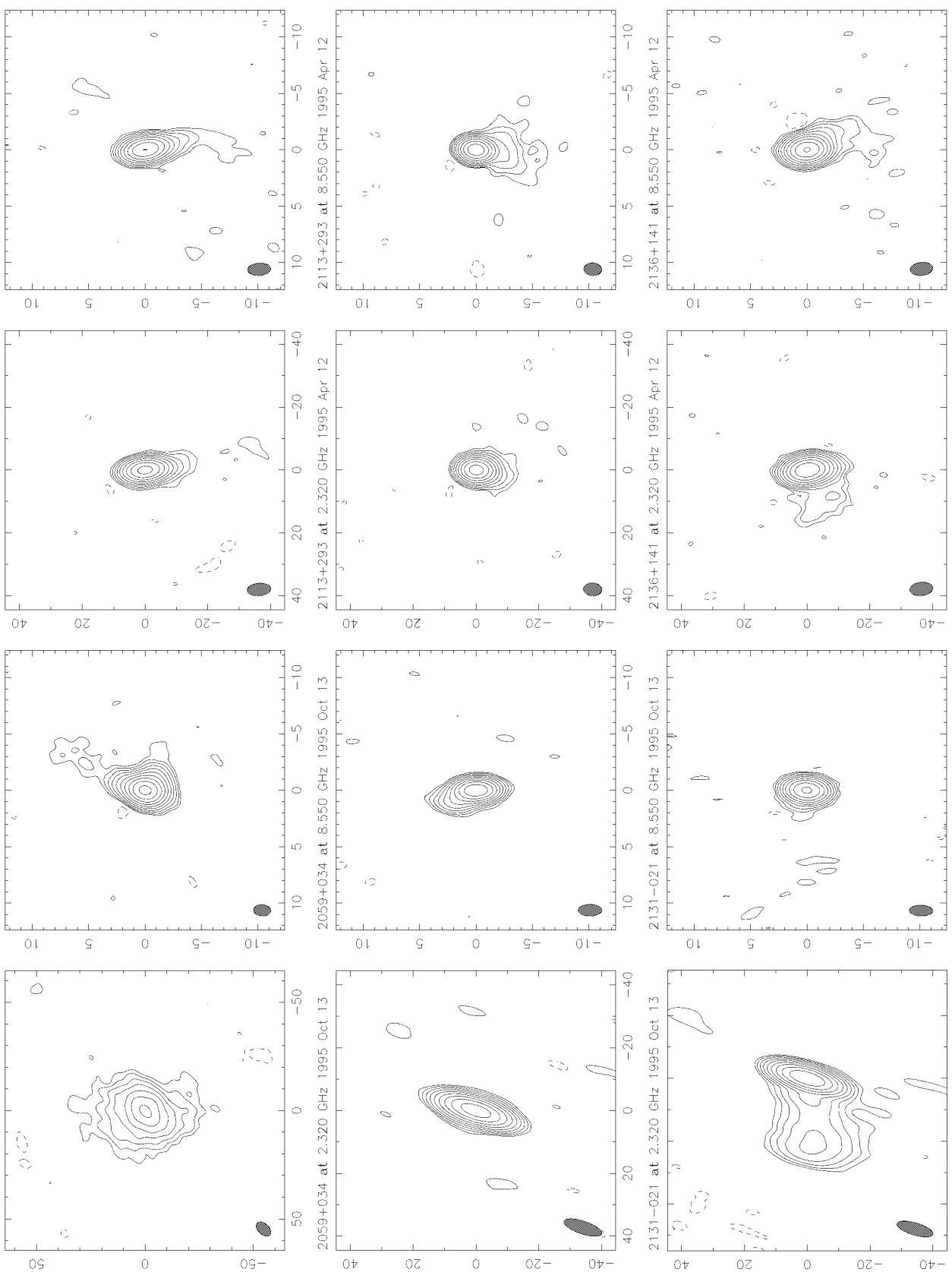

FIG. 1—*Continued*

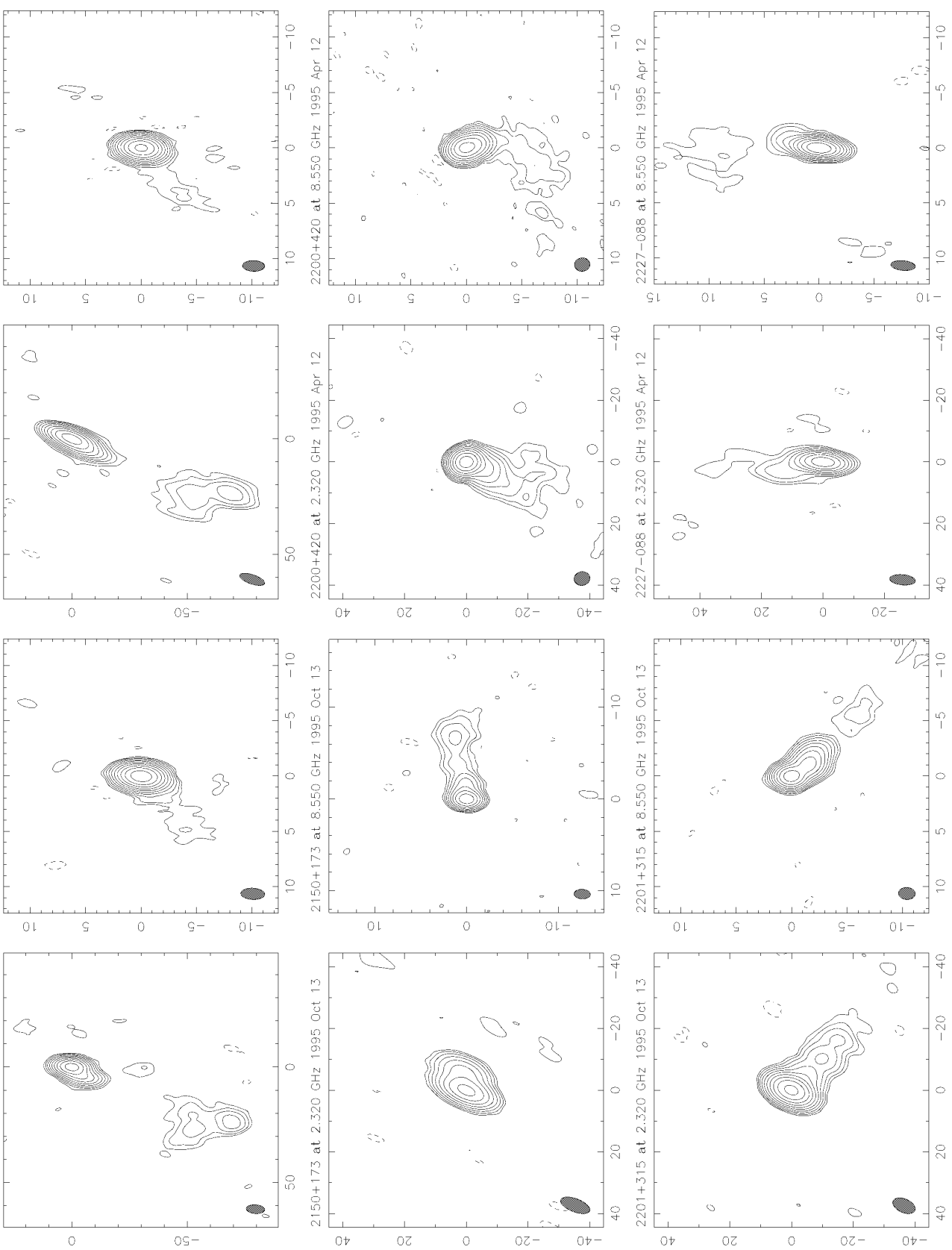

FIG. 1—*Continued*

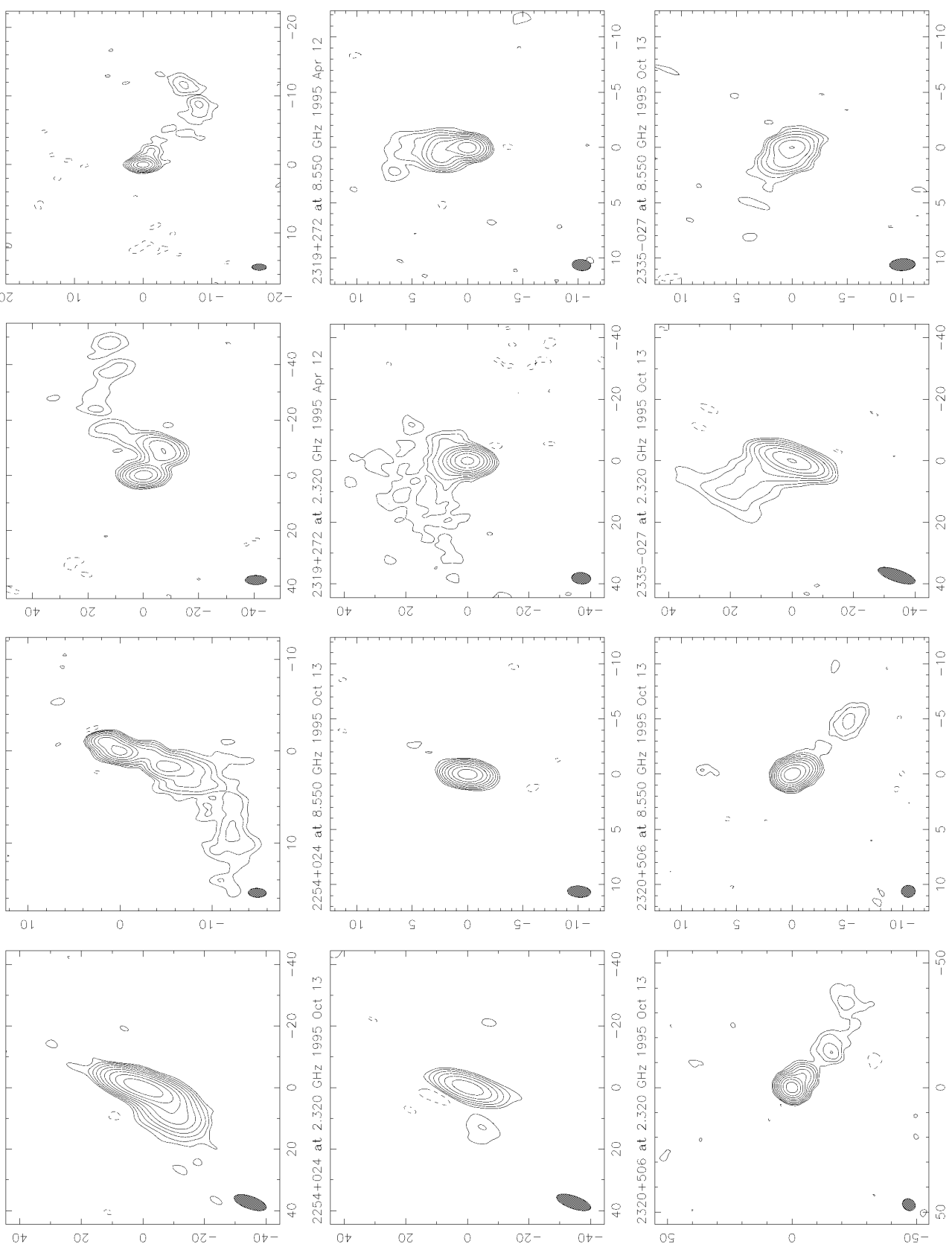

FIG. 1—*Continued*

TABLE 1

PARAMETERS OF NATURALLY WEIGHTED IMAGES

SOURCE	ν (GHz)	BEAM[a] a (mas)	b (mas)	ϕ (deg)	PEAK (Jy beam^{-1})	rms[b] (mJy beam^{-1})	CONTOUR LEVELS[c] (mJy beam^{-1})
0003−066	2.32	13.5	4.0	−15	2.30	1.5	$4.5 \times (1, \ldots, 2^8)$
	8.55	2.3	1.0	−1	1.62	1.2	$3.7 \times (1, \ldots, 2^8)$
0010+405	2.32	5.3	3.7	−5	0.40	0.9	$2.4 \times (1, \ldots, 2^7)$
	8.55	1.4	1.0	−5	0.57	0.8	$2.0 \times (1, \ldots, 2^8)$
0016+731	2.32	5.5	4.7	29	1.61	0.8	$2.5 \times (1, \ldots, 2^9)$
	8.55	1.3	1.2	24	0.88	0.6	$1.8 \times (1, \ldots, 2^8)$
0026+346	2.32	6.0	3.9	−7	0.86	0.9	$2.8 \times (1, \ldots, 2^8)$
	8.55	1.9	1.5	9	0.28	0.8	$2.3 \times (1, \ldots, 2^6)$
0059+581	2.32	5.5	4.8	2	1.05	1.0	$2.6 \times (1, \ldots, 2^8)$
	8.55	1.3	1.1	15	1.19	0.6	$1.9 \times (1, \ldots, 2^9)$
0108+388	2.32	5.6	3.8	−2	0.62	1.2	$3.7 \times (1, \ldots, 2^7)$
	8.55	1.5	1.0	−2	0.33	0.8	$2.4 \times (1, \ldots, 2^7)$
0116+319	2.32	10.4	9.8	24	0.44	0.9	$2.8 \times (1, \ldots, 2^7)$
	8.55	8.4	7.2	−75	0.22	4.1	$9.5 \times (1, \ldots, 2^4)$
0119+115	2.32	11.3	4.1	−19	0.97	0.8	$2.1 \times (1, \ldots, 2^8)$
	8.55	2.1	1.0	−3	0.87	0.7	$2.2 \times (1, \ldots, 2^8)$
0138−097	2.32	12.6	4.2	−15	0.50	1.2	$2.4 \times (1, \ldots, 2^7)$
	8.55	2.2	1.0	1	0.33	0.7	$1.7 \times (1, \ldots, 2^7)$
0153+744	2.32	4.7	4.1	−78	1.34	0.9	$2.7 \times (1, \ldots, 2^8)$
	8.55	1.5	1.1	−86	0.32	0.7	$2.0 \times (1, \ldots, 2^7)$
0201+113	2.32	11.7	4.4	−14	0.90	1.2	$2.9 \times (1, \ldots, 2^8)$
	8.55	2.0	1.0	5	0.58	0.7	$1.8 \times (1, \ldots, 2^8)$
0215+015	2.32	12.1	4.3	−19	0.73	0.9	$2.2 \times (1, \ldots, 2^8)$
	8.55	2.1	1.1	−4	1.26	0.7	$2.1 \times (1, \ldots, 2^9)$
0221+067	2.32	11.8	4.1	−19	0.41	1.1	$2.7 \times (1, \ldots, 2^7)$
	8.55	2.0	1.0	−2	0.63	0.7	$2.0 \times (1, \ldots, 2^8)$
0229+131	2.32	7.4	3.6	−2	1.44	1.7	$3.4 \times (1, \ldots, 2^8)$
	8.55	2.0	1.0	−1	1.10	0.9	$2.9 \times (1, \ldots, 2^8)$
0237+040	2.32	12.1	4.0	−19	0.81	1.1	$2.6 \times (1, \ldots, 2^8)$
	8.55	2.0	1.0	−3	0.56	0.7	$1.9 \times (1, \ldots, 2^8)$
0238−084	2.32	9.0	3.8	−1	0.77	1.3	$3.8 \times (1, \ldots, 2^7)$
	8.55	2.5	1.0	−2	1.15	1.2	$3.7 \times (1, \ldots, 2^8)$
0259+121	2.32	7.3	3.6	−1	0.63	1.0	$2.3 \times (1, \ldots, 2^8)$
	8.55	2.0	1.2	−2	0.24	1.0	$2.4 \times (1, \ldots, 2^6)$
0302+625	2.32	5.3	4.9	63	0.41	0.8	$2.0 \times (1, \ldots, 2^7)$
	8.55	1.2	1.1	23	0.22	0.5	$1.4 \times (1, \ldots, 2^7)$
0317+188	2.32	10.0	4.5	−21	0.64	0.9	$2.4 \times (1, \ldots, 2^8)$
	8.55	1.8	1.1	−2	0.40	0.6	$1.7 \times (1, \ldots, 2^7)$
0334+014	2.32	15.5	8.7	30	0.25	2.5	$6.9 \times (1, \ldots, 2^5)$
	8.55	2.4	1.4	14	0.14	3.8	$11.5 \times (1, \ldots, 2^3)$
0341+158	2.32	10.6	4.5	−20	0.31	1.0	$2.2 \times (1, \ldots, 2^7)$
	8.55	2.2	1.3	14	0.18	0.8	$2.0 \times (1, \ldots, 2^6)$
0400+258	2.32	6.7	3.7	−4	0.62	0.9	$2.7 \times (1, \ldots, 2^7)$
	8.55	1.8	1.0	−4	0.41	0.8	$2.3 \times (1, \ldots, 2^7)$
0406+121	2.32	11.4	4.4	−13	0.70	1.1	$2.2 \times (1, \ldots, 2^8)$
	8.55	2.1	1.0	7	0.57	0.8	$2.0 \times (1, \ldots, 2^8)$
0422+004	2.32	8.1	3.9	−3	0.70	1.1	$3.3 \times (1, \ldots, 2^7)$
	8.55	2.2	1.1	−3	0.61	0.9	$2.6 \times (1, \ldots, 2^7)$
0425+048	2.32	11.8	4.8	−13	0.26	1.4	$3.4 \times (1, \ldots, 2^6)$
	8.55	2.2	1.1	10	0.24	0.8	$2.0 \times (1, \ldots, 2^6)$
0440+345	2.32	5.9	3.7	2	1.01	0.8	$1.9 \times (1, \ldots, 2^9)$
	8.55	1.6	1.0	2	0.63	0.7	$2.2 \times (1, \ldots, 2^8)$
0440−003	2.32	12.2	5.2	−12	2.09	1.4	$3.4 \times (1, \ldots, 2^9)$
	8.55	2.3	1.1	11	1.01	0.7	$1.9 \times (1, \ldots, 2^9)$
0458+138	2.32	9.9	4.9	−20	0.27	1.0	$2.5 \times (1, \ldots, 2^6)$
	8.55	1.9	1.1	5	0.30	0.8	$2.1 \times (1, \ldots, 2^7)$
0459+060	2.32	7.7	3.4	−3	0.87	1.1	$3.1 \times (1, \ldots, 2^8)$
	8.55	2.1	0.9	−3	0.47	1.0	$2.8 \times (1, \ldots, 2^7)$
0507+179	2.32	6.7	4.2	−4	0.52	1.0	$2.4 \times (1, \ldots, 2^7)$
	8.55	1.8	1.1	−4	0.50	0.9	$2.3 \times (1, \ldots, 2^7)$
0518+165	2.32	9.8	5.0	−20	0.35	14.4	$38.8 \times (1, \ldots, 2^3)$
	8.55	2.0	1.1	8	0.15	1.5	$3.5 \times (1, \ldots, 2^5)$
0536+145	2.32	10.3	5.9	−32	0.51	1.5	$3.7 \times (1, \ldots, 2^7)$
	8.55	1.8	1.5	5	0.46	1.0	$2.4 \times (1, \ldots, 2^7)$
0539−057	2.32	9.1	4.2	−1	0.65	1.2	$3.0 \times (1, \ldots, 2^7)$
	8.55	2.5	1.0	−4	0.89	1.2	$3.6 \times (1, \ldots, 2^7)$
0544+273	2.32	8.3	4.8	−38	0.38	1.1	$2.8 \times (1, \ldots, 2^7)$
	8.55	1.6	1.3	−26	0.77	0.8	$2.2 \times (1, \ldots, 2^8)$
0552+398[d]	2.32	5.7	4.0	−13	3.88	2.1	$6.2 \times (1, \ldots, 2^9)$
	8.55	1.6	1.1	−13	4.41	2.0	$5.9 \times (1, \ldots, 2^9)$

TABLE 1—*Continued*

Source	ν (GHz)	Beam[a] a (mas)	b (mas)	ϕ (deg)	Peak (Jy beam^{-1})	rms[b] (mJy beam^{-1})	Contour Levels[c] (mJy beam^{-1})
0552+398[e]	2.32	7.4	4.9	−42	3.83	1.3	$4.0 \times (1, \ldots, 2^9)$
	8.55	1.4	1.3	19	4.34	1.5	$4.8 \times (1, \ldots, 2^9)$
0600+177	2.32	6.7	3.8	−2	0.48	1.1	$3.2 \times (1, \ldots, 2^7)$
	8.55	1.8	1.1	−2	0.35	1.0	$2.7 \times (1, \ldots, 2^6)$
0609+607	2.32	7.0	4.7	−89	0.89	0.9	$2.3 \times (1, \ldots, 2^8)$
	8.55	1.5	1.1	88	0.33	0.5	$1.5 \times (1, \ldots, 2^7)$
0636+680	2.32	4.7	4.4	3	0.41	0.7	$1.8 \times (1, \ldots, 2^7)$
	8.55	1.3	1.2	5	0.32	0.6	$1.5 \times (1, \ldots, 2^7)$
0642+449	2.32	6.8	5.0	−62	0.74	1.0	$3.0 \times (1, \ldots, 2^7)$
	8.55	1.4	1.3	−38	1.78	0.7	$2.1 \times (1, \ldots, 2^9)$
0657+172	2.32	9.6	5.0	−28	0.63	0.9	$2.4 \times (1, \ldots, 2^8)$
	8.55	1.7	1.3	1	0.77	0.7	$1.9 \times (1, \ldots, 2^8)$
0707+476	2.32	4.9	4.3	−29	0.79	0.9	$2.3 \times (1, \ldots, 2^8)$
	8.55	1.3	1.2	−27	0.75	0.8	$1.9 \times (1, \ldots, 2^8)$
0718+793	2.32	5.7	4.3	−55	0.75	0.8	$2.1 \times (1, \ldots, 2^8)$
	8.55	1.4	1.0	−56	0.57	0.6	$1.5 \times (1, \ldots, 2^8)$
0723−008	2.32	8.0	3.5	1	0.97	1.4	$4.2 \times (1, \ldots, 2^7)$
	8.55	2.2	1.0	1	0.69	1.4	$4.2 \times (1, \ldots, 2^7)$
0727−115[d]	2.32	9.2	3.6	0	3.27	1.6	$4.8 \times (1, \ldots, 2^9)$
	8.55	2.5	1.0	0	2.75	1.9	$5.6 \times (1, \ldots, 2^8)$
0727−115[e]	2.32	15.2	5.2	−9	3.01	1.5	$3.7 \times (1, \ldots, 2^9)$
	8.55	2.7	1.1	11	2.05	1.6	$4.7 \times (1, \ldots, 2^8)$
0742+103	2.32	7.4	3.6	−1	4.11	2.2	$6.7 \times (1, \ldots, 2^9)$
	8.55	2.0	1.0	−1	1.21	1.1	$3.2 \times (1, \ldots, 2^8)$
0743−006	2.32	13.5	4.9	−14	1.23	1.2	$3.3 \times (1, \ldots, 2^8)$
	8.55	2.4	1.1	10	1.57	1.0	$2.9 \times (1, \ldots, 2^9)$
0749+540	2.32	4.7	4.3	22	1.13	0.9	$2.7 \times (1, \ldots, 2^8)$
	8.55	1.3	1.2	19	1.00	0.8	$2.4 \times (1, \ldots, 2^8)$
0805−077	2.32	14.2	4.0	−15	0.99	1.4	$3.8 \times (1, \ldots, 2^8)$
	8.55	2.3	1.0	−2	0.48	1.2	$3.3 \times (1, \ldots, 2^7)$
0808+019	2.32	8.1	3.8	−4	0.78	1.0	$2.4 \times (1, \ldots, 2^8)$
	8.55	2.2	1.0	−4	1.06	0.9	$2.5 \times (1, \ldots, 2^8)$
0820+560	2.32	6.0	4.3	−34	1.09	1.0	$2.4 \times (1, \ldots, 2^8)$
	8.55	1.3	1.1	−19	0.66	0.6	$1.7 \times (1, \ldots, 2^8)$
0823+033	2.32	8.0	3.4	−4	1.50	1.2	$3.7 \times (1, \ldots, 2^8)$
	8.55	2.2	0.9	−4	0.92	1.2	$3.7 \times (1, \ldots, 2^7)$
0831+557	2.32	5.6	4.4	−35	2.98	2.4	$7.1 \times (1, \ldots, 2^8)$
	8.55	2.0	1.9	−64	0.41	1.8	$5.5 \times (1, \ldots, 2^6)$
0833+585	2.32	4.9	4.2	−41	0.70	0.8	$2.5 \times (1, \ldots, 2^8)$
	8.55	1.4	1.2	−63	0.27	0.8	$2.5 \times (1, \ldots, 2^6)$
0851+202[d]	2.32	6.8	3.6	−7	1.47	1.1	$3.3 \times (1, \ldots, 2^8)$
	8.55	1.9	1.0	−7	0.89	1.1	$3.4 \times (1, \ldots, 2^8)$
0851+202[e]	2.32	9.4	4.2	−28	1.21	1.0	$2.5 \times (1, \ldots, 2^8)$
	8.55	1.7	1.0	−10	1.56	0.7	$1.9 \times (1, \ldots, 2^9)$
0859+470	2.32	5.1	4.0	−11	0.74	1.1	$2.9 \times (1, \ldots, 2^8)$
	8.55	1.4	1.1	−11	0.44	0.8	$2.1 \times (1, \ldots, 2^7)$
0912+297	2.32	7.7	4.0	−26	0.20	1.4	$3.5 \times (1, \ldots, 2^5)$
	8.55	1.6	1.0	−8	0.17	0.8	$2.1 \times (1, \ldots, 2^6)$
0917+624	2.32	4.6	4.3	−88	1.34	1.2	$3.7 \times (1, \ldots, 2^8)$
	8.55	1.3	1.2	89	1.34	0.8	$2.2 \times (1, \ldots, 2^9)$
0945+408	2.32	7.0	3.9	−17	1.25	1.1	$2.7 \times (1, \ldots, 2^8)$
	8.55	1.5	0.9	3	1.12	1.1	$3.2 \times (1, \ldots, 2^8)$
0955+476	2.32	6.8	3.9	−21	1.10	0.8	$2.1 \times (1, \ldots, 2^9)$
	8.55	1.5	1.0	−7	1.00	0.6	$1.8 \times (1, \ldots, 2^9)$
1004+141	2.32	7.4	3.7	−0	0.60	1.0	$2.8 \times (1, \ldots, 2^7)$
	8.55	2.0	1.0	−0	0.76	1.2	$3.0 \times (1, \ldots, 2^8)$
1020+400	2.32	8.1	4.0	−25	0.68	0.9	$2.3 \times (1, \ldots, 2^8)$
	8.55	1.6	1.0	−8	0.84	0.7	$1.9 \times (1, \ldots, 2^8)$
1022+194	2.32	6.7	3.9	−2	0.35	0.9	$2.8 \times (1, \ldots, 2^6)$
	8.55	1.8	1.1	−3	0.52	0.8	$1.9 \times (1, \ldots, 2^8)$
1038+064	2.32	11.9	3.9	−18	1.44	1.1	$2.6 \times (1, \ldots, 2^9)$
	8.55	2.0	0.9	−1	0.94	0.7	$2.0 \times (1, \ldots, 2^8)$
1049+215	2.32	6.6	3.8	−3	1.09	1.2	$2.9 \times (1, \ldots, 2^8)$
	8.55	1.8	1.0	−3	1.15	1.2	$3.5 \times (1, \ldots, 2^8)$
1053+815	2.32	5.0	4.3	−1	0.26	0.8	$2.1 \times (1, \ldots, 2^6)$
	8.55	1.2	1.0	−11	0.40	0.5	$1.3 \times (1, \ldots, 2^8)$
1116+128	2.32	7.2	3.7	0	1.12	1.3	$3.8 \times (1, \ldots, 2^8)$
	8.55	2.0	1.0	1	0.71	1.5	$4.6 \times (1, \ldots, 2^7)$
1117+146	2.32	11.6	7.8	−13	0.51	4.2	$10.6 \times (1, \ldots, 2^5)$
	8.55	8.9	5.9	21	0.20	6.7	$20.2 \times (1, \ldots, 2^3)$

TABLE 1—*Continued*

Source	ν (GHz)	Beam[a] a (mas)	b (mas)	ϕ (deg)	Peak (Jy beam^{-1})	rms[b] (mJy beam^{-1})	Contour Levels[c] (mJy beam^{-1})
1130+009	2.32	7.9	3.6	−1	0.32	1.1	$2.8 \times (1, \ldots, 2^6)$
	8.55	2.1	1.0	−1	0.21	1.1	$3.3 \times (1, \ldots, 2^6)$
1145−071	2.32	12.0	4.2	−15	0.70	0.9	$2.4 \times (1, \ldots, 2^8)$
	8.55	2.3	1.0	−2	0.45	0.6	$1.7 \times (1, \ldots, 2^8)$
1150+812	2.32	4.1	4.0	−41	1.24	0.9	$2.8 \times (1, \ldots, 2^8)$
	8.55	1.1	1.1	−27	0.89	0.6	$1.7 \times (1, \ldots, 2^9)$
1156−094	2.32	13.0	4.0	−14	0.25	2.1	$5.3 \times (1, \ldots, 2^5)$
	8.55	2.2	1.0	1	0.21	0.8	$2.4 \times (1, \ldots, 2^6)$
1213+350	2.32	5.5	4.3	−6	0.86	1.1	$3.1 \times (1, \ldots, 2^8)$
	8.55	1.5	1.2	−8	0.32	1.0	$2.9 \times (1, \ldots, 2^6)$
1219+044	2.32	11.8	4.0	−18	0.69	1.1	$2.8 \times (1, \ldots, 2^7)$
	8.55	2.0	1.0	−2	0.67	0.7	$1.9 \times (1, \ldots, 2^8)$
1221+809	2.32	4.4	3.9	−52	0.32	0.7	$2.0 \times (1, \ldots, 2^7)$
	8.55	1.2	1.0	−52	0.42	0.6	$1.5 \times (1, \ldots, 2^8)$
1226+373	2.32	6.5	4.2	−27	0.47	0.8	$2.1 \times (1, \ldots, 2^7)$
	8.55	1.4	1.0	−8	0.27	0.6	$1.7 \times (1, \ldots, 2^7)$
1236+077	2.32	8.0	3.6	−5	0.57	1.0	$2.7 \times (1, \ldots, 2^7)$
	8.55	2.2	1.0	−6	0.53	1.0	$2.6 \times (1, \ldots, 2^7)$
1307+121	2.32	7.6	3.7	−2	0.72	1.1	$3.3 \times (1, \ldots, 2^7)$
	8.55	2.1	1.0	−2	0.36	0.9	$2.7 \times (1, \ldots, 2^7)$
1315+346	2.32	6.9	4.1	−25	0.28	0.8	$2.1 \times (1, \ldots, 2^7)$
	8.55	1.5	1.0	−5	0.26	0.6	$1.7 \times (1, \ldots, 2^7)$
1342+662	2.32	4.8	4.5	80	0.26	0.8	$2.1 \times (1, \ldots, 2^6)$
	8.55	1.2	1.1	55	0.18	0.5	$1.3 \times (1, \ldots, 2^7)$
1347+539	2.32	4.6	4.3	31	0.43	0.9	$2.2 \times (1, \ldots, 2^7)$
	8.55	1.3	1.2	28	0.32	0.7	$1.9 \times (1, \ldots, 2^7)$
1357+769	2.32	4.6	4.3	−31	0.66	0.7	$2.0 \times (1, \ldots, 2^8)$
	8.55	1.1	1.0	−26	0.63	0.5	$1.3 \times (1, \ldots, 2^8)$
1402+044	2.32	8.0	3.8	−7	0.91	1.0	$2.4 \times (1, \ldots, 2^8)$
	8.55	2.2	1.1	−7	0.70	0.8	$2.2 \times (1, \ldots, 2^8)$
1413+135	2.32	10.1	5.7	−20	0.26	1.8	$4.6 \times (1, \ldots, 2^5)$
	8.55	1.9	1.0	−3	1.38	0.8	$2.3 \times (1, \ldots, 2^9)$
1416+067	2.32	7.0	3.5	−2	0.40	2.4	$5.9 \times (1, \ldots, 2^6)$
	8.55	3.2	2.0	−13	0.19	1.1	$3.2 \times (1, \ldots, 2^5)$
1432+200	2.32	6.4	4.0	−1	0.44	1.0	$2.4 \times (1, \ldots, 2^7)$
	8.55	1.7	1.1	−1	0.32	0.9	$2.1 \times (1, \ldots, 2^7)$
1433+304	2.32	7.9	4.5	−22	0.21	0.8	$2.0 \times (1, \ldots, 2^6)$
	8.55	1.7	1.2	13	0.15	0.8	$2.0 \times (1, \ldots, 2^6)$
1458+718	2.32	5.0	4.1	61	0.96	1.6	$4.1 \times (1, \ldots, 2^7)$
	8.55	1.4	1.1	61	0.85	0.9	$2.6 \times (1, \ldots, 2^8)$
1459+480	2.32	5.7	4.4	−29	0.32	0.8	$1.9 \times (1, \ldots, 2^7)$
	8.55	1.3	1.1	3	0.49	0.5	$1.4 \times (1, \ldots, 2^8)$
1510−089	2.32	8.7	3.6	−3	3.07	1.6	$4.8 \times (1, \ldots, 2^9)$
	8.55	2.4	1.0	−3	1.87	1.6	$4.9 \times (1, \ldots, 2^8)$
1532+016	2.32	12.0	3.8	−17	1.08	0.9	$2.2 \times (1, \ldots, 2^8)$
	8.55	2.1	1.0	−1	0.42	0.8	$2.4 \times (1, \ldots, 2^7)$
1546+027	2.32	8.3	4.1	−6	1.14	1.3	$3.8 \times (1, \ldots, 2^8)$
	8.55	2.3	1.1	−6	1.09	1.2	$3.4 \times (1, \ldots, 2^8)$
1600+335	2.32	8.0	4.0	−24	2.17	1.7	$4.4 \times (1, \ldots, 2^8)$
	8.55	1.5	1.0	−8	0.73	0.9	$2.6 \times (1, \ldots, 2^8)$
1607+268	2.32	6.9	3.7	−8	1.42	1.9	$5.7 \times (1, \ldots, 2^7)$
	8.55	1.9	1.0	−8	0.23	0.8	$2.5 \times (1, \ldots, 2^6)$
1624+416	2.32	6.8	4.2	−25	1.12	0.9	$2.1 \times (1, \ldots, 2^9)$
	8.55	1.4	1.0	−7	0.33	0.6	$1.6 \times (1, \ldots, 2^7)$
1633+382	2.32	6.1	3.8	−7	2.37	1.2	$3.7 \times (1, \ldots, 2^9)$
	8.55	1.6	1.1	−6	1.10	1.5	$4.8 \times (1, \ldots, 2^7)$
1642+690	2.32	4.9	4.6	12	0.97	0.9	$2.4 \times (1, \ldots, 2^8)$
	8.55	1.3	1.1	−14	0.61	0.5	$1.6 \times (1, \ldots, 2^8)$
1652+398	2.32	4.9	4.6	19	0.72	1.7	$4.2 \times (1, \ldots, 2^7)$
	8.55	1.3	1.3	19	0.53	1.1	$2.8 \times (1, \ldots, 2^7)$
1705+018	2.32	12.6	4.1	−18	0.62	1.0	$2.1 \times (1, \ldots, 2^8)$
	8.55	2.2	1.0	−5	0.47	0.7	$2.0 \times (1, \ldots, 2^7)$
1705+456	2.32	4.9	4.6	−68	0.33	1.0	$2.4 \times (1, \ldots, 2^7)$
	8.55	1.3	1.3	−67	0.27	1.0	$2.7 \times (1, \ldots, 2^6)$
1725+044	2.32	7.7	3.5	−1	0.84	1.3	$3.9 \times (1, \ldots, 2^7)$
	8.55	2.1	1.0	−1	0.51	0.9	$2.5 \times (1, \ldots, 2^7)$
1738+476	2.32	5.9	4.4	−27	1.03	0.9	$2.2 \times (1, \ldots, 2^8)$
	8.55	1.3	1.0	−0	0.78	0.6	$1.6 \times (1, \ldots, 2^8)$
1741−038	2.32	13.3	4.0	−18	1.75	1.2	$3.1 \times (1, \ldots, 2^9)$
	8.55	2.3	1.0	−7	3.20	0.9	$3.0 \times (1, \ldots, 2^{10})$

TABLE 1—*Continued*

Source	ν (GHz)	Beam[a] a (mas)	Beam[a] b (mas)	Beam[a] ϕ (deg)	Peak (Jy beam^{-1})	rms[b] (mJy beam^{-1})	Contour Levels[c] (mJy beam^{-1})
1743+173	2.32	7.2	3.7	−6	0.98	1.0	$3.0 \times (1, \ldots, 2^8)$
	8.55	2.0	1.0	−6	0.66	0.9	$2.5 \times (1, \ldots, 2^8)$
1749+096[d]	2.32	7.4	3.7	−2	1.47	1.0	$3.1 \times (1, \ldots, 2^8)$
	8.55	2.0	1.0	−4	3.91	1.4	$4.5 \times (1, \ldots, 2^9)$
1749+096[e]	2.32	10.7	4.0	−20	1.42	1.1	$2.8 \times (1, \ldots, 2^8)$
	8.55	1.9	1.0	−2	3.66	1.1	$3.5 \times (1, \ldots, 2^{10})$
1751+288	2.32	6.5	3.8	3	0.47	1.1	$2.6 \times (1, \ldots, 2^7)$
	8.55	1.8	1.0	3	0.32	0.9	$2.8 \times (1, \ldots, 2^6)$
1823+568	2.32	5.3	4.7	−11	0.81	1.0	$2.4 \times (1, \ldots, 2^8)$
	8.55	1.3	1.1	9	1.46	0.7	$2.0 \times (1, \ldots, 2^9)$
1842+681	2.32	5.0	4.8	−8	0.72	0.8	$2.2 \times (1, \ldots, 2^8)$
	8.55	1.2	1.1	6	0.58	0.5	$1.4 \times (1, \ldots, 2^8)$
1849+670	2.32	4.7	4.5	−3	0.41	0.7	$1.8 \times (1, \ldots, 2^7)$
	8.55	1.3	1.2	−2	0.80	0.6	$1.6 \times (1, \ldots, 2^8)$
1929+226	2.32	6.7	4.0	8	0.45	0.7	$1.8 \times (1, \ldots, 2^7)$
	8.55	1.8	1.1	8	0.41	0.6	$1.7 \times (1, \ldots, 2^7)$
1932+204	2.32	9.9	4.1	−17	0.47	1.0	$2.6 \times (1, \ldots, 2^7)$
	8.55	1.8	1.0	1	0.39	0.7	$2.0 \times (1, \ldots, 2^7)$
1947+079	2.32	7.5	3.8	−1	0.81	1.1	$3.4 \times (1, \ldots, 2^7)$
	8.55	2.1	1.0	−1	0.41	0.7	$2.2 \times (1, \ldots, 2^7)$
1951+355	2.32	13.3	10.1	21	0.35	1.3	$3.3 \times (1, \ldots, 2^6)$
	8.55	1.5	1.1	−15	0.24	0.6	$1.3 \times (1, \ldots, 2^7)$
1954+513	2.32	5.1	4.4	16	1.00	1.3	$3.3 \times (1, \ldots, 2^8)$
	8.55	1.4	1.3	15	1.00	0.9	$2.4 \times (1, \ldots, 2^8)$
2007+777	2.32	4.8	4.4	−29	1.64	0.8	$2.3 \times (1, \ldots, 2^9)$
	8.55	1.1	1.0	−20	0.98	0.6	$1.9 \times (1, \ldots, 2^9)$
2017+743	2.32	4.6	4.4	45	0.29	0.7	$1.8 \times (1, \ldots, 2^7)$
	8.55	1.2	1.2	−8	0.44	0.6	$1.5 \times (1, \ldots, 2^8)$
2021+317	2.32	7.5	4.2	−21	2.33	1.2	$3.3 \times (1, \ldots, 2^9)$
	8.55	1.6	1.0	−2	1.57	0.8	$2.4 \times (1, \ldots, 2^9)$
2023+336	2.32	8.0	5.0	−44	0.49	2.6	$6.4 \times (1, \ldots, 2^6)$
	8.55	1.5	1.0	−3	1.65	0.9	$2.5 \times (1, \ldots, 2^9)$
2029+121	2.32	7.6	4.0	5	0.93	1.1	$2.8 \times (1, \ldots, 2^8)$
	8.55	2.1	1.1	4	0.67	0.9	$2.6 \times (1, \ldots, 2^8)$
2059+034	2.32	12.7	4.1	−18	0.86	0.9	$2.2 \times (1, \ldots, 2^8)$
	8.55	2.1	1.0	0	0.80	0.6	$1.6 \times (1, \ldots, 2^8)$
2113+293	2.32	5.9	4.1	−4	0.94	0.8	$2.5 \times (1, \ldots, 2^8)$
	8.55	1.6	1.1	−4	0.88	0.7	$2.0 \times (1, \ldots, 2^8)$
2131−021	2.32	11.9	3.9	−17	1.42	1.2	$2.9 \times (1, \ldots, 2^8)$
	8.55	2.1	1.0	−2	1.01	1.3	$3.4 \times (1, \ldots, 2^8)$
2136+141	2.32	7.4	4.3	6	1.37	0.9	$2.7 \times (1, \ldots, 2^8)$
	8.55	2.0	1.2	6	1.99	1.1	$3.6 \times (1, \ldots, 2^9)$
2145+067[d]	2.32	8.0	3.9	−4	2.50	2.2	$6.7 \times (1, \ldots, 2^8)$
	8.55	2.2	1.0	−3	8.44	3.1	$9.8 \times (1, \ldots, 2^9)$
2145+067[e]	2.32	11.4	4.1	−19	2.61	2.2	$6.7 \times (1, \ldots, 2^8)$
	8.55	2.0	1.0	−2	7.37	3.6	$11.5 \times (1, \ldots, 2^9)$
2150+173	2.32	10.1	4.3	−21	0.43	1.1	$2.6 \times (1, \ldots, 2^7)$
	8.55	1.8	1.1	−3	0.35	0.6	$1.6 \times (1, \ldots, 2^7)$
2200+420	2.32	5.2	4.5	9	3.23	1.3	$4.0 \times (1, \ldots, 2^9)$
	8.55	1.4	1.2	7	2.17	1.9	$6.0 \times (1, \ldots, 2^8)$
2201+315	2.32	7.7	4.5	−24	1.97	1.1	$3.0 \times (1, \ldots, 2^9)$
	8.55	1.5	1.1	−4	1.02	0.8	$2.4 \times (1, \ldots, 2^8)$
2227−088	2.32	8.4	3.4	−5	0.81	1.3	$3.8 \times (1, \ldots, 2^7)$
	8.55	2.2	0.9	−5	1.60	1.2	$3.2 \times (1, \ldots, 2^8)$
2230+114	2.32	11.0	4.1	−19	4.21	3.1	$9.2 \times (1, \ldots, 2^8)$
	8.55	2.0	1.0	−2	1.02	1.7	$5.4 \times (1, \ldots, 2^7)$
2252−089	2.32	7.8	3.4	−0	0.37	1.4	$3.6 \times (1, \ldots, 2^6)$
	8.55	2.1	0.9	−0	0.30	1.0	$2.8 \times (1, \ldots, 2^6)$
2254+024	2.32	11.7	4.1	−19	0.20	1.3	$3.6 \times (1, \ldots, 2^5)$
	8.55	2.1	1.0	−4	0.32	0.6	$1.6 \times (1, \ldots, 2^7)$
2319+272	2.32	6.3	3.8	−5	0.68	0.8	$2.1 \times (1, \ldots, 2^8)$
	8.55	1.7	1.0	−5	0.38	0.6	$1.7 \times (1, \ldots, 2^7)$
2320+506	2.32	5.4	4.6	−34	1.21	1.0	$2.8 \times (1, \ldots, 2^8)$
	8.55	1.3	1.1	2	0.94	0.7	$2.0 \times (1, \ldots, 2^8)$
2335−027	2.32	12.7	3.9	−19	0.35	1.1	$2.6 \times (1, \ldots, 2^7)$
	8.55	2.3	1.1	3	0.18	1.0	$2.8 \times (1, \ldots, 2^6)$

[a] The restoring beam is an elliptical Gaussian with FWHM major axis a and minor axis b, with the major axis in position angle ϕ (measured north through east).

[b] The rms of the residuals of the final hybrid image.

[c] Contours levels are represented by the geometric series $1, \ldots, 2^n$, e.g., for $n = 5$, the contour levels would be $\pm 1, 2, 4, 8, 16, 32$.

[d] Epoch 1995 April 12–13.

[e] Epoch 1995 October 12–13.

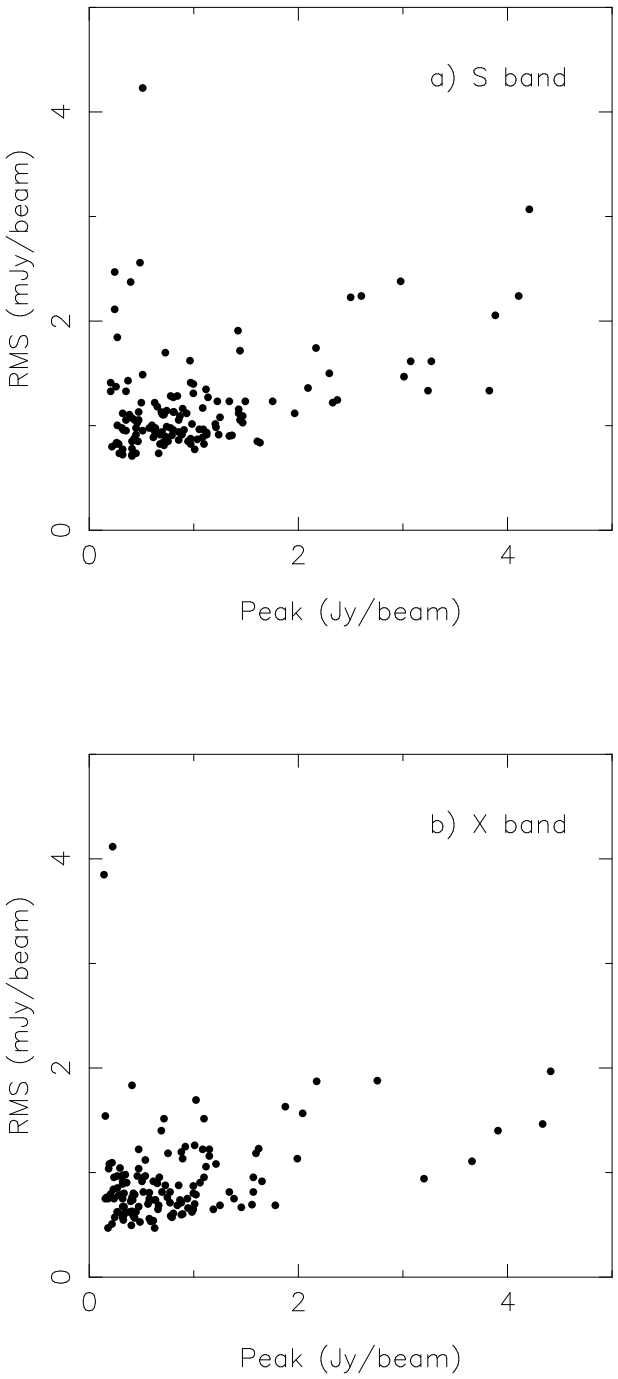

FIG. 2.—The rms noise plotted against the peak of the images for most sources at (*a*) the *S* band and (*b*) the *X* band.

model satisfactorily with the available data. The sources 0831+557, 2021+317, and 2023+336 are also too complex to model at the *X* band. For these sources, we list in Table 2 only the total integrated flux densities (as measured from the images).

Although the agreement between the fitted models and the data is not as good as that produced by the hybrid images (models with many CLEAN components), an inspection of plots of residuals in the image plane, after subtracting the Gaussian models from the visibility data, revealed that the Gaussian models generally describe the visibility data quite well. However, because of incomplete sampling in the (*u*, *v*)-plane, these models may not be unique. They represent only one *possible* deconvolution of complex source structure. Such deconvolutions can be misleading.

4. DISCUSSION

In this section, we attempt to quantify the expected effects of intrinsic source structure on astrometric bandwidth synthesis VLBI observations. We also define a source "structure index," which can be used as an estimate of the astrometric quality of the observed sources. The analysis described here is based on that of Charlot (1990b).

4.1. *Source Structure Corrections and the Structure Index*

The complex visibility V of a spatially extended source measured by an interferometer with baseline $\boldsymbol{b}$ is given by

$$V(\boldsymbol{b}, \omega, t) = \int_{\Omega_s} I(\boldsymbol{s}, \omega, t) \exp\left(-\frac{i\omega}{c}\,\boldsymbol{b}\cdot\boldsymbol{s}\right) d\Omega\,, \qquad (1)$$

where $I(\boldsymbol{s}, \omega, t)$ is the source brightness distribution that depends on the direction $\boldsymbol{s}$ on the sky, the frequency $\omega = 2\pi c/\lambda$, and time t, while the integration is over the extended source of solid angle Ω_s. If we adopt a reference direction $\boldsymbol{s}_0$ within the source, $\boldsymbol{s}$ can be written as $\boldsymbol{s} = \boldsymbol{s}_0 + \boldsymbol{\sigma}$, where $\boldsymbol{\sigma}$ is in the plane of the sky. The visibility function then can be written as

$$V(\boldsymbol{b}, \omega, t) = \exp\left(-\frac{i\omega}{c}\,\boldsymbol{b}\cdot\boldsymbol{s}_0\right) \times \int_{\Omega_s} I(\boldsymbol{s}_0 + \boldsymbol{\sigma}, \omega, t) \exp\left(-\frac{i\omega}{c}\,\boldsymbol{b}\cdot\boldsymbol{\sigma}\right) d\Omega\,, \qquad (2)$$

which also can be written as

$$\begin{aligned} V &= A \exp\left[i(\phi_g + \phi_s)\right]\,, \\ &= A \exp\left(i\phi_t\right)\,, \end{aligned} \qquad (3)$$

where the total phase ϕ_t is the sum of the geometric phase for the reference direction $\boldsymbol{s}_0$,

$$\phi_g = -\frac{\omega}{c}\,\boldsymbol{b}\cdot\boldsymbol{s}_0\,, \qquad (4)$$

and the additional structure phase introduced by the source brightness distribution,

$$\phi_s = \arg\left[\int_{\Omega_s} I(\boldsymbol{s}_0 + \boldsymbol{\sigma}, \omega, t) \exp\left(-\frac{i\omega}{c}\,\boldsymbol{b}\cdot\boldsymbol{\sigma}\right) d\Omega\right]. \qquad (5)$$

The amplitude A observed by the interferometer is given by

$$A = \left|\int_{\Omega_s} I(\boldsymbol{s}_0 + \boldsymbol{\sigma}, \omega, t) \exp\left(-\frac{i\omega}{c}\,\boldsymbol{b}\cdot\boldsymbol{\sigma}\right) d\Omega\right|. \qquad (6)$$

The VLBI delay observable used in astrometry is defined by the partial derivative of the total phase with respect to frequency. For an extended source, the delay can be written as

$$\begin{aligned} \tau &= \frac{\partial\phi_t}{\partial\omega} = \frac{\partial\phi_g}{\partial\omega} + \frac{\partial\phi_s}{\partial\omega}\,, \\ &= -\frac{1}{c}\,\boldsymbol{b}\cdot\boldsymbol{s}_0 + \tau_s\,, \end{aligned} \qquad (7)$$

TABLE 2

GAUSSIAN MODELS[a]

SOURCE	ν (GHz)	Component	S (Jy)	r (mas)	θ (deg)	a (mas)	b/a	ϕ (deg)	χ^2
0003−066.....	2.32	1	2.27	0.0	...	1.21	1.00	...	1.05
		2	0.55	4.0	−71	3.56	1.00	...	
	8.55	1	1.57	0.0	...	0.54	0.46	2	0.93
		2	0.31	0.8	−37	0.34	1.00	...	
		3	0.21	1.3	−69	0.49	1.00	...	
		4	0.11	2.0	−66	0.56	1.00	...	
		5	0.12	4.3	−72	3.50	1.00	...	
		6	0.04	6.2	−75	1.07	1.00	...	
0010+405.....	2.32	1	0.41	0.0	...	0.92	0.15	−30	0.82
		2	0.02	6.0	−31	3.05	1.00	...	
	8.55	1	0.55	0.0	...	0.40	0.00	−27	0.78
		2	0.09	0.7	−29	0.12	1.00	...	
		3	0.01	1.8	−31	0.54	1.00	...	
0016+731.....	2.32	1	1.53	0.0	...	1.23	0.00	−64	0.98
		2	0.17	1.4	174	2.09	1.00	...	
		3	0.02	9.3	156	11.36	1.00	...	
	8.55	1	0.82	0.0	...	0.47	0.80	−73	1.00
		2	0.25	0.5	−50	0.23	1.00	...	
0026+346.....	2.32	1	0.73	0.0	...	2.12	0.45	47	0.95
		2	0.41	2.2	42	3.07	1.00	...	
		3	0.18	10.5	53	6.97	1.00	...	
		4	0.21	27.5	54	1.84	1.00	...	
		5	0.14	28.7	61	2.95	1.00	...	
		6	0.48	30.2	56	1.83	1.00	...	
	8.55	1	0.40	0.0	...	1.51	0.68	33	0.88
		2	0.23	2.1	43	2.77	0.62	3	
		3	0.05	10.5	51	5.74	1.00	...	
		4	0.09	27.6	54	2.28	0.41	37	
		5	0.05	29.0	58	2.38	1.00	...	
		6	0.10	30.4	56	1.61	0.81	14	
0059+581.....	2.32	1	1.09	0.0	...	1.33	1.00	...	0.88
		2	0.07	2.8	−101	1.21	1.00	...	
		3	0.03	7.6	−100	2.78	1.00	...	
	8.55	1	0.93	0.0	...	0.10	1.00	...	0.95
		2	0.23	0.3	175	0.24	1.00	...	
		3	0.22	0.8	−146	0.76	1.00	...	
		4	0.03	2.5	−116	1.55	1.00	...	
0108+388.....	2.32	1	0.68	0.0	...	1.70	0.43	73	0.83
		2	0.03	5.3	70	1.65	1.00	...	
		3	0.46	5.4	−111	1.85	0.28	−56	
	8.55	1	0.24	0.0	...	0.23	0.91	−68	0.81
		2	0.35	1.0	−109	1.86	0.21	77	
		3	0.08	5.1	−123	0.99	1.00	...	
		4	0.20	5.8	−120	0.59	0.55	−53	
0116+319.....	2.32	1	2.65[b]	...	...	...	...	...	...
	8.55	1	0.31	0.0	...	5.47	1.00	...	0.60
0119+115.....	2.32	1	0.99	0.0	...	1.67	0.00	3	0.95
		2	0.07	13.1	2	3.39	1.00	...	
		3	0.05	21.3	6	5.85	1.00	...	
		4	0.06	28.4	16	6.24	1.00	...	
		5	0.02	36.3	29	7.31	1.00	...	
	8.55	1	0.85	0.0	...	0.53	0.22	11	0.87
		2	0.16	1.3	4	0.16	1.00	...	
		3	0.01	14.1	3	1.11	1.00	...	
0138−097.....	2.32	1	0.42	0.0	...	0.54	1.00	...	1.11
		2	0.12	2.0	−147	0.93	1.00	...	
		3	0.02	9.6	−151	6.32	1.00	...	
	8.55	1	0.37	0.0	...	0.56	0.22	66	1.02
		2	0.05	1.9	−137	1.19	1.00	...	
0153+744.....	2.32	1	1.16	0.0	...	1.29	0.86	6	1.26
		2	0.29	1.8	−57	1.40	1.00	...	
		3	0.54	4.3	16	6.08	0.23	−15	
		4	0.54	10.0	−22	1.97	0.28	−67	
	8.55	1	0.41	0.0	...	1.05	0.28	85	1.02
		2	0.03	7.6	130	2.42	1.00	...	
		3	0.02	9.4	144	1.35	1.00	...	
		4	0.25	10.3	155	1.79	0.51	−63	
0201+113.....	2.32	1	0.92	0.0	...	1.33	0.56	−53	0.87
		2	0.02	23.1	−138	16.26	1.00	...	
	8.55	1	0.58	0.0	...	0.52	0.00	−27	0.86
		2	0.13	1.2	−36	0.89	1.00	...	

TABLE 2—*Continued*

Source	ν (GHz)	Component	S (Jy)	r (mas)	θ (deg)	a (mas)	b/a	ϕ (deg)	χ^2
0215+015.....	2.32	1	0.65	0.0	...	0.49	1.00	...	1.03
		2	0.14	2.4	100	1.65	1.00	...	
		3	0.03	5.5	113	4.96	1.00	...	
		4	0.02	18.5	95	8.71	1.00	...	
	8.55	1	1.26	0.0	...	0.12	1.00	...	0.95
		2	0.03	1.1	112	0.93	1.00	...	
		3	0.06	2.4	100	1.96	1.00	...	
0221+067.....	2.32	1	0.38	0.0	...	0.34	1.00	...	0.92
		2	0.09	4.6	−52	1.84	1.00	...	
		3	0.02	8.6	−57	1.90	1.00	...	
	8.55	1	0.64	0.0	...	0.26	1.00	...	0.96
		2	0.06	0.9	−62	0.75	1.00	...	
		3	0.03	5.4	−56	2.55	1.00	...	
0229+131.....	2.32	1	1.53	0.0	...	1.80	0.00	37	1.00
		2	0.12	6.5	59	6.60	1.00	...	
		3	0.09	26.7	84	12.61	1.00	...	
	8.55	1	0.93	0.0	...	0.36	0.32	−81	0.77
		2	0.34	0.4	63	0.37	1.00	...	
		3	0.06	2.2	37	1.13	1.00	...	
0237+040.....	2.32	1	0.82	0.0	...	0.86	1.00	...	0.96
		2	0.06	6.0	−56	4.70	1.00	...	
	8.55	1	0.57	0.0	...	0.39	0.04	−44	0.92
		2	0.09	1.2	−38	0.33	1.00	...	
		3	0.03	2.1	−53	0.63	1.00	...	
0238−084.....	2.32	1	1.12	0.0	...	4.44	0.11	61	1.10
		2	0.28	6.4	65	2.15	1.00	...	
		3	0.02	11.7	−111	2.31	1.00	...	
		4	0.05	12.5	65	3.26	1.00	...	
		5	0.04	16.6	−114	0.00	1.00	...	
	8.55	1	1.00	0.0	...	0.58	1.00	...	0.98
		2	0.74	0.8	−117	0.60	1.00	...	
		3	0.24	0.9	79	0.88	1.00	...	
		4	0.20	2.3	73	0.99	1.00	...	
		5	0.18	4.1	−110	0.93	1.00	...	
		6	0.14	4.1	64	1.43	1.00	...	
		7	0.17	7.1	−115	1.40	1.00	...	
		8	0.09	8.9	65	2.66	1.00	...	
		9	0.08	11.8	−111	2.40	1.00	...	
0259+121.....	2.32	1	0.70	0.0	...	2.01	0.48	55	0.95
		2	0.08	4.0	−82	4.03	1.00	...	
	8.55	1	0.18	0.0	...	0.35	1.00	...	0.84
		2	0.15	0.7	43	1.72	1.00	...	
		3	0.07	1.3	−127	0.76	1.00	...	
		4	0.03	4.9	−70	2.16	1.00	...	
0302+625.....	2.32	1	0.36	0.0	...	1.05	1.00	...	0.94
		2	0.10	1.6	−17	2.61	1.00	...	
	8.55	1	0.23	0.0	...	0.29	1.00	...	0.96
		2	0.06	1.4	−31	1.22	1.00	...	
0317+188.....	2.32	1	0.63	0.0	...	1.18	1.00	...	0.94
		2	0.14	4.1	108	3.01	1.00	...	
	8.55	1	0.46	0.0	...	0.68	0.44	−33	0.92
		2	0.03	1.6	98	0.87	1.00	...	
		3	0.03	3.7	89	1.42	1.00	...	
0334+014.....	2.32	1	0.26	0.0	...	2.59	1.00	...	0.73
	8.55	1	0.15	0.0	...	0.44	1.00	...	0.81
0341+158.....	2.32	1	0.33	0.0	...	1.44	1.00	...	0.90
		2	0.03	7.0	23	3.60	1.00	...	
	8.55	1	0.18	0.0	...	0.82	0.00	29	0.91
		2	0.02	1.6	33	0.83	1.00	...	
0400+258.....	2.32	1	0.60	0.0	...	1.98	0.07	69	0.91
		2	0.39	4.1	40	5.13	0.30	13	
		3	0.06	10.7	31	6.72	1.00	...	
	8.55	1	0.42	0.0	...	0.30	1.00	...	1.01
		2	0.12	1.3	87	1.30	1.00	...	
		3	0.07	3.8	59	1.78	1.00	...	
		4	0.10	6.0	38	2.54	1.00	...	
0406+121.....	2.32	1	0.72	0.0	...	0.96	0.52	61	0.75
	8.55	1	0.67	0.0	...	0.83	0.41	−21	0.86
0422+004.....	2.32	1	0.66	0.0	...	0.48	1.00	...	1.13
		2	0.10	2.5	29	3.31	1.00	...	
	8.55	1	0.62	0.0	...	0.60	0.27	−8	0.97
		2	0.08	1.1	11	0.71	1.00	...	

TABLE 2—*Continued*

Source	ν (GHz)	Component	S (Jy)	r (mas)	θ (deg)	a (mas)	b/a	ϕ (deg)	χ^2
0425+048.....	2.32	1	0.17	0.0	...	0.00	1.00	...	0.88
		2	0.15	1.0	−125	4.44	1.00	...	
		3	0.06	13.1	−105	7.90	1.00	...	
		4	0.10	18.5	−99	2.43	1.00	...	
		5	0.01	18.5	78	2.62	1.00	...	
		6	0.02	26.7	−80	6.99	1.00	...	
	8.55	1	0.22	0.0	...	0.22	1.00	...	0.88
		2	0.04	0.6	−118	0.44	1.00	...	
		3	0.04	2.3	−102	1.92	1.00	...	
		4	0.04	19.1	−100	2.50	1.00	...	
0440+345.....	2.32	1	1.01	0.0	...	0.92	0.46	21	0.87
		2	0.09	4.1	−27	3.41	1.00	...	
		3	0.02	5.7	−177	0.27	1.00	...	
	8.55	1	0.69	0.0	...	0.53	0.55	4	0.92
		2	0.04	2.2	−174	0.32	1.00	...	
0440−003.....	2.32	1	2.11	0.0	...	1.16	0.00	56	1.08
		2	0.03	2.7	102	4.02	1.00	...	
	8.55	1	0.85	0.0	...	1.06	0.30	59	0.99
		2	0.35	0.1	99	0.16	1.00	...	
0458+138.....	2.32	1	0.28	0.0	...	1.25	1.00	...	0.92
		2	0.02	4.4	46	2.98	1.00	...	
		3	0.06	7.9	−131	4.03	1.00	...	
		4	0.01	11.0	55	1.63	1.00	...	
		5	0.01	20.5	51	4.25	1.00	...	
		6	0.02	28.9	−134	16.04	1.00	...	
	8.55	1	0.30	0.0	...	0.66	0.07	23	0.89
		2	0.08	1.1	39	0.42	1.00	...	
0459+060.....	2.32	1	0.86	0.0	...	1.13	1.00	...	0.93
		2	0.18	2.5	76	2.95	1.00	...	
	8.55	1	0.63	0.0	...	0.89	0.27	61	0.91
		2	0.03	1.3	124	1.31	1.00	...	
		3	0.02	3.1	79	1.68	1.00	...	
0507+179.....	2.32	1	0.45	0.0	...	1.06	1.00	...	1.01
		2	0.23	2.7	−99	1.54	1.00	...	
		3	0.09	9.8	−101	5.42	1.00	...	
	8.55	1	0.47	0.0	...	0.20	1.00	...	1.01
		2	0.11	0.7	−104	0.43	1.00	...	
		3	0.07	3.1	−99	0.84	1.00	...	
		4	0.02	8.9	−102	3.98	1.00	...	
0518+165.....	2.32	1	2.70[b]	...	...	...	...	...	...
	8.55	1	0.17	0.0	...	0.75	0.54	40	0.95
		2	0.04	3.3	105	3.03	1.00	...	
		3	0.04	5.4	−90	0.47	1.00	...	
0536+145.....	2.32	1	0.50	0.0	...	0.37	1.00	...	0.99
		2	0.03	5.1	158	3.65	1.00	...	
	8.55	1	0.47	0.0	...	0.32	0.56	−32	0.92
0539−057.....	2.32	1	0.77	0.0	...	3.07	1.00	...	1.08
		2	0.14	4.4	173	3.50	1.00	...	
	8.55	1	0.89	0.0	...	0.53	0.57	−2	1.07
		2	0.21	1.2	149	1.45	1.00	...	
0544+273.....	2.32	1	0.34	0.0	...	1.31	1.00	...	0.88
		2	0.08	2.0	6	2.07	1.00	...	
		3	0.02	15.1	16	2.67	1.00	...	
	8.55	1	0.77	0.0	...	0.15	1.00	...	0.89
		2	0.04	1.1	12	0.70	1.00	...	
0552+398[c].....	2.32	1	4.14	0.0	...	1.39	0.59	−68	1.04
	8.55	1	4.39	0.0	...	0.46	0.75	79	1.30
		2	1.21	0.7	−74	0.71	1.00	...	
0552+398[d].....	2.32	1	3.94	0.0	...	1.37	0.60	−56	0.76
	8.55	1	4.07	0.0	...	0.44	0.80	−83	0.92
		2	1.19	0.7	−74	0.67	1.00	...	
0600+177.....	2.32	1	0.52	0.0	...	2.51	0.31	−19	0.95
		2	0.06	8.2	125	8.06	1.00	...	
	8.55	1	0.39	0.0	...	0.72	0.26	−21	0.98
		2	0.04	2.8	157	1.23	1.00	...	
0609+607.....	2.32	1	0.83	0.0	...	1.58	0.33	−19	0.95
		2	0.12	4.2	116	2.54	1.00	...	
		3	0.27	4.3	145	1.82	1.00	...	
	8.55	1	0.34	0.0	...	0.53	0.29	−30	0.96
		2	0.13	1.1	164	0.58	1.00	...	
		3	0.09	4.7	143	2.32	1.00	...	
0636+680.....	2.32	1	0.42	0.0	...	0.55	1.00	...	1.11
	8.55	1	0.37	0.0	...	0.58	0.52	−46	1.00

TABLE 2—*Continued*

Source	ν (GHz)	Component	S (Jy)	r (mas)	θ (deg)	a (mas)	b/a	ϕ (deg)	χ^2
0642+449.....	2.32	1	0.70	0.0	...	0.57	1.00	...	0.89
		2	0.11	3.7	95	1.23	1.00	...	
	8.55	1	1.83	0.0	...	0.33	0.39	−89	0.88
		2	0.03	0.6	91	0.50	1.00	...	
		3	0.02	3.3	91	1.50	1.00	...	
0657+172.....	2.32	1	0.63	0.0	...	0.96	1.00	...	0.86
		2	0.07	5.3	−154	2.40	1.00	...	
		3	0.05	10.7	−161	0.00	1.00	...	
	8.55	1	0.78	0.0	...	0.25	0.59	−81	0.89
		2	0.03	0.9	−93	0.47	1.00	...	
		3	0.02	5.7	−147	1.56	1.00	...	
		4	0.02	11.0	−162	2.57	1.00	...	
0707+476.....	2.32	1	0.79	0.0	...	1.31	0.40	−4	1.06
		2	0.09	2.9	12	1.62	1.00	...	
		3	0.07	6.0	28	3.35	1.00	...	
	8.55	1	0.75	0.0	...	0.35	0.23	−22	1.14
		2	0.13	1.1	−12	0.79	1.00	...	
		3	0.04	4.4	19	3.26	1.00	...	
0718+793.....	2.32	1	0.77	0.0	...	1.14	0.68	−67	0.97
		2	0.01	3.2	71	4.28	1.00	...	
	8.55	1	0.50	0.0	...	0.60	0.22	−89	1.01
		2	0.16	0.2	−173	0.53	1.00	...	
		3	0.03	0.9	−63	0.60	1.00	...	
0723−008.....	2.32	1	0.99	0.0	...	1.72	0.54	−29	1.07
		2	0.21	4.2	−30	1.30	1.00	...	
		3	0.07	11.7	−24	3.09	1.00	...	
		4	0.18	20.8	−16	7.43	1.00	...	
		5	0.12	29.0	−3	7.28	1.00	...	
	8.55	1	0.80	0.0	...	0.72	0.47	−40	1.22
		2	0.09	1.2	−27	0.57	1.00	...	
		3	0.09	3.4	−32	1.23	1.00	...	
		4	0.06	6.0	−27	1.35	1.00	...	
0727−115[c].....	2.32	1	2.36	0.0	...	0.52	1.00	...	1.31
		2	1.24	1.1	−43	2.47	1.00	...	
		3	0.22	7.9	−28	8.49	1.00	...	
		4	0.03	22.5	−36	7.80	1.00	...	
	8.55	1	2.77	0.0	...	0.32	0.39	60	1.31
		2	0.54	1.1	−60	3.65	0.33	−32	
0727−115[d].....	2.32	1	2.63	0.0	...	0.97	1.00	...	1.00
		2	0.50	2.3	−44	2.37	1.00	...	
		3	0.19	7.9	−26	10.12	1.00	...	
		4	0.02	23.6	−44	3.10	1.00	...	
	8.55	1	2.10	0.0	...	0.45	0.61	44	1.02
		2	0.34	1.5	−55	3.21	0.36	−33	
0742+103.....	2.32	1	3.85	0.0	...	2.22	0.39	6	1.04
		2	0.82	1.5	43	3.12	1.00	...	
		3	0.28	5.8	101	5.45	1.00	...	
		4	0.09	12.0	132	7.04	1.00	...	
	8.55	1	0.90	0.0	...	0.71	1.00	...	1.14
		2	0.79	0.9	152	0.62	0.51	−35	
		3	0.56	1.6	6	1.15	1.00	...	
		4	0.13	1.9	40	2.89	1.00	...	
0743−006.....	2.32	1	1.07	0.0	...	0.45	1.00	...	0.96
		2	0.22	2.0	56	0.85	1.00	...	
		3	0.06	10.7	42	6.82	1.00	...	
	8.55	1	1.78	0.0	...	0.90	0.13	50	0.86
		2	0.11	1.0	45	0.41	1.00	...	
		3	0.01	2.9	44	0.53	1.00	...	
0749+540.....	2.32	1	1.14	0.0	...	0.71	0.53	12	1.12
		2	0.03	7.4	3	15.03	0.23	24	
	8.55	1	1.00	0.0	...	0.32	0.12	70	1.11
		2	0.08	0.7	29	0.49	1.00	...	
		3	0.01	2.0	1	0.75	1.00	...	
0805−077.....	2.32	1	0.98	0.0	...	0.60	1.00	...	1.03
		2	0.08	7.9	−34	5.13	1.00	...	
		3	0.20	20.6	−28	9.17	1.00	...	
	8.55	1	0.49	0.0	...	0.60	0.39	−26	0.93
		2	0.23	1.2	−44	0.45	1.00	...	
0808+019.....	2.32	1	0.64	0.0	...	0.00	1.00	...	1.01
		2	0.16	1.4	−157	0.96	1.00	...	
		3	0.03	7.7	−144	6.66	1.00	...	
	8.55	1	1.09	0.0	...	0.33	0.35	9	1.00
		2	0.01	3.0	−175	1.03	1.00	...	

TABLE 2—*Continued*

Source	ν (GHz)	Component	S (Jy)	r (mas)	θ (deg)	a (mas)	b/a	ϕ (deg)	χ^2
0820+560.....	2.32	1	0.92	0.0	...	0.37	1.00	...	0.81
		2	0.22	1.6	92	0.26	1.00	...	
		3	0.10	4.4	76	1.79	1.00	...	
		4	0.05	7.8	73	4.13	1.00	...	
		5	0.14	17.7	71	5.54	1.00	...	
		6	0.09	23.1	82	5.66	1.00	...	
	8.55	1	0.70	0.0	...	0.51	0.27	−72	0.88
		2	0.11	0.9	101	0.41	1.00	...	
		3	0.04	2.6	93	1.00	1.00	...	
		4	0.03	5.1	77	2.37	1.00	...	
		5	0.03	17.7	72	5.33	1.00	...	
0823+033.....	2.32	1	1.10	0.0	...	0.00	1.00	...	0.97
		2	0.51	2.0	23	0.74	1.00	...	
		3	0.07	8.4	29	5.20	1.00	...	
	8.55	1	0.99	0.0	...	0.80	0.08	19	1.12
		2	0.21	1.9	17	2.24	0.38	26	
0831+557.....	2.32	1	9.30[b]	...	...	...	...	...	...
	8.55	1	2.26[b]	...	...	...	...	...	...
0833+585.....	2.32	1	0.78	0.0	...	2.21	0.15	82	1.09
		2	0.04	8.0	79	4.49	1.00	...	
	8.55	1	0.33	0.0	...	0.94	0.16	82	1.03
		2	0.13	2.0	83	0.73	1.00	...	
		3	0.01	2.3	−98	0.10	1.00	...	
0851+202[c].....	2.32	1	1.55	0.0	...	1.46	0.00	83	0.89
		2	0.14	3.0	−117	2.82	1.00	...	
		3	0.03	7.3	−119	3.94	1.00	...	
		4	0.01	15.0	−124	5.15	1.00	...	
	8.55	1	0.88	0.0	...	0.32	0.00	89	0.96
		2	0.45	1.0	−90	0.70	0.73	86	
		3	0.06	2.9	−107	3.52	1.00	...	
0851+202[d].....	2.32	1	1.23	0.0	...	1.37	0.00	87	0.82
		2	0.11	2.8	−109	2.36	1.00	...	
		3	0.05	7.3	−121	5.45	1.00	...	
	8.55	1	1.60	0.0	...	0.30	0.00	−87	0.90
		2	0.26	1.2	−90	0.56	0.95	1	
		3	0.05	3.5	−109	2.88	1.00	...	
0859+470.....	2.32	1	0.72	0.0	...	2.32	0.34	5	1.05
		2	0.33	3.6	−0	2.43	1.00	...	
		3	0.10	24.9	−6	17.31	1.00	...	
		4	0.22	53.6	1	14.03	1.00	...	
	8.55	1	0.44	0.0	...	0.33	0.36	−13	1.08
		2	0.13	1.6	−9	1.14	0.66	4	
		3	0.03	2.8	8	0.67	1.00	...	
		4	0.09	4.6	−0	1.82	1.00	...	
0912+297.....	2.32	1	0.20	0.0	...	0.77	1.00	...	0.81
		2	0.02	3.1	−124	1.51	1.00	...	
	8.55	1	0.17	0.0	...	0.26	0.65	45	0.88
0917+624.....	2.32	1	1.37	0.0	...	0.97	0.15	−22	1.22
		2	0.33	5.7	−19	2.39	1.00	...	
		3	0.09	21.2	−25	11.59	1.00	...	
	8.55	1	1.37	0.0	...	0.31	0.57	−44	1.11
		2	0.08	0.7	−13	0.27	1.00	...	
		3	0.03	1.4	−6	0.49	1.00	...	
		4	0.10	5.9	−19	1.68	1.00	...	
0945+408.....	2.32	1	1.25	0.0	...	0.35	1.00	...	0.74
		2	0.27	6.8	122	2.89	1.00	...	
		3	0.25	9.9	114	2.51	1.00	...	
		4	0.08	14.9	112	4.82	1.00	...	
		5	0.08	22.4	115	6.21	1.00	...	
	8.55	1	0.96	0.0	...	0.23	1.00	...	0.88
		2	0.34	0.5	−73	0.29	1.00	...	
		3	0.07	6.9	124	2.00	1.00	...	
		4	0.07	9.7	114	2.31	1.00	...	
0955+476.....	2.32	1	1.11	0.0	...	0.48	1.00	...	0.70
		2	0.03	6.0	138	2.95	1.00	...	
	8.55	1	1.03	0.0	...	0.25	0.75	−69	0.89
		2	0.02	1.0	134	1.21	1.00	...	
1004+141.....	2.32	1	0.61	0.0	...	1.00	1.00	...	0.89
		2	0.05	3.9	125	3.78	1.00	...	
		3	0.29	11.0	133	2.83	1.00	...	
	8.55	1	0.68	0.0	...	0.18	1.00	...	1.02
		2	0.16	0.5	113	0.32	1.00	...	
		3	0.07	1.5	121	1.02	1.00	...	

TABLE 2—*Continued*

Source	ν (GHz)	Component	S (Jy)	r (mas)	θ (deg)	a (mas)	b/a	ϕ (deg)	χ^2
		4	0.08	11.4	130	1.73	1.00	…	
1020+400.....	2.32	1	0.61	0.0	…	0.45	1.00	…	0.68
		2	0.14	3.9	−41	0.48	1.00	…	
		3	0.08	11.4	−36	3.29	1.00	…	
		4	0.04	16.8	−32	3.66	1.00	…	
	8.55	1	0.79	0.0	…	0.27	0.08	−53	0.89
		2	0.20	0.7	−58	0.22	1.00	…	
		3	0.02	2.8	−41	0.99	1.00	…	
		4	0.03	4.6	−42	0.97	1.00	…	
1022+194.....	2.32	1	0.33	0.0	…	2.16	0.00	36	1.03
		2	0.17	4.5	50	8.22	0.17	42	
	8.55	1	0.48	0.0	…	0.33	0.00	34	1.13
		2	0.07	0.4	45	1.11	0.00	28	
		3	0.03	2.6	41	0.60	1.00	…	
		4	0.02	4.5	52	1.79	1.00	…	
		5	0.02	9.1	44	2.72	1.00	…	
1038+064.....	2.32	1	1.32	0.0	…	0.18	1.00	…	0.86
		2	0.21	4.7	151	1.65	1.00	…	
		3	0.07	16.1	154	4.17	1.00	…	
		4	0.06	23.0	155	2.69	1.00	…	
		5	0.05	34.7	156	9.59	1.00	…	
	8.55	1	0.79	0.0	…	0.23	1.00	…	0.89
		2	0.34	0.9	−25	0.00	1.00	…	
		3	0.06	1.1	156	0.24	1.00	…	
		4	0.04	2.5	148	1.03	1.00	…	
1049+215.....	2.32	1	1.14	0.0	…	1.00	1.00	…	0.98
		2	0.16	5.8	118	2.69	1.00	…	
		3	0.09	8.1	106	2.05	1.00	…	
		4	0.05	11.2	88	5.36	1.00	…	
	8.55	1	1.08	0.0	…	0.32	0.64	−47	1.02
		2	0.17	0.5	121	0.33	1.00	…	
		3	0.07	7.1	114	2.59	1.00	…	
		4	0.12	1.3	110	1.09	1.00	…	
1053+815.....	2.32	1	0.27	0.0	…	0.89	0.50	39	0.93
	8.55	1	0.40	0.0	…	0.08	1.00	…	1.00
		2	0.01	0.8	−144	0.49	1.00	…	
		3	0.01	1.9	−145	0.93	1.00	…	
1116+128.....	2.32	1	1.05	0.0	…	0.85	1.00	…	1.04
		2	0.46	5.0	21	2.95	1.00	…	
		3	0.34	9.5	18	4.12	1.00	…	
		4	0.16	14.9	27	5.53	1.00	…	
		5	0.08	23.8	13	8.59	1.00	…	
	8.55	1	0.71	0.0	…	0.58	0.27	−1	1.12
		2	0.22	1.5	2	1.40	1.00	…	
		3	0.13	6.0	19	2.70	1.00	…	
		4	0.14	10.0	18	4.52	1.00	…	
1117+146.....	2.32	1	2.05[b]	…	…	…	…	…	…
	8.55	1	0.24	0.0	…	3.22	1.00	…	0.90
1130+009.....	2.32	1	0.32	0.0	…	0.60	1.00	…	1.05
		2	0.04	9.7	137	3.40	1.00	…	
		3	0.03	4.5	132	2.53	1.00	…	
	8.55	1	0.19	0.0	…	0.10	1.00	…	1.02
		2	0.05	0.7	145	0.55	1.00	…	
1145−071.....	2.32	1	0.78	0.0	…	2.55	0.38	−65	1.14
		2	0.04	11.0	−53	8.00	1.00	…	
	8.55	1	0.46	0.0	…	0.20	1.00	…	1.12
		2	0.10	1.9	−86	0.59	1.00	…	
		3	0.10	2.1	−63	1.22	1.00	…	
1150+812.....	2.32	1	1.11	0.0	…	1.38	0.15	−5	1.12
		2	0.29	1.8	166	1.08	1.00	…	
		3	0.12	4.0	158	1.07	1.00	…	
		4	0.04	7.1	143	3.10	1.00	…	
		5	0.03	11.6	134	5.92	1.00	…	
		6	0.02	30.3	127	7.79	1.00	…	
	8.55	1	0.91	0.0	…	0.43	0.26	32	1.01
		2	0.30	1.2	176	1.26	0.41	−4	
		3	0.09	3.5	161	3.09	0.32	−20	
1156−094.....	2.32	1	0.14	0.0	…	0.00	1.00	…	1.25
		2	0.20	0.5	56	8.07	0.37	28	
		3	0.07	14.3	50	6.89	1.00	…	
		4	0.04	36.6	70	2.86	1.00	…	
		5	0.06	40.3	67	0.34	1.00	…	
	8.55	1	0.21	0.0	…	0.23	1.00	…	1.16

TABLE 2—*Continued*

Source	ν (GHz)	Component	S (Jy)	r (mas)	θ (deg)	a (mas)	b/a	ϕ (deg)	χ^2
		2	0.02	1.3	−75	1.99	1.00	…	
		3	0.02	23.3	−98	2.17	1.00	…	
		4	0.02	29.1	−103	2.46	1.00	…	
		5	0.04	37.5	−107	2.48	1.00	…	
		6	0.05	41.0	−114	2.73	1.00	…	
1213+350.....	2.32	1	0.82	0.0	…	1.62	0.77	−7	0.98
		2	0.52	3.0	102	9.38	0.66	45	
		3	0.02	35.4	−125	0.00	1.00	…	
	8.55	1	0.30	0.0	…	0.45	1.00	…	0.99
		2	0.18	0.7	−160	2.13	1.00	…	
		3	0.12	2.5	119	6.60	1.00	…	
		4	0.03	37.0	−126	0.46	1.00	…	
1219+044.....	2.32	1	0.65	0.0	…	0.14	1.00	…	1.01
		2	0.06	4.5	172	1.38	1.00	…	
	8.55	1	0.65	0.0	…	0.00	1.00	…	0.97
		2	0.08	1.4	172	0.40	1.00	…	
		3	0.01	6.4	174	1.75	1.00	…	
1221+809.....	2.32	1	0.30	0.0	…	1.02	0.00	−14	1.08
		2	0.16	5.4	−8	8.76	0.22	−14	
		3	0.06	21.4	−15	13.67	1.00	…	
	8.55	1	0.43	0.0	…	0.22	0.00	−6	0.99
		2	0.05	1.1	−5	0.44	1.00	…	
		3	0.01	4.1	−5	0.59	1.00	…	
		4	0.02	6.0	−6	1.48	1.00	…	
		5	0.03	9.4	−12	2.21	1.00	…	
1226+373.....	2.32	1	0.46	0.0	…	0.41	1.00	…	0.88
		2	0.03	3.8	−70	1.82	1.00	…	
	8.55	1	0.26	0.0	…	0.35	0.00	−55	0.95
		2	0.03	0.6	−28	0.25	1.00	…	
1236+077.....	2.32	1	0.50	0.0	…	0.72	0.48	−57	0.89
		2	0.21	2.9	−52	6.80	0.07	−43	
		3	0.01	20.4	−41	4.02	1.00	…	
	8.55	1	0.60	0.0	…	0.64	0.15	−58	1.09
		2	0.08	1.7	−48	1.46	1.00	…	
		3	0.05	5.5	−48	2.01	1.00	…	
1307+121.....	2.32	1	0.65	0.0	…	2.31	0.00	42	0.88
		2	0.34	3.1	43	1.70	1.00	…	
		3	0.05	8.2	42	5.44	1.00	…	
	8.55	1	0.39	0.0	…	0.62	0.08	41	0.97
		2	0.08	1.6	44	0.93	1.00	…	
		3	0.17	3.4	40	1.43	1.00	…	
1315+346.....	2.32	1	0.26	0.0	…	0.52	1.00	…	0.79
		2	0.05	2.9	9	0.94	1.00	…	
		3	0.02	9.5	11	4.51	1.00	…	
	8.55	1	0.24	0.0	…	0.00	1.00	…	0.92
		2	0.05	0.9	6	0.26	1.00	…	
		3	0.02	3.3	8	1.36	1.00	…	
1342+662.....	2.32	1	0.26	0.0	…	1.15	0.00	42	0.93
		2	0.02	2.2	26	3.15	1.00	…	
	8.55	1	0.17	0.0	…	0.14	1.00	…	0.96
		2	0.03	0.8	37	0.71	1.00	…	
		3	0.00	2.8	30	1.18	1.00	…	
1347+539.....	2.32	1	0.38	0.0	…	1.11	0.00	−44	0.98
		2	0.24	4.2	137	7.69	0.13	−38	
		3	0.06	12.9	136	3.11	1.00	…	
		4	0.11	18.4	125	4.15	1.00	…	
		5	0.17	58.0	141	13.03	1.00	…	
	8.55	1	0.37	0.0	…	0.71	0.15	−27	0.94
		2	0.03	2.3	138	1.33	1.00	…	
		3	0.03	5.9	139	2.20	1.00	…	
		4	0.02	12.0	142	5.02	1.00	…	
		5	0.03	19.1	124	3.35	1.00	…	
1357+769.....	2.32	1	0.65	0.0	…	0.40	1.00	…	0.94
		2	0.04	2.2	−117	2.27	1.00	…	
	8.55	1	0.59	0.0	…	0.03	1.00	…	1.01
		2	0.06	0.3	179	0.55	1.00	…	
		3	0.01	1.4	−130	2.26	1.00	…	
1402+044.....	2.32	1	0.90	0.0	…	0.32	1.00	…	0.98
		2	0.03	3.0	−50	0.79	1.00	…	
		3	0.14	8.7	−48	3.11	1.00	…	
		4	0.08	12.3	−78	4.14	1.00	…	
	8.55	1	0.77	0.0	…	0.83	0.26	−21	0.93
		2	0.06	9.0	−47	2.51	1.00	…	

TABLE 2—*Continued*

Source	ν (GHz)	Component	S (Jy)	r (mas)	θ (deg)	a (mas)	b/a	ϕ (deg)	χ^2
		3	0.02	12.9	−79	1.64	1.00	…	
1413+135.....	2.32	1	0.26	0.0	…	1.90	1.00	…	1.09
		2	0.11	6.2	−105	6.04	1.00	…	
		3	0.10	8.1	72	8.86	1.00	…	
		4	0.15	19.7	58	5.92	1.00	…	
		5	0.04	23.6	−118	13.70	1.00	…	
		6	0.16	26.1	75	11.59	1.00	…	
		7	0.09	35.5	74	5.29	1.00	…	
	8.55	1	1.41	0.0	…	0.16	1.00	…	1.04
		2	0.04	1.5	−118	0.56	1.00	…	
		3	0.02	2.4	−114	0.62	1.00	…	
		4	0.01	3.6	−109	0.81	1.00	…	
		5	0.02	6.9	−109	1.99	1.00	…	
		6	0.01	7.6	59	0.58	1.00	…	
		7	0.03	19.8	59	3.75	1.00	…	
1416+067.....	2.32	1	0.42	0.0	…	1.12	1.00	…	1.00
		2	0.05	10.9	101	3.57	1.00	…	
		3	0.03	17.7	105	4.44	1.00	…	
	8.55	1	0.21	0.0	…	0.82	0.60	−78	0.71
1432+200.....	2.32	1	0.39	0.0	…	0.36	1.00	…	0.94
		2	0.09	2.0	−132	0.90	1.00	…	
		3	0.03	5.9	−127	3.69	1.00	…	
		4	0.02	33.5	−124	9.30	1.00	…	
	8.55	1	0.32	0.0	…	0.35	0.00	41	0.96
		2	0.04	1.0	−131	0.42	1.00	…	
		3	0.03	2.7	−139	1.53	1.00	…	
1433+304.....	2.32	1	0.22	0.0	…	1.21	0.00	73	0.77
		2	0.03	3.7	63	0.00	1.00	…	
		3	0.02	8.8	65	3.43	1.00	…	
		4	0.01	17.3	82	6.79	1.00	…	
	8.55	1	0.17	0.0	…	0.56	0.35	77	0.93
		2	0.01	3.2	70	1.48	1.00	…	
1458+718.....	2.32	1	3.65[b]	…	…	…	…	…	…
	8.55	1	0.88	0.0	…	0.26	0.46	−12	1.17
		2	0.11	22.3	169	2.71	1.00	…	
		3	0.25	24.4	163	1.33	1.00	…	
		4	0.21	26.3	166	3.07	1.00	…	
		5	0.20	41.4	164	8.31	1.00	…	
1459+480.....	2.32	1	0.33	0.0	…	1.55	0.00	−88	0.86
		2	0.04	3.5	83	1.19	1.00	…	
		3	0.04	6.8	73	1.66	1.00	…	
		4	0.03	10.9	52	4.58	1.00	…	
	8.55	1	0.49	0.0	…	0.16	1.00	…	0.94
		2	0.04	1.1	82	0.59	1.00	…	
		3	0.01	3.3	86	0.67	1.00	…	
		4	0.02	6.9	71	2.07	1.00	…	
1510−089.....	2.32	1	2.97	0.0	…	0.54	1.00	…	1.18
		2	0.23	2.2	−33	0.84	1.00	…	
		3	0.06	12.8	−26	5.51	1.00	…	
		4	0.05	27.2	−22	10.95	1.00	…	
	8.55	1	1.56	0.0	…	0.36	0.45	−6	1.01
		2	0.67	0.7	−43	0.37	1.00	…	
		3	0.03	3.4	−35	0.99	1.00	…	
1532+016.....	2.32	1	0.13	0.0	…	8.08	0.66	35	0.93
		2	0.91	1.5	−9	1.79	0.28	−39	
		3	0.37	4.1	135	2.94	0.86	−46	
	8.55	1	0.29	0.0	…	0.36	1.00	…	1.00
		2	0.22	0.6	−52	0.37	1.00	…	
		3	0.10	0.9	136	0.41	1.00	…	
		4	0.06	2.0	144	1.24	1.00	…	
		5	0.14	6.1	145	2.29	1.00	…	
1546+027.....	2.32	1	1.13	0.0	…	0.81	0.20	−28	1.11
		2	0.05	5.4	170	1.22	1.00	…	
		3	0.02	13.7	−175	3.36	1.00	…	
		4	0.03	27.2	175	8.66	1.00	…	
	8.55	1	1.17	0.0	…	0.86	0.13	−8	1.07
		2	0.04	2.8	160	0.53	1.00	…	
1600+335.....	2.32	1	1.89	0.0	…	1.45	0.38	−3	0.87
		2	0.62	3.5	−8	4.42	0.51	−5	
		3	0.16	5.2	−137	7.14	0.48	21	
		4	0.06	8.5	115	3.99	0.73	62	
		5	0.12	16.1	−161	18.97	0.89	−86	
		6	0.18	40.3	86	23.64	1.00	…	

TABLE 2—*Continued*

Source	ν (GHz)	Component	S (Jy)	r (mas)	θ (deg)	a (mas)	b/a	ϕ (deg)	χ^2
	8.55	1	0.81	0.0	...	0.64	0.78	28	1.01
		2	0.21	1.0	1	0.35	1.00	...	
		3	0.06	1.8	12	0.41	1.00	...	
		4	0.09	3.1	−16	1.43	1.00	...	
		5	0.12	4.9	−4	1.90	1.00	...	
		6	0.03	5.8	−136	3.40	1.00	...	
		7	0.01	9.0	114	0.00	1.00	...	
1607+268.....	2.32	1	1.61	0.0	...	2.79	0.79	−62	1.12
		2	0.40	3.8	−157	2.39	1.00	...	
		3	0.38	5.0	−130	6.11	1.00	...	
		4	0.52	43.5	−154	9.06	0.28	17	
		5	1.17	49.4	−154	4.49	0.47	8	
		6	0.33	51.7	−158	2.88	1.00	...	
	8.55	1	0.21	0.0	...	0.51	1.00	...	0.84
		2	0.29	0.8	−156	2.78	1.00	...	
		3	0.05	42.1	−154	2.38	1.00	...	
		4	0.29	50.0	−154	4.95	0.45	7	
1624+416.....	2.32	1	0.82	0.0	...	1.41	0.49	86	0.85
		2	0.51	1.9	−144	2.36	1.00	...	
		3	0.12	4.6	−17	3.99	1.00	...	
		4	0.04	13.7	−18	5.73	1.00	...	
		5	0.04	25.5	−6	9.78	1.00	...	
	8.55	1	0.26	0.0	...	0.31	0.00	84	1.02
		2	0.22	0.8	−106	0.98	0.44	55	
		3	0.20	1.8	−116	2.36	1.00	...	
		4	0.05	3.7	−143	1.68	1.00	...	
		5	0.04	4.4	−23	4.18	1.00	...	
1633+382.....	2.32	1	2.41	0.0	...	1.25	0.58	−85	0.86
		2	0.26	2.7	−64	2.26	1.00	...	
		3	0.19	14.6	−73	13.48	1.00	...	
	8.55	1	1.03	0.0	...	0.34	0.54	−65	0.99
		2	0.73	1.0	−85	0.65	1.00	...	
		3	0.19	1.7	−66	1.48	1.00	...	
		4	0.02	4.7	−62	0.00	1.00	...	
1642+690.....	2.32	1	0.65	0.0	...	1.45	0.78	38	0.94
		2	0.56	1.1	−17	4.98	0.19	−70	
		3	0.13	4.2	−166	1.52	1.00	...	
		4	0.13	8.2	−164	2.27	1.00	...	
	8.55	1	0.63	0.0	...	0.49	0.46	−23	1.04
		2	0.41	1.3	−159	0.75	0.40	29	
		3	0.05	5.6	−166	2.40	1.00	...	
		4	0.05	9.9	−165	2.05	1.00	...	
1652+398.....	2.32	1	0.69	0.0	...	2.03	0.00	−31	1.10
		2	0.34	4.1	124	6.86	0.34	−75	
		3	0.14	17.0	121	12.51	1.00	...	
		4	0.39	47.9	66	53.15	1.00	...	
	8.55	1	0.49	0.0	...	0.28	0.27	−13	1.06
		2	0.13	0.7	170	0.67	1.00	...	
		3	0.10	2.4	146	1.22	1.00	...	
		4	0.05	4.2	133	1.52	1.00	...	
		5	0.07	7.5	114	2.77	1.00	...	
1705+018.....	2.32	1	0.47	0.0	...	0.61	0.00	28	1.02
		2	0.20	1.4	61	1.45	1.00	...	
	8.55	1	0.43	0.0	...	0.07	1.00	...	1.00
		2	0.08	1.1	4	0.33	1.00	...	
		3	0.01	2.2	42	0.78	1.00	...	
1705+456.....	2.32	1	0.38	0.0	...	2.67	0.18	62	0.96
		2	0.16	8.4	−119	4.26	0.68	70	
		3	0.02	26.2	−85	6.83	1.00	...	
	8.55	1	0.27	0.0	...	0.26	0.00	60	1.02
		2	0.08	1.9	−110	2.12	0.16	56	
		3	0.04	9.7	−117	3.03	1.00	...	
1725+044.....	2.32	1	0.84	0.0	...	0.77	1.00	...	0.94
		2	0.05	2.0	95	1.73	1.00	...	
		3	0.10	52.5	101	10.89	1.00	...	
	8.55	1	0.51	0.0	...	0.40	1.00	...	0.84
		2	0.17	0.8	113	0.65	1.00	...	
1738+476.....	2.32	1	0.93	0.0	...	0.57	1.00	...	0.78
		2	0.16	1.3	−92	2.03	1.00	...	
	8.55	1	0.77	0.0	...	0.26	0.14	44	0.90
		2	0.11	0.9	−128	0.54	1.00	...	
		3	0.02	2.0	−78	1.30	1.00	...	

TABLE 2—*Continued*

Source	ν (GHz)	Component	S (Jy)	r (mas)	θ (deg)	a (mas)	b/a	ϕ (deg)	χ^2
1741−038.....	2.32	1	1.77	0.0	...	0.70	1.00	...	1.12
		2	0.05	7.2	171	2.59	1.00	...	
	8.55	1	2.72	0.0	...	0.13	1.00	...	1.06
		2	0.65	0.4	−159	0.52	1.00	...	
1743+173.....	2.32	1	0.91	0.0	...	0.32	1.00	...	0.97
		2	0.18	3.5	156	2.79	1.00	...	
		3	0.08	9.2	152	3.57	1.00	...	
		4	0.04	14.9	165	8.11	1.00	...	
	8.55	1	0.62	0.0	...	0.88	0.00	−18	0.89
		2	0.15	0.6	152	0.61	1.00	...	
		3	0.01	3.1	140	0.76	1.00	...	
		4	0.05	5.8	161	4.12	1.00	...	
1749+096[c].....	2.32	1	1.48	0.0	...	1.19	0.13	43	0.83
		2	0.11	3.5	28	1.42	1.00	...	
		3	0.03	8.9	35	5.22	1.00	...	
		4	0.02	31.7	34	14.12	1.00	...	
	8.55	1	3.91	0.0	...	0.08	1.00	...	0.76
		2	0.08	1.0	29	0.00	1.00	...	
		3	0.03	3.3	16	1.06	1.00	...	
1749+096[d].....	2.32	1	1.40	0.0	...	0.82	1.00	...	0.97
		2	0.14	3.3	26	1.95	1.00	...	
		3	0.03	8.4	26	3.88	1.00	...	
		4	0.01	29.6	36	6.98	1.00	...	
	8.55	1	3.65	0.0	...	0.06	1.00	...	1.11
		2	0.05	1.0	28	0.32	1.00	...	
		3	0.03	2.6	24	1.24	1.00	...	
1751+288.....	2.32	1	0.46	0.0	...	1.35	0.36	46	0.91
		2	0.07	2.5	62	4.52	1.00	...	
		3	0.01	14.4	64	1.86	1.00	...	
	8.55	1	0.31	0.0	...	0.16	1.00	...	1.04
		2	0.07	1.2	31	1.18	1.00	...	
1823+568.....	2.32	1	0.84	0.0	...	1.39	0.19	23	0.97
		2	0.08	6.4	−162	3.54	0.23	18	
		3	0.05	25.6	−159	6.56	1.00	...	
		4	0.04	41.7	−161	10.62	1.00	...	
	8.55	1	1.48	0.0	...	0.33	0.13	22	1.02
		2	0.07	0.7	−153	0.35	1.00	...	
		3	0.05	1.8	−157	0.24	1.00	...	
		4	0.03	6.5	−161	1.26	1.00	...	
1842+681.....	2.32	1	0.77	0.0	...	1.82	0.43	−56	0.96
		2	0.02	3.8	148	1.89	1.00	...	
		3	0.04	10.3	156	3.75	1.00	...	
		4	0.01	18.4	160	7.85	1.00	...	
	8.55	1	0.61	0.0	...	0.32	0.35	−34	0.98
		2	0.12	1.5	126	0.82	0.63	−45	
		3	0.01	3.5	137	0.96	1.00	...	
1849+670.....	2.32	1	0.39	0.0	...	1.02	0.25	−58	1.09
		2	0.09	3.1	−56	1.23	1.00	...	
		3	0.05	5.4	−53	1.54	1.00	...	
		4	0.02	10.1	−52	6.97	1.00	...	
	8.55	1	0.80	0.0	...	0.17	0.00	−40	0.90
		2	0.03	1.2	−56	1.68	0.22	−66	
		3	0.04	4.4	−55	3.36	0.39	−56	
1929+226.....	2.32	1	0.46	0.0	...	1.12	1.00	...	0.92
		2	0.04	3.4	−46	3.38	1.00	...	
		3	0.02	11.6	−41	6.97	1.00	...	
	8.55	1	0.40	0.0	...	0.15	1.00	...	0.88
		2	0.03	0.8	−31	0.71	1.00	...	
1932+204.....	2.32	1	0.63	0.0	...	3.60	0.73	−86	0.78
	8.55	1	0.35	0.0	...	0.33	1.00	...	0.83
		2	0.07	0.5	−180	0.30	1.00	...	
		3	0.01	2.0	−161	0.58	1.00	...	
1947+079.....	2.32	1	0.87	0.0	...	1.53	0.67	55	1.04
		2	0.04	3.7	69	0.61	1.00	...	
		3	0.23	18.7	165	3.20	1.00	...	
		4	0.45	21.5	162	0.87	1.00	...	
	8.55	1	0.34	0.0	...	0.35	1.00	...	0.81
		2	0.15	0.6	171	0.81	1.00	...	
		3	0.05	19.2	165	2.51	1.00	...	
		4	0.08	21.3	162	1.25	1.00	...	
		5	0.15	22.4	162	0.35	1.00	...	
1951+355.....	2.32	1	0.47	0.0	...	10.36	0.32	21	0.98
	8.55	1	0.25	0.0	...	1.31	0.24	28	0.96

TABLE 2—*Continued*

Source	ν (GHz)	Component	S (Jy)	r (mas)	θ (deg)	a (mas)	b/a	ϕ (deg)	χ^2
		2	0.07	0.1	−118	0.17	1.00	…	
		3	0.02	4.7	−178	1.55	1.00	…	
1954+513.....	2.32	1	1.02	0.0	…	1.18	0.11	−51	0.94
		2	0.17	5.8	−62	5.11	0.51	−73	
		3	0.17	12.0	−68	3.65	0.70	−59	
		4	0.04	23.2	−64	7.35	1.00	…	
		5	0.05	44.8	−72	17.19	1.00	…	
		6	0.05	87.1	−73	20.45	1.00	…	
	8.55	1	1.14	0.0	…	0.73	0.04	−51	0.90
		2	0.07	1.2	−54	0.95	1.00	…	
		3	0.04	6.4	−58	2.57	1.00	…	
		4	0.05	11.8	−68	2.70	1.00	…	
2007+777.....	2.32	1	1.59	0.0	…	1.25	0.00	87	1.01
		2	0.15	1.4	−96	1.22	1.00	…	
		3	0.07	6.3	−93	1.95	1.00	…	
		4	0.05	18.5	−97	4.71	1.00	…	
		5	0.03	35.8	−94	11.23	1.00	…	
	8.55	1	0.84	0.0	…	0.35	0.00	87	1.06
		2	0.37	0.6	−97	0.26	1.00	…	
		3	0.21	1.4	−88	0.20	1.00	…	
		4	0.10	1.7	−97	0.35	1.00	…	
		5	0.03	6.7	−92	1.51	1.00	…	
2017+743.....	2.32	1	0.29	0.0	…	1.21	0.00	74	1.01
		2	0.03	3.4	86	1.29	1.00	…	
		3	0.01	5.7	87	1.24	1.00	…	
		4	0.01	15.1	92	8.39	1.00	…	
	8.55	1	0.44	0.0	…	0.32	0.00	76	0.97
		2	0.05	0.9	82	0.39	1.00	…	
		3	0.01	3.6	86	1.32	1.00	…	
2021+317.....	2.32	1	3.66[b]	…	…	…	…	…	…
	8.55	1	2.31[b]	…	…	…	…	…	…
2023+336.....	2.32	1	2.41[b]	…	…	…	…	…	…
	8.55	1	2.84[b]	…	…	…	…	…	…
2029+121.....	2.32	1	0.96	0.0	…	1.78	0.00	22	0.82
		2	0.04	6.8	−174	3.09	1.00	…	
	8.55	1	0.59	0.0	…	0.43	0.00	38	0.76
		2	0.21	0.9	−154	0.38	1.00	…	
		3	0.03	2.7	−167	0.93	1.00	…	
2059+034.....	2.32	1	0.78	0.0	…	0.72	1.00	…	0.99
		2	0.13	2.3	22	0.71	1.00	…	
	8.55	1	0.73	0.0	…	0.03	1.00	…	0.96
		2	0.11	0.6	24	0.27	1.00	…	
		3	0.07	1.9	29	0.71	1.00	…	
2113+293.....	2.32	1	0.84	0.0	…	0.85	0.00	15	0.90
		2	0.23	2.4	177	3.54	1.00	…	
		3	0.01	10.6	166	2.76	1.00	…	
	8.55	1	0.89	0.0	…	0.33	0.19	−7	0.78
		2	0.09	1.9	176	2.48	0.80	−27	
2131−021.....	2.32	1	1.44	0.0	…	0.65	1.00	…	0.97
		2	0.09	6.7	96	5.09	1.00	…	
		3	0.19	19.4	99	10.05	1.00	…	
		4	0.03	23.2	85	3.11	1.00	…	
	8.55	1	0.70	0.0	…	0.37	1.00	…	0.97
		2	0.50	0.5	−73	0.22	1.00	…	
		3	0.02	1.1	75	1.12	1.00	…	
2136+141.....	2.32	1	1.32	0.0	…	1.72	0.14	44	0.96
		2	0.23	3.7	−168	3.48	0.00	−43	
		3	0.05	10.3	120	10.75	1.00	…	
	8.55	1	1.95	0.0	…	0.41	0.16	−62	0.85
		2	0.24	0.5	−110	1.56	0.00	42	
		3	0.05	3.0	−154	2.10	1.00	…	
2145+067[c].....	2.32	1	2.43	0.0	…	1.20	0.00	−57	1.07
		2	0.84	5.1	134	7.36	0.15	−27	
		3	0.21	58.1	154	12.86	1.00	…	
		4	0.17	73.7	161	5.15	1.00	…	
	8.55	1	7.82	0.0	…	0.38	0.59	−46	0.95
		2	1.72	0.6	132	0.38	0.41	−68	
		3	0.05	2.6	131	0.67	1.00	…	
		4	0.07	6.3	135	2.09	1.00	…	
2145+067[d].....	2.32	1	2.47	0.0	…	1.42	0.00	−51	0.98
		2	0.69	5.5	136	5.90	0.19	−24	
		3	0.19	58.8	154	12.03	1.00	…	
		4	0.15	73.6	161	5.93	1.00	…	

TABLE 2—*Continued*

Source	ν (GHz)	Component	S (Jy)	r (mas)	θ (deg)	a (mas)	b/a	ϕ (deg)	χ^2
	8.55	1	7.41	0.0	...	0.44	0.56	−55	1.36
		2	1.10	0.7	134	0.30	1.00	...	
		3	0.03	2.8	126	1.34	1.00	...	
		4	0.04	5.7	132	0.91	1.00	...	
2150+173.....	2.32	1	0.45	0.0	...	1.85	0.00	−86	0.89
		2	0.17	5.8	−79	4.17	0.33	89	
	8.55	1	0.35	0.0	...	0.26	1.00	...	0.91
		2	0.05	0.8	−74	0.50	1.00	...	
		3	0.05	1.9	−88	0.94	1.00	...	
		4	0.02	4.0	−74	1.12	1.00	...	
		5	0.05	6.9	−79	2.15	1.00	...	
2200+420.....	2.32	1	3.27	0.0	...	1.34	0.28	16	0.90
		2	0.20	3.3	−179	3.34	0.33	−35	
		3	0.31	7.3	158	5.05	1.00	...	
		4	0.05	15.1	149	5.70	1.00	...	
		5	0.12	21.9	166	13.29	1.00	...	
	8.55	1	1.78	0.0	...	0.45	0.00	5	1.00
		2	1.32	1.0	−164	0.87	0.48	41	
		3	0.13	0.9	32	0.12	1.00	...	
		4	0.07	2.2	−171	0.69	1.00	...	
		5	0.19	6.2	169	4.62	1.00	...	
2201+315.....	2.32	1	2.21	0.0	...	2.30	0.55	37	0.93
		2	0.10	6.7	−134	2.92	1.00	...	
		3	0.09	14.6	−134	4.41	1.00	...	
		4	0.03	22.3	−133	0.00	1.00	...	
	8.55	1	1.06	0.0	...	0.49	0.20	29	0.98
		2	0.35	1.8	−151	0.95	0.42	30	
		3	0.49	2.3	−138	1.69	0.40	50	
		4	0.03	8.5	−137	2.53	1.00	...	
2227−088.....	2.32	1	0.84	0.0	...	2.18	0.33	−10	1.05
		2	0.10	8.4	8	5.78	1.00	...	
		3	0.03	25.5	4	10.26	1.00	...	
	8.55	1	1.53	0.0	...	0.11	1.00	...	0.78
		2	0.12	0.5	−31	0.37	1.00	...	
		3	0.05	2.7	−15	1.21	1.00	...	
		4	0.03	9.6	5	5.30	1.00	...	
2230+114.....	2.32	1	2.11	0.0	...	1.31	1.00	...	0.95
		2	0.80	3.8	170	1.24	1.00	...	
		3	2.30	4.8	−20	0.70	1.00	...	
		4	0.70	6.4	149	2.21	1.00	...	
		5	0.69	11.8	135	3.68	1.00	...	
		6	0.05	16.7	127	4.11	1.00	...	
	8.55	1	1.20	0.0	...	0.92	0.50	−15	1.32
		2	0.70	1.7	−36	0.62	0.00	−39	
		3	0.19	2.9	177	1.50	0.39	−12	
		4	0.54	5.4	163	2.46	0.39	−5	
		5	0.35	7.9	160	3.20	0.81	1	
		6	0.23	14.7	145	7.71	0.38	−84	
2252−089.....	2.32	1	0.36	0.0	...	1.30	1.00	...	1.06
		2	0.08	2.5	−124	1.16	1.00	...	
		3	0.11	10.7	−138	2.03	1.00	...	
		4	0.15	12.6	−121	4.77	0.00	−44	
		5	0.05	19.3	−57	11.68	1.00	...	
		6	0.03	38.4	−72	6.70	1.00	...	
		7	0.02	49.2	−73	4.23	1.00	...	
	8.55	1	0.29	0.0	...	0.16	1.00	...	0.79
		2	0.04	0.9	−117	0.50	1.00	...	
		3	0.02	2.5	−120	0.53	1.00	...	
		4	0.04	11.8	−135	2.31	1.00	...	
		5	0.03	13.1	−117	1.62	1.00	...	
2254+024.....	2.32	1	0.20	0.0	...	0.85	1.00	...	0.90
		2	0.02	12.3	107	4.21	1.00	...	
	8.55	1	0.33	0.0	...	0.27	0.31	−41	0.89
2319+272.....	2.32	1	0.76	0.0	...	2.92	0.37	12	0.86
		2	0.10	4.5	3	6.88	1.00	...	
	8.55	1	0.39	0.0	...	0.35	0.18	7	0.77
		2	0.15	2.0	2	1.07	1.00	...	
		3	0.08	2.7	20	0.62	1.00	...	
		4	0.03	4.7	1	2.46	1.00	...	
2320+506.....	2.32	1	1.26	0.0	...	1.42	0.18	28	0.83
		2	0.13	6.2	−135	3.01	1.00	...	
		3	0.04	21.6	−136	5.53	1.00	...	
		4	0.03	42.0	−123	10.33	1.00	...	

TABLE 2—*Continued*

SOURCE	ν (GHz)	Component	S (Jy)	r (mas)	θ (deg)	a (mas)	b/a	ϕ (deg)	χ^2
	8.55	1	0.76	0.0	...	0.47	0.00	28	0.92
		2	0.54	0.8	−157	1.14	0.30	26	
		3	0.03	7.3	−137	1.89	1.00	...	
2335−027.....	2.32	1	0.37	0.0	...	1.52	1.00	...	0.92
		2	0.04	5.7	31	4.02	1.00	...	
		3	0.05	19.8	26	9.53	1.00	...	
	8.55	1	0.19	0.0	...	0.34	1.00	...	0.92
		2	0.02	1.3	−126	0.00	1.00	...	
		3	0.08	1.3	72	0.51	1.00	...	
		4	0.01	3.2	46	1.30	1.00	...	

[a] The models fitted to the visibility data are of Gaussian form with flux density S and FWHM major axis a and minor axis b, with the major axis in position angle ϕ (measured north through east). Components are separated from the (arbitrary) origin of the image by an amount r in position angle θ, which is the position angle (measured north through east) of a line joining the components with the origin.

[b] The emission structure is too complex to fit a model; only the total integrated flux density (as measured from the image) is listed.

[c] Epoch 1995 April 12–13.

[d] Epoch 1995 October 12–13.

where the first term is the geometric delay corresponding to the reference direction $\boldsymbol{s}_0$, and the second term τ_s is the additional delay introduced by the source brightness distribution. Thus, the absolute VLBI position determined in astrometry is the position of the adopted reference direction $\boldsymbol{s}_0$ if structure effects are accounted for in the modeled delays according to equation (7). In practice, the delay structure corrections τ_s are determined as the slope of a straight line fitted to the individual structure phases calculated for each frequency channel used during the observations, in order to match precisely the scheme used to build the bandwidth synthesis delay observable at the correlator (see Charlot 1990b). The phase-delay rate, defined by the partial derivative of the total phase with respect to time, must be accounted for in a complete astrometric analysis also. For the purposes of this paper, we will deal with delay only. The interested reader is referred to Charlot (1990b) for a more thorough discussion of the phase-delay rate observable.

With an estimate of the brightness distribution $I(\boldsymbol{s}, \omega, t)$ for an extended source and the choice of a reference direction $\boldsymbol{s}_0$ within that source, structure corrections τ_s can be calculated (see Charlot 1990b for a detailed expression of τ_s). For the analysis presented here, we use CLEAN component models obtained from the hybrid imaging procedure described previously. The method used to select an appropriate reference position for each source is described below. As shown by Charlot (1990b), structure corrections τ_s then depend on the coordinates u and v only, which are the coordinates of the baseline $\boldsymbol{b}$ projected on the plane of the sky. To obtain an estimate of the overall magnitude of intrinsic source structure effects on a hypothetical bandwidth synthesis delay measurement, we calculate τ_s for all pixels of a 512 × 512 (u, v) grid lying within a circle of radius equal to the diameter of the Earth. This length corresponds to the longest baseline that can be theoretically observed using Earth-based VLBI. Next, the mean, rms, maximum, and median values of the structure corrections (absolute values) are determined. The calculation is done separately for the S-band and the X-band images. The structure corrections are then scaled by 0.08 at the S band and by 1.08 at the X band (these numbers correspond to the factors used in the linear combination of the S-band and the X-band observables in order to get the dual-frequency–calibrated bandwidth synthesis delay). Without scaling, the S-band corrections are very large (because the structures at the S band are generally more extended) and do not reflect the actual contribution to the dual-frequency–calibrated bandwidth synthesis delay. The results of these calculations are listed in Table 3. For convenience, we identify values in Table 3 by only a single fiducial frequency (2.32 and 8.55 GHz, respectively), even though these corrections represent bandwidth synthesis delay structure corrections determined over all frequency channels, as discussed above. For some sources, the maximum delay corrections are as large as several nanoseconds. The mean, rms, and median delay corrections range anywhere from a few picoseconds up to several hundred picoseconds. With the calculated values listed in Table 3, the additional noise introduced into a bandwidth synthesis delay measurement by intrinsic source structure can be estimated.

The calculation of τ_s for a particular source also requires the choice of a reference direction $\boldsymbol{s}_0$ within the source brightness distribution (i.e., a delay center). As discussed previously, this reference direction is equivalent to the absolute position of the source in the extragalactic reference frame so that, if these delay corrections were to be applied to measured bandwidth synthesis delays, an appropriate choice of the reference position would be critical for the stability of the celestial reference frame. Indeed, the calculated delay is very sensitive to the choice of the reference position. For example, a change of 0.1 mas in the reference position with respect to the source brightness distribution (equivalent to a change of 0.1 mas of the position of the source in the extragalactic reference frame) would produce a change in the calculated delay of up to 10 ps for a 6000 km baseline. Since the absolute positions of the source brightness distributions are unknown with respect to the celestial reference frame, and in order to avoid the difficult problem of choosing a reference position subjectively, we decided to select automatically during the calculation (using a least-squares procedure) the reference position for each source that minimizes the calculated rms delay for that source. In other words, the reference position determined by this method is such that any other choice of reference position would produce a larger rms delay. We felt that this least-squares method was most appropriate for the goal of this paper, which is simply to quantify the magnitude of the

source structure delay contributions without choosing subjectively an absolute position within the source brightness distribution. By examining the results of this analysis, we noted that the reference positions determined in this way are generally located at or near the *peak* of the brightness distributions (and not at the centroid of the brightness distributions as one would expect).

Finally, we classify the sources according to the median value of the calculated structure corrections, $\tau_{\text{median}} \equiv \tau_s(\text{median})$, as follows:

$$\text{Structure Index} = \begin{cases} 1\,, & \text{if } 0 \text{ ps} \le \tau_{\text{median}} < 3 \text{ ps}\,, \\ 2\,, & \text{if } 3 \text{ ps} \le \tau_{\text{median}} < 10 \text{ ps}\,, \\ 3\,, & \text{if } 10 \text{ ps} \le \tau_{\text{median}} < 30 \text{ ps}\,, \\ 4\,, & \text{if } 30 \text{ ps} \le \tau_{\text{median}} < \infty\,. \end{cases} \quad (8)$$

Two structure indices are defined for each source, one at the S band and one at the X band. We have chosen the median rather than the rms to define the structure index because we think that it better reflects the expected magnitude of the additional delay introduced by intrinsic source structure. Also, the median appears more "stable" and is not affected by a limited number of very large corrections (where VLBI observation probably could not be made anyway because the visibility amplitude would be too low). The divisions between the different indices could be considered somewhat arbitrary. However, the choices that we have made are based on our experience both in developing the formalism for calculating structure corrections and in analyzing the results. Figure 3 shows the distribution of the S band and the X band structure index for the observed sources. About 40% of these sources have an X-band structure index of either 3 or 4. As noted in Fey et al. (1996), some of the observed sources were chosen because they were the most troublesome, and hence the most interesting, of the sources in the Johnston et al. (1995) astrometric analysis. Consequently, the large number of sources with a structure index of either 3 or 4 is understandable since these sources are also the most spatially extended sources in our sample and were initially expected to produce large, calculated structure corrections.

To obtain an estimate of the influence of the noise in the CLEAN component models on the calculated structure corrections, all calculations were repeated, this time with the negative CLEAN components removed from the source models. The results were such that the mean differences were less than 0.1 ps (in the median) for the most compact sources (structure index 1) to $\sim$1 ps for the most extended sources (structure index 4). Thus, the noise in the models (at least the negative part) does not appear to affect these calculations significantly.

4.2. *Structure Index as an Indicator for Astrometry*

The structure index as defined by equation (8) can be used as an estimate of the astrometric quality of the observed sources. We have made a comparison between the X band structure index of the observed sources and the formal uncertainties of their astrometric positions obtained from the catalog of Johnston et al. (1995). The results of this comparison are listed in Table 4. The first column lists the X-band structure index, while the second column lists the number of observed sources that have this value of the structure index. For these sources, the third, fourth, and fifth columns list the mean number of bandwidth synthesis

TABLE 3

SOURCE STRUCTURE INDEX

SOURCE	ν (GHz)	τ_{mean} (ps)	τ_{rms} (ps)	τ_{max} (ps)	τ_{median} (ps)	Structure Index
0003−066.....	2.32	2.3	3.1	9.8	1.7	1
	8.55	14.8	18.8	60.2	12.5	3
0010+405.....	2.32	1.8	2.3	10.1	1.5	1
	8.55	8.0	10.0	24.9	7.2	2
0016+731.....	2.32	0.4	0.5	2.4	0.4	1
	8.55	13.7	19.8	62.5	9.3	2
0026+346.....	2.32	95.9	154.2	536.8	44.1	4
	8.55	191.4	508.1	4727.3	95.1	4
0056−001.....	2.32	18.4	26.9	449.4	12.8	3
	8.55	59.1	77.9	362.0	45.4	4
0059+581.....	2.32	1.1	1.4	4.8	0.8	1
	8.55	4.5	5.9	19.6	3.5	2
0108+388.....	2.32	20.9	56.3	473.3	6.2	2
	8.55	159.8	239.8	1869.8	111.0	4
0116+319.....	2.32	73.2	131.2	1266.1	45.1	4
	8.55	42.1	55.2	246.2	32.9	4
0119+115.....	2.32	2.9	3.8	15.2	2.2	1
	8.55	12.5	16.7	50.3	9.5	2
0138−097.....	2.32	1.6	2.1	6.4	1.2	1
	8.55	14.2	20.6	64.3	8.1	2
0153+744.....	2.32	20.5	31.1	274.9	14.8	3
	8.55	89.1	119.7	1738.4	69.0	4
0201+113.....	2.32	0.3	0.4	2.2	0.2	1
	8.55	10.5	13.2	40.6	9.5	2
0212+735.....	2.32	13.2	20.0	198.8	8.0	2
	8.55	8.9	11.9	54.6	6.7	2
0215+015.....	2.32	1.9	2.4	8.8	1.5	1
	8.55	2.1	2.9	13.6	1.5	1
0221+067.....	2.32	3.7	4.6	14.8	3.2	2
	8.55	5.1	7.2	34.4	3.6	2
0229+131.....	2.32	2.4	3.2	11.9	1.9	1
	8.55	5.8	8.6	36.0	3.6	2
0234+285.....	2.32	6.2	8.2	35.5	4.8	2
	8.55	20.6	28.7	163.2	14.4	3
0237+040.....	2.32	0.7	1.0	3.8	0.5	1
	8.55	6.0	7.8	21.8	4.8	2
0237−233.....	2.32	29.3	55.9	514.4	12.7	3
	8.55	345.0	500.9	2422.3	238.0	4
0238−084.....	2.32	11.5	16.3	57.6	7.7	2
	8.55	96.3	191.0	2240.8	44.7	4
0259+121.....	2.32	1.6	2.0	7.1	1.3	1
	8.55	24.4	33.0	146.7	17.9	3
0300+470.....	2.32	1.8	2.3	6.9	1.6	1
	8.55	7.7	9.8	27.5	6.7	2
0302+625.....	2.32	0.8	1.1	2.9	0.6	1
	8.55	7.6	10.1	54.5	5.9	2
0317+188.....	2.32	1.5	1.9	4.7	1.3	1
	8.55	9.7	13.5	53.6	6.7	2
0334+014.....	2.32	5.0	6.3	27.3	4.1	2
	8.55	6.1	8.1	29.6	4.6	2
0341+158.....	2.32	2.5	3.4	11.9	1.9	1
	8.55	6.0	7.4	19.0	5.5	2
0400+258.....	2.32	8.6	12.6	88.1	5.2	2
	8.55	21.0	28.0	155.9	16.1	3
0406+121.....	2.32	0.3	0.4	1.4	0.2	1
	8.55	4.1	5.4	17.3	3.0	2
0420−014.....	2.32	0.8	1.1	4.7	0.6	1
	8.55	24.7	31.8	124.3	19.7	3
0422+004.....	2.32	1.1	1.4	5.1	0.9	1
	8.55	6.0	7.8	34.9	4.5	2
0425+048.....	2.32	15.6	21.3	99.0	10.9	3
	8.55	16.5	21.5	88.3	13.1	3
0430+052.....	2.32	21.3	34.8	324.2	13.3	3
	8.55	118.3	236.8	2938.3	49.5	4
0440+345.....	2.32	0.8	1.0	5.0	0.6	1
	8.55	9.4	12.1	38.6	7.7	2
0440−003.....	2.32	0.2	0.3	1.3	0.1	1
	8.55	3.1	3.9	11.6	2.6	1
0454−234.....	2.32	0.7	0.9	3.0	0.5	1
	8.55	9.0	11.4	35.1	7.7	2
0458+138.....	2.32	5.8	7.6	32.2	4.5	2
	8.55	12.2	16.1	42.7	8.8	2

TABLE 3—*Continued*

Source	ν (GHz)	τ_{mean} (ps)	τ_{rms} (ps)	τ_{max} (ps)	τ_{median} (ps)	Structure Index
0459+060.....	2.32	1.9	2.6	11.8	1.4	1
	8.55	63.5	156.3	1639.2	18.4	3
0507+179.....	2.32	7.5	10.1	39.7	5.9	2
	8.55	13.2	18.2	78.8	9.6	2
0518+165.....	2.32	116.5	208.9	1332.5	66.0	4
	8.55	50.8	68.4	274.9	36.8	4
0536+145.....	2.32	0.6	0.8	2.7	0.5	1
	8.55	1.3	1.7	4.7	1.1	1
0539−057.....	2.32	3.5	5.3	44.2	2.3	1
	8.55	7.9	10.2	35.3	6.5	2
0544+273.....	2.32	1.9	2.6	10.4	1.4	1
	8.55	2.1	2.8	8.6	1.6	1
0552+398[a].....	2.32	0.4	0.6	2.3	0.3	1
	8.55	8.3	10.6	27.6	7.2	2
0552+398[b].....	2.32	0.1	0.1	0.5	0.1	1
	8.55	8.7	11.3	30.7	7.1	2
0552+398[c].....	2.32	0.1	0.1	0.4	0.1	1
	8.55	8.0	10.6	29.7	5.6	2
0600+177.....	2.32	2.3	3.1	10.4	1.7	1
	8.55	7.0	9.9	34.0	4.8	2
0609+607.....	2.32	6.9	9.4	42.1	5.4	2
	8.55	27.6	41.6	296.8	17.4	3
0636+680.....	2.32	0.8	1.0	3.7	0.6	1
	8.55	2.8	3.6	9.6	2.2	1
0642+449.....	2.32	1.6	2.0	4.6	1.5	1
	8.55	1.4	1.9	9.7	1.0	1
0646−306.....	2.32	5.2	7.1	29.0	3.5	2
	8.55	5.7	7.7	30.2	4.4	2
0657+172.....	2.32	3.0	4.2	14.8	2.2	1
	8.55	3.6	4.5	16.4	3.2	2
0707+476.....	2.32	1.5	1.9	6.2	1.3	1
	8.55	7.7	10.0	38.5	6.2	2
0710+439.....	2.32	34.4	55.9	477.0	20.6	3
	8.55	340.5	492.3	2410.9	229.8	4
0718+793.....	2.32	0.2	0.2	0.6	0.2	1
	8.55	3.5	4.3	12.1	3.1	2
0723−008.....	2.32	8.1	11.6	63.7	5.4	2
	8.55	19.9	27.3	106.6	14.1	3
0727−115[a].....	2.32	1.1	1.4	5.5	0.9	1
	8.55	4.6	5.8	16.8	3.8	2
0727−115[b].....	2.32	1.5	2.1	7.7	1.0	1
	8.55	4.4	6.1	23.2	2.9	1
0727−115[c].....	2.32	0.9	1.2	4.9	0.7	1
	8.55	4.2	5.4	18.6	3.2	2
0742+103.....	2.32	1.5	2.1	8.7	1.1	1
	8.55	81.1	166.8	2257.8	33.8	4
0743−006.....	2.32	1.5	2.0	8.6	1.2	1
	8.55	5.4	7.0	21.6	4.3	2
0749+540.....	2.32	0.6	0.8	2.6	0.4	1
	8.55	2.5	3.3	13.6	1.9	1
0805−077.....	2.32	3.7	4.8	19.1	2.9	1
	8.55	20.0	27.5	104.7	14.7	3
0808+019.....	2.32	0.7	0.9	3.9	0.5	1
	8.55	2.6	3.4	14.3	1.9	1
0820+560.....	2.32	3.1	4.4	20.0	2.1	1
	8.55	11.1	15.0	77.4	8.3	2
0823+033.....	2.32	1.0	1.4	5.4	0.6	1
	8.55	13.5	18.0	54.7	9.0	2
0831+557.....	2.32	39.3	97.9	1483.7	19.2	3
	8.55	236.7	376.5	2122.1	123.6	4
0833+585.....	2.32	2.1	3.6	18.7	0.8	1
	8.55	38.4	75.1	897.6	21.9	3
0851+202[a].....	2.32	1.0	1.3	5.0	0.8	1
	8.55	20.9	25.8	68.4	19.7	3
0851+202[b].....	2.32	1.2	1.7	5.7	0.7	1
	8.55	13.4	17.2	51.9	11.2	3
0851+202[c].....	2.32	1.2	1.6	4.7	0.9	1
	8.55	8.1	11.4	37.5	6.1	2
0859+470.....	2.32	9.6	13.5	75.4	6.5	2
	8.55	15.6	21.8	103.6	10.7	3
0912+297.....	2.32	1.5	1.9	9.1	1.2	1
	8.55	1.3	1.7	5.5	1.0	1
0917+624.....	2.32	3.1	4.2	20.4	2.2	1
	8.55	6.5	8.9	46.6	4.9	2

TABLE 3—*Continued*

Source	ν (GHz)	τ_{mean} (ps)	τ_{rms} (ps)	τ_{max} (ps)	τ_{median} (ps)	Structure Index
0919−260.....	2.32	11.3	20.8	457.3	7.1	2
	8.55	17.0	22.5	69.6	12.8	3
0945+408.....	2.32	4.1	5.6	22.6	3.0	2
	8.55	12.3	18.1	82.6	7.2	2
0953+254.....	2.32	0.5	0.6	2.6	0.4	1
	8.55	6.5	8.5	21.0	5.0	2
0955+476.....	2.32	0.3	0.4	1.3	0.2	1
	8.55	1.5	1.9	7.9	1.3	1
1004+141.....	2.32	9.8	12.8	42.4	7.6	2
	8.55	13.2	17.0	66.0	10.5	3
1020+400.....	2.32	2.9	3.9	18.7	2.2	1
	8.55	14.5	19.1	53.5	11.5	3
1022+194.....	2.32	6.3	8.6	35.6	4.4	2
	8.55	7.9	11.2	47.6	5.1	2
1034−293.....	2.32	1.5	2.0	9.4	1.2	1
	8.55	3.2	4.3	15.3	2.5	1
1038+064.....	2.32	3.4	4.5	19.7	2.5	1
	8.55	27.9	35.7	99.3	25.3	3
1049+215.....	2.32	2.3	3.3	12.8	1.5	1
	8.55	9.0	12.6	53.0	6.1	2
1053+815.....	2.32	0.4	0.5	1.5	0.3	1
	8.55	1.3	1.7	5.0	1.1	1
1116+128.....	2.32	8.5	13.0	83.1	5.5	2
	8.55	18.5	25.0	124.7	13.5	3
1117+146.....	2.32	87.7	155.3	1231.2	53.0	4
	8.55	24.3	31.0	117.2	19.7	3
1127−145.....	2.32	4.8	6.3	24.8	3.8	2
	8.55	58.5	82.7	441.5	40.8	4
1130+009.....	2.32	2.0	2.5	8.3	1.5	1
	8.55	6.2	7.8	24.6	5.2	2
1145−071.....	2.32	1.6	2.2	11.5	1.1	1
	8.55	12.3	15.6	47.5	10.6	3
1150+812.....	2.32	3.9	5.1	17.4	3.4	2
	8.55	12.9	18.5	103.8	8.6	2
1156+295.....	2.32	6.1	8.0	36.4	4.6	2
	8.55	7.7	10.6	47.4	5.6	2
1156−094.....	2.32	26.0	32.8	122.1	22.2	3
	8.55	26.1	35.0	223.7	20.0	3
1213+350.....	2.32	3.5	4.5	18.4	2.8	1
	8.55	32.5	41.6	193.9	26.5	3
1219+044.....	2.32	0.6	0.8	2.1	0.5	1
	8.55	4.9	6.2	20.4	4.5	2
1221+809.....	2.32	3.9	5.5	27.0	2.7	1
	8.55	8.3	11.4	43.3	5.9	2
1226+373.....	2.32	0.5	0.6	2.1	0.4	1
	8.55	3.2	4.1	10.5	2.5	1
1236+077.....	2.32	2.4	3.1	13.7	2.0	1
	8.55	16.6	24.7	157.9	9.4	2
1307+121.....	2.32	10.2	14.8	73.5	6.9	2
	8.55	33.2	48.6	272.8	19.6	3
1308+326.....	2.32	0.9	1.2	5.1	0.7	1
	8.55	2.1	2.6	7.8	1.8	1
1313−333.....	2.32	2.0	2.6	9.4	1.6	1
	8.55	3.1	4.2	19.0	2.2	1
1315+346.....	2.32	2.4	3.1	10.9	2.0	1
	8.55	8.9	11.4	31.1	7.8	2
1323+321.....	2.32	124.0	180.2	1039.4	89.1	4
	8.55	78.7	102.7	1013.9	63.6	4
1334−127.....	2.32	0.7	1.0	4.6	0.6	1
	8.55	8.4	10.4	26.0	7.7	2
1342+662.....	2.32	0.7	0.8	2.0	0.5	1
	8.55	3.7	4.7	13.0	3.2	2
1345+125.....	2.32	84.8	128.4	952.0	57.2	4
	8.55	255.5	441.2	4963.0	150.3	4
1347+539.....	2.32	10.2	14.4	74.8	7.1	2
	8.55	23.7	33.9	188.8	14.8	3
1357+769.....	2.32	0.3	0.5	1.3	0.2	1
	8.55	1.2	1.5	4.6	1.0	1
1402+044.....	2.32	2.9	3.9	16.9	2.1	1
	8.55	10.1	13.5	59.0	7.5	2
1404+286.....	2.32	1.8	2.5	14.2	1.3	1
	8.55	23.5	32.6	154.5	16.1	3
1413+135.....	2.32	35.1	60.9	653.4	20.7	3
	8.55	2.9	4.0	14.9	2.0	1

TABLE 3—*Continued*

Source	ν (GHz)	τ_{mean} (ps)	τ_{rms} (ps)	τ_{max} (ps)	τ_{median} (ps)	Structure Index
1416+067.....	2.32	4.1	6.3	28.1	2.2	1
	8.55	10.8	14.8	89.4	8.0	2
1432+200.....	2.32	2.1	2.8	11.0	1.6	1
	8.55	7.2	9.8	31.5	4.9	2
1433+304.....	2.32	3.7	4.9	21.8	2.8	1
	8.55	8.2	11.8	55.2	5.2	2
1458+718.....	2.32	51.8	93.9	694.0	24.1	3
	8.55	20.4	27.9	261.5	15.4	3
1459+480.....	2.32	2.8	3.7	12.1	2.3	1
	8.55	4.7	6.4	24.9	3.4	2
1502+106.....	2.32	1.7	2.3	8.9	1.3	1
	8.55	8.5	10.6	45.4	7.5	2
1510−089.....	2.32	0.8	1.0	4.1	0.6	1
	8.55	17.5	22.1	57.7	14.8	3
1532+016.....	2.32	4.3	5.6	17.8	3.4	2
	8.55	68.0	133.3	1856.0	35.4	4
1546+027.....	2.32	1.0	1.4	5.7	0.8	1
	8.55	6.6	9.2	38.6	4.7	2
1600+335.....	2.32	2.8	3.5	12.6	2.4	1
	8.55	28.4	38.4	213.0	21.3	3
1607+268.....	2.32	130.0	193.0	690.9	79.6	4
	8.55	68.4	93.2	685.9	51.2	4
1611+343.....	2.32	2.6	3.6	16.9	2.0	1
	8.55	18.8	27.8	146.9	12.2	3
1622−253.....	2.32	1.2	1.6	7.1	0.9	1
	8.55	2.4	3.3	10.5	1.9	1
1624+416.....	2.32	4.7	6.3	28.6	3.5	2
	8.55	30.7	40.9	178.1	23.1	3
1633+382.....	2.32	1.5	2.2	12.3	1.0	1
	8.55	25.2	39.8	255.7	15.5	3
1642+690.....	2.32	4.7	6.5	25.6	3.3	2
	8.55	26.6	38.7	222.2	17.3	3
1652+398.....	2.32	6.8	9.2	52.6	5.2	2
	8.55	17.8	23.6	103.2	13.6	3
1705+018.....	2.32	1.2	1.7	6.2	0.8	1
	8.55	6.1	7.6	22.0	5.1	2
1705+456.....	2.32	10.0	15.1	105.1	5.7	2
	8.55	16.6	22.2	80.6	12.3	3
1725+044.....	2.32	2.0	2.7	10.7	1.5	1
	8.55	11.1	15.1	55.0	7.7	2
1738+476.....	2.32	0.6	0.8	2.7	0.5	1
	8.55	4.2	5.3	17.0	3.6	2
1739+522.....	2.32	1.7	2.2	10.6	1.3	1
	8.55	6.4	8.7	47.6	4.8	2
1741−038[a].....	2.32	0.5	0.7	2.7	0.4	1
	8.55	2.5	3.1	9.4	2.1	1
1741−038[c].....	2.32	0.3	0.4	1.3	0.3	1
	8.55	2.2	3.0	13.2	1.7	1
1743+173.....	2.32	2.3	3.0	17.0	1.7	1
	8.55	9.2	13.2	71.4	6.6	2
1749+096[a].....	2.32	1.6	2.2	7.9	1.1	1
	8.55	1.9	2.5	9.2	1.3	1
1749+096[b].....	2.32	1.2	1.5	5.6	1.0	1
	8.55	0.9	1.1	3.8	0.7	1
1749+096[c].....	2.32	1.0	1.2	3.5	0.9	1
	8.55	0.7	0.9	2.4	0.5	1
1751+288.....	2.32	1.4	1.9	8.5	1.1	1
	8.55	5.9	7.7	26.7	4.8	2
1803+784.....	2.32	3.6	5.1	25.0	2.3	1
	8.55	5.8	8.1	37.2	4.0	2
1821+107.....	2.32	1.3	1.7	7.9	1.0	1
	8.55	28.7	43.7	232.1	19.8	3
1823+568.....	2.32	3.1	4.3	17.8	2.0	1
	8.55	4.0	5.6	21.8	2.9	1
1826+796.....	2.32	4.9	6.3	21.1	4.0	2
	8.55	69.6	95.6	409.5	47.7	4
1842+681.....	2.32	1.4	2.0	7.8	0.9	1
	8.55	8.9	12.1	33.9	6.4	2
1849+670.....	2.32	3.8	4.9	19.8	3.1	2
	8.55	2.8	3.7	14.3	2.1	1
1921−293.....	2.32	3.6	4.6	13.8	2.9	1
	8.55	8.1	11.0	54.5	5.9	2

TABLE 3—*Continued*

Source	ν (GHz)	τ_{mean} (ps)	τ_{rms} (ps)	τ_{max} (ps)	τ_{median} (ps)	Structure Index
1929+226.....	2.32	1.4	1.8	7.4	1.0	1
	8.55	3.3	4.3	17.7	2.6	1
1932+204.....	2.32	4.1	6.7	63.7	2.3	1
	8.55	1.3	1.8	5.6	1.0	1
1947+079.....	2.32	57.8	78.9	351.4	44.5	4
	8.55	129.7	166.7	557.9	105.4	4
1951+355.....	2.32	2.5	3.5	14.7	1.7	1
	8.55	10.5	15.4	92.6	6.9	2
1954+513.....	2.32	3.6	4.9	19.5	2.6	1
	8.55	10.2	14.9	87.1	6.4	2
2007+777.....	2.32	1.3	2.0	9.2	0.7	1
	8.55	52.3	97.5	805.6	26.0	3
2017+743.....	2.32	1.8	2.4	9.5	1.5	1
	8.55	4.8	6.5	19.1	3.6	2
2021+317.....	2.32	3.1	4.4	34.9	2.3	1
	8.55	17.9	24.7	121.9	12.7	3
2021+614.....	2.32	22.5	44.5	476.8	11.2	3
	8.55	99.9	130.4	383.3	77.7	4
2023+336.....	2.32	50.5	89.1	747.3	23.1	3
	8.55	14.8	21.4	135.2	10.2	3
2029+121.....	2.32	0.6	0.8	2.3	0.5	1
	8.55	15.9	20.4	67.6	12.9	3
2059+034.....	2.32	0.7	1.0	3.7	0.6	1
	8.55	4.6	6.2	19.1	3.4	2
2113+293.....	2.32	1.4	1.8	6.1	1.1	1
	8.55	2.9	3.9	17.5	2.3	1
2128−123.....	2.32	4.2	5.6	19.3	3.1	2
	8.55	45.7	66.8	246.3	28.5	3
2131−021.....	2.32	2.1	2.9	13.6	1.6	1
	8.55	6.7	9.2	35.7	4.5	2
2134+004.....	2.32	0.5	0.6	2.3	0.3	1
	8.55	83.6	184.4	1645.8	38.5	4
2136+141.....	2.32	2.3	3.0	8.7	1.9	1
	8.55	3.5	4.8	20.3	2.7	1
2145+067[a].....	2.32	4.4	5.4	17.7	3.8	2
	8.55	9.6	12.2	26.8	8.5	2
2145+067[b].....	2.32	3.9	5.1	28.6	3.1	2
	8.55	8.3	10.7	29.0	6.7	2
2145+067[c].....	2.32	4.0	5.3	23.8	3.2	2
	8.55	8.3	10.6	23.0	6.7	2
2150+173.....	2.32	7.0	9.9	39.5	4.6	2
	8.55	11.3	15.6	72.0	7.9	2
2200+420.....	2.32	1.5	1.9	8.0	1.2	1
	8.55	25.7	35.1	157.4	17.5	3
2201+315.....	2.32	2.9	4.3	15.3	1.5	1
	8.55	31.3	50.4	473.3	18.9	3
2216−038.....	2.32	0.4	0.5	2.0	0.3	1
	8.55	24.4	32.1	93.1	20.6	3
2227−088.....	2.32	1.7	2.2	8.2	1.4	1
	8.55	2.0	2.6	8.0	1.6	1
2230+114.....	2.32	11.9	16.0	132.4	8.9	2
	8.55	69.1	98.4	1636.3	51.1	4
2234+282.....	2.32	0.4	0.5	2.4	0.3	1
	8.55	4.8	6.7	25.9	3.3	2
2252−089.....	2.32	18.2	29.3	329.1	11.2	3
	8.55	14.7	19.4	88.1	11.1	3
2254+024.....	2.32	3.1	4.0	18.6	2.5	1
	8.55	1.4	1.8	4.8	1.3	1
2255−282.....	2.32	6.1	8.6	36.2	4.5	2
	8.55	4.1	5.8	25.7	2.8	1
2319+272.....	2.32	2.6	3.5	16.9	1.9	1
	8.55	22.3	33.3	149.1	12.5	3
2320+506.....	2.32	2.3	3.4	12.8	1.5	1
	8.55	24.0	30.5	102.5	21.7	3
2335−027.....	2.32	3.4	4.7	25.7	2.4	1
	8.55	24.0	31.4	99.5	18.8	3
2337+264.....	2.32	29.2	53.6	499.3	15.1	3
	8.55	100.8	138.2	641.7	70.7	4

[a] Epoch 1994 July 8–9.
[b] Epoch 1995 April 12–13.
[c] Epoch 1995 October 12–13.

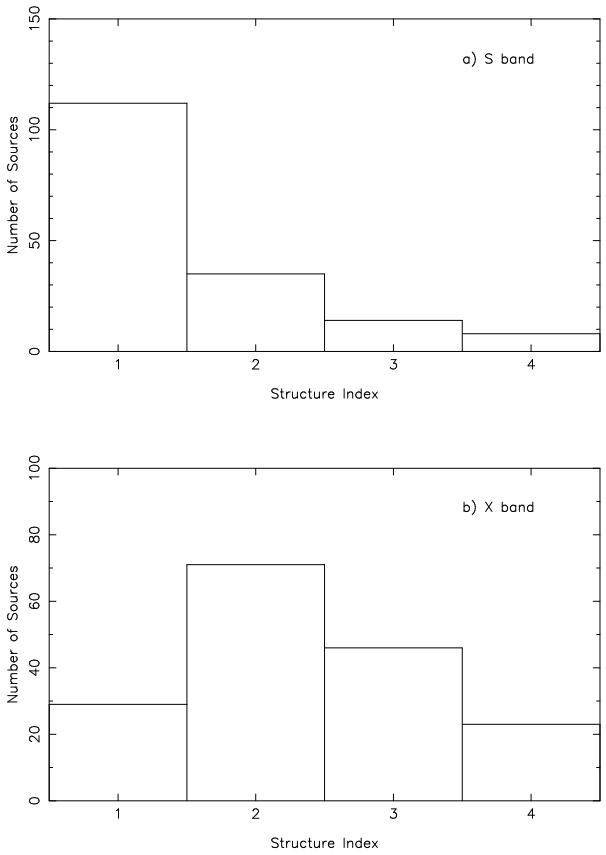

FIG. 3.—The distribution of the structure index (eq. [8]) for the sources presented in this paper and in Fey et al. (1996) at (*a*) the *S* band and (*b*) the *X* band.

delay measurements used in the astrometric solution from which Johnston et al. (1995) estimate positions, the mean formal uncertainties in right ascension, and the mean formal uncertainties in declination, respectively. Right ascension formal uncertainties have been scaled by the cosine of their respective declinations. The results of this comparison indicate that, in the mean, sources with larger formal position uncertainties have a larger structure index than those with smaller uncertainties, as would be expected if the structure index traces the complexity of intrinsic source structure accurately.

We have also made a comparison between the *X*-band structure index listed in Table 3 and the *X*-band core flux

TABLE 4

STRUCTURE INDEX VERSUS FORMAL POSITION UNCERTAINTY

STRUCTURE INDEX	NUMBER OF SOURCES	MEAN N_{obs}	MEAN UNCERTAINTY $\sigma_\alpha \cos(\delta)$ (mas)	MEAN UNCERTAINTY σ_δ (mas)
1	29	2637 ± 1128	0.15 ± 0.03	0.19 ± 0.03
2	70	6381 ± 1727	0.22 ± 0.04	0.29 ± 0.06
3	46	3540 ± 1125	0.34 ± 0.12	0.46 ± 0.15
4	23	683 ± 410	1.50 ± 0.76	1.03 ± 0.37

NOTE.—Formal position uncertainties are from Johnston et al. 1995. All sources for which we have images are included in the analysis here except 0334+014, which had a very poorly determined position in Johnston et al. 1995. In the case of sources observed at multiple epochs, only results from the most recent epoch were used. The structure index is that defined at the *X* band.

TABLE 5

STRUCTURE INDEX VERSUS CORE FLUX DENSITY

Structure Index	Number of Sources	Mean Ratio (S_{core}/S_{total})
1	29	0.92 ± 0.01
2	71	0.82 ± 0.01
3	44	0.64 ± 0.02
4	22	0.48 ± 0.04

NOTES.—The *X*-band flux density values are taken from the Gaussian models fitted to the visibility data and are listed in Table 2 of this paper and in Table 2 of Fey et al. 1996. The core flux density, S_{core}, is the value of the Gaussian model component defined to be at the origin of the image, while the total flux density, S_{total}, is the sum of all model components. All sources for which we have images are included in the analysis here except 0831+557, 2021+317, and 2023+336, which were too complex to model satisfactorily with the available data. In the case of sources observed at multiple epochs, only results from the most recent epoch were used. The structure index is that defined at the *X* band.

densities of the observed sources. The results of this comparison are listed in Table 5. The first column lists the *X*-band structure index, while the second column lists the number of observed sources that have this value of the structure index. The last column in this table lists for these sources the mean ratio of the *X*-band core flux density to the total *X*-band flux density. The *X*-band flux density values are taken from the Gaussian models fitted to the visibility data listed in Table 2 of this paper and in Table 2 of Fey et al. (1996). The core flux density, S_{core}, is the value of the Gaussian model component defined to be at the origin of the image, while the total flux density, S_{total}, is the sum of all model components. Since the core-to-total flux density ratio is an indication of the "compactness" of a source, the results of this comparison indicate that, in the mean, more extended sources have a larger structure index than more compact sources. Thus, the compactness of the sources has a direct bearing on the structure index. A comparison of Table 4 and Table 5 then indicates that the more extended sources have larger formal position uncertainties.

A specific example from the above analysis would be for the source 0851+202 (OJ 287). This BL Lac object has a redshift of $z = 0.306$ and regularly ejects superluminal components that separate from the core with an angular velocity of ~ 0.3 mas yr^{-1} (Gabuzda, Wardle, & Roberts 1989; Vicente, Charlot, & Sol 1996) . From our data, we find that the ratio S_{core}/S_{total} varies from 0.60 at epoch 1994 July 8 to 0.63 at epoch 1995 April 12 to 0.84 at epoch 1995 October 12. The median structure correction, τ_{median}, varies from 19.7 ps to 11.2 ps to 6.1 ps at these same epochs. Consequently, the *X*-band structure index changes from an initial value of 3 to a value of 2 at the last epoch. We interpret this result as a consequence of the fact that the observed superluminal component is fading (with respect to the core) as it moves away from the core, and thus the source becomes more compact with time with a corresponding decrease in the magnitude of the intrinsic structure effects. This result strongly suggests that variable intrinsic structure can negatively impact bandwidth synthesis astrometry, as was pre-

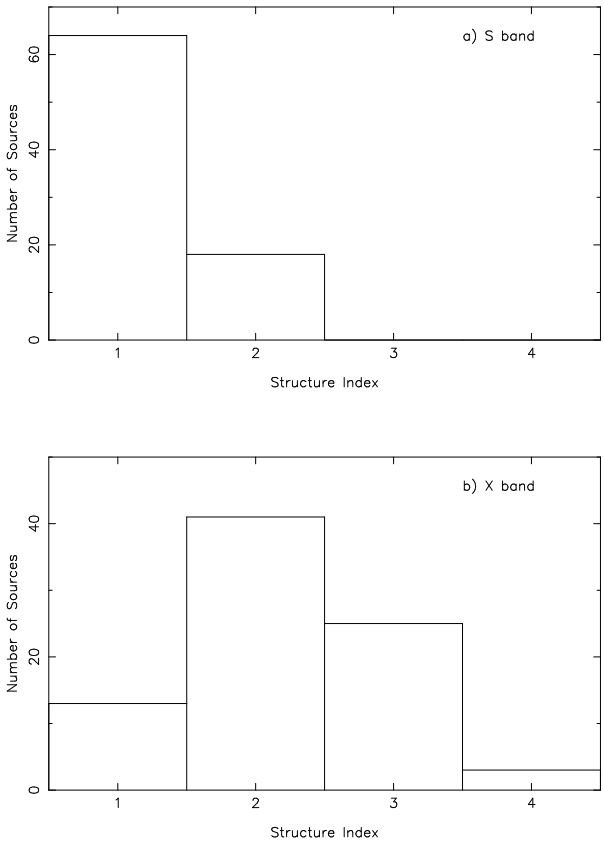

FIG. 4.—The distribution of the structure index (eq. [8]) for 82 of the sources presented in this paper and in Fey et al. (1996) that were classified as defining reference frame objects by Johnston et al. (1995) at (*a*) the *S* band and (*b*) the *X* band.

viously shown by Charlot (1994) in the case of the more extended source 1226+023 (3C 273). The source 0851+202 should be monitored regularly for future ejection events and should be used for astrometry only with caution.

Of the sources we have imaged, 82 are Johnston et al. (1995) class I sources, i.e., they were selected as the best reference frame sources based on the number of bandwidth synthesis delay measurements, repeatability of observations, etc. The distribution of the *S*-band and the *X*-band structure index for these 82 sources is shown in Figure 4. All 82 of these sources have an *S*-band structure index of either 1 or 2, indicating that they are relatively spatially compact at this frequency. However, roughly one-third of these sources have an *X*-band structure index of either 3 or 4, indicating that they are somewhat spatially extended and thus are probably not very good reference frame sources. This result suggests that, if images had been available, use of the structure index would have been an invaluable addition to the selection criteria of Johnston et al. (1995), for their choice of defining reference frame objects, since a large number of extended sources were obviously included in their list.

Based on the above results, we suggest that the structure index defined by equation (8) can be used as an estimate of the astrometric quality of the sources and should be given at least equal weight with other selection criteria when choosing compact extragalactic radio sources for precise astrometry. We suggest that sources be evaluated for astrometric use based on the *S*-band and the *X*-band structure index as follows. Sources with an *X*-band structure index of 1 may be considered very good astrometric sources. Sources with an *X*-band index of 2 may be considered good sources, while sources with an *X*-band index of 3 should be considered marginal (and should only be used with caution). Finally, sources with an *X*-band index of 4 should not be used at all for astrometric work unless the effects caused by their extended structures can be modeled. Additionally, sources should have an *S*-band structure index of either 1 or 2, with a preferred value of 1, independent of the value of their *X*-band structure index.

5. SUMMARY

Charlot (1990b) has modeled the effects of radio source structure on measured VLBI bandwidth synthesis delays and delay rates. The results of this modeling suggest that these effects can be significant for extended sources (typically at a level of 100 ps [$\sim$3 cm at the surface of the Earth $\sim$1 mas] in the bandwidth synthesis delay). We have calculated structure delay corrections based on the Charlot (1990b) analysis by using source models derived from VLBA observations of 169 extragalactic sources presented in this paper and in Fey et al. (1996). The results of these calculations show that intrinsic structure contributions to the measured bandwidth synthesis delay are significant, ranging from maximum delay corrections of only a few picoseconds for the most compact sources to maximum delay corrections of several nanoseconds for the most extended sources. The structure corrections presented in this paper can be used to estimate the additional noise introduced into a bandwidth synthesis delay measurement by intrinsic source structure. A correlation between the compactness of the sources and their formal position uncertainties was found, indicating that the more extended sources have larger position uncertainties. We also define a source "structure index" based on the median structure corrections and suggest that this index can be used as an estimate of the astrometric quality of the sources.

The authors would like to thank Tim Pearson for helpful comments on the manuscript.

REFERENCES

Charlot, P. 1990a, A&A, 229, 51
———. 1990b, AJ, 99, 1309
———. 1994, in Proc. Int. Symp., VLBI Technology: Progress and Future Observational Possibilities, ed. T. Sasao, S. Manabe, O. Kameya, & M. Inoue (Tokyo: Terra Scientific Publishing Co.), 286
Fey, A. L., Clegg, A. W., & Fomalont, E. B. 1996, ApJS, 105, 299
Gabuzda, D. C., Wardle, J. F. C., & Roberts, D. H. 1989, ApJ, 336, L59
Henstock, D. R., Browne, I. W. A., Wilkinson, P. N., Taylor, G. B., Vermeulen, R. C., Pearson, T. J., & Readhead, A. C. S. 1995, ApJS, 100, 1
Johnston, K. J., Fey, A. L., Zacharias, N., Russell, J. L., Ma, C., & De Vegt, C. 1995, AJ, 110, 880
Napier, P. J., Bagri, D. S., Clark, B. G., Rogers, A. E. E., Romney, J. D., Thompson, A. R., & Walker, R. C. 1994, Proc. IEEE, 82, 658
Pearson, T. J., & Readhead, A. C. S. 1984, ARA&A, 22, 97
Pearson, T. J., Shepherd, M. C., Taylor, G. B., & Myers, S. T. 1994, BAAS, 26, 1318
Rogers, A. E. E. 1970, Radio Sci., 5, 1239
Shepherd, M. C., Pearson, T. J., & Taylor, G. B. 1995, BAAS, 27, 903
Vicente, L., Charlot, P., & Sol, H. 1996, A&A, 312, 727